CONTROLLED DELIVERY OF BASAL LEVEL OF INSULIN

A Dissertation
Submitted to the Graduate Faculty
of the
North Dakota State University
of Agriculture and Applied Science

By
Mayura Arvind Oak

In Partial Fulfillment of the Requirements
for the Degree of
DOCTOR OF PHILOSOPHY

Major Department:
Pharmaceutical Sciences

August 2012

Fargo, North Dakota

North Dakota State University
Graduate School

Title

Controlled delivery of basal level of insulin

By

Mayura Arvind Oak

The Supervisory Committee certifies that this ***disquisition*** complies with North Dakota State University's regulations and meets the accepted standards for the degree of

DOCTOR OF PHILOSOPHY

SUPERVISORY COMMITTEE:

Dr. Jagdish Singh

Chair

Dr. Sanku Mallik

Dr. Chengwen Sun

Dr. Rhonda Magel

Approved by Department Chair:

02/25/2013 — Date

Dr. Jagdish Singh — Signature

ABSTRACT

Present study was aimed at developing a delivery system for controlled release of insulin at basal level from chitosan-zinc-insulin complex incorporated into thermosensitive polymer, poly(lactic acid)-poly(ethylene glycol)-poly(lactic acid) (PLA-PEG-PLA). Chitosan-zinc-insulin complex was optimized to restrict the insulin diffusion from the delivery system by complex formation and thereby reducing initial burst release. Polymer concentration, insulin loading, chitosan and $Zinc^{+2}$ addition were shown to affect the insulin release in vitro. Formulations containing insulin, zinc-insulin, and chitosan-insulin exhibited high initial burst (~7-14%), accompanied with a large secondary burst and incomplete release. Chitosan-zinc-insulin containing formulations showed extended release profiles of insulin for 84-90 days with a significant ($P<0.05$) reduction in initial burst release and minimal secondary burst. Increasing chitosan amount had no effect ($P>0.05$) on the initial burst, and release rate. Insulin alone and zinc-insulin containing formulations showed significant ($p<0.05$) attenuation in secondary and tertiary structure of insulin, as compared to chitosan-zinc-insulin. The complex formation conserved the physical and chemical stability of insulin and protected it from aggregation during release and storage. It also protected insulin from the acidic degradation product of copolymer.

The delivery systems were investigated for continuous in vivo insulin delivery at basal level for prolonged period after a single subcutaneous injection. In vivo absorption and bioactivity of insulin released were studied in streptozotocin-induced diabetic rats. Chitosan-zinc-insulin complex significantly ($P<0.05$) reduced the initial burst release of insulin in comparison to zinc-insulin or insulin alone. The delivery system released insulin for ~70 days in biologically active form with corresponding reduction in blood glucose. Blood glucose levels were comparable to that of control for longer duration, and were significantly ($P<0.05$) lower

than untreated diabetic animals. No significant difference ($P>0.05$) in blood glucose levels in two consecutive time points until 56-63 days indicated a pharmacodynamic manifestation of continuous release of insulin at steady rate. The delivery systems showed increase in bioavailability of insulin (1.2-2 fold increase in AUC) as compared to zinc-insulin and insulin alone. Insulin released from the delivery systems did not provoke any immune response. The delivery systems were biocompatible in vitro and in vivo and were non-toxic.

ACKNOWLEDGEMENTS

I would like to express my sincere gratitude to my advisor, Dr. Jagdish Singh, whose expertise, constructive criticism, and understanding added considerably to my graduate experience.

I would like to extend my genuine thanks to my graduate advisory committee members, Dr. Sanku Mallik, Dr. Rhonda Magel, and Dr. Chengwen Sun for their helpful suggestions, and guidance throughout the study.

My warm and sincere thanks to my seniors, Dr. Khaled Al-Tahami, Dr. Sibao Chen, Dr. Yu Tang, Dr. Chandrasekar Manoharan, and Dr. Babu Medi, for their valuable suggestions.

I would also like to thank my friends and fellow graduate students Venkata Shravan Kumar Indurthi, Mukta Sane, Anil Wagh, and Neha Singh for their help during my studies.

I would like to acknowledge the help and assistance of Janet Krom, Jean Trautmann, and Lori Peterson during my stay at NDSU.

I gratefully acknowledge the financial support from the National Institute of Health (NIH), and graduate school.

I would also like to acknowledge Heidi Docktor for her help with GPC analysis. I would also like to thank Scott Payne for sample preparation and SEM measurements.

I am extremely grateful to Dr. Steven Qian, Dr. Scott Walden, and Josie Hayden for providing a continuous guidance and help during in vivo studies.

I would like to thank Rhishi and my family members for their support and understanding during my entire graduate studies.

DEDICATION

This dissertation is dedicated to my parents for their never-ending support and encouragement during my higher education.

TABLE OF CONTENTS

LIST OF TABLES

LIST OF FIGURES

LIST OF ABBREVIATIONS

ANOVA…….. Analysis of variance

CD…… Circular dichroism

DMEM……..... Dulbecco's modified eagle medium

DSC……. Differential scanning calorimetry

ELISA……. Enzyme linked immunosorbent assay

FBS……. Fetal bovine serum

GPC…… Gel permeation chromatography

H&E……..... Hematoxylin-eosin

HRP……. Horseradish peroxidase

HEK293…….. Human embryonic kidney 293 cells

HPLC…….. High performance liquid chromatography

IACUC…… Institutional animal care and use committee

MALDI-TOF MS…… Matrix assisted laser desorption ionization time of flight mass spectroscopy

MW……. Molecular weight

MTT…… 3-(4,5-dimethylthiazol-2-yl)-2, 5-diphenyltetrazolium bromide

NMR……. Nuclear magnetic resonance

PAGE…….. Polyacrylamide gel electrophoresis

PBS……. Phosphate-buffered saline

PBST…….. Phosphate-buffered saline containing 0.02% Tween 20

PDI…….. Polydispersity index

PEG……. Polyethylene glycol

PLA……. Poly lactic acid

PLGA…….. Poly lactic-co-glycolic acid

RPM…… Revolutions per minute

RT…… Room temperature

SDS-PAGE……. Sodium dodecyl sulfate- polyacrylamide gel electrophoresis

SD Rats…… Sprague dawley rats

STZ……. Streptozotocin

TFA……. Trifluoroacetic acid

Tris…….. Tris(hydroxymethyl) aminomethane

% v/v…… Percent volume by volume

% w/v…….. Percent weight by volume

% w/w…….. Percent weight by weight

1. INTRODUCTION

1.1. Controlled Release Systems

The 'biologics portfolio' of biotechnology and pharmaceutical industry represents an important sector for sustainable advancements in a market that is estimated to be growing at a rate of ~13% annually (1). Protein and peptide drugs such as insulin, salmon calcitonin, growth hormone, and vascular endothelial growth factor (VEGF), which represent a vast majority of these biologics, are often constrained with issues like short half-life, delicate structure and the physical/chemical instabilities (2-6). These problems, combined with the delivery issues, necessitate the frequent injections of these biologics to obtain the desired therapeutic effect. The proteins and peptides usually suffer with physical and/or chemical instabilities. Physical instability includes the alteration of higher order protein structures without any covalent modification, and can lead to undesirable processes such as denaturation (protein unfolding), aggregation, precipitation, and adsorption to the surfaces. The chemical instability includes breaking or formation of covalent bonds, which may lead to formation of new chemical entities with altered properties. Reactions such as hydrolysis, oxidation, deamidation, racemization, and isomerization are reported to contribute towards the chemical instability of the biologics (7). The diverse nature of these physicochemical instabilities of proteins and peptides warrants individualized approach to the development of their formulations. Smart (stimuli-responsive, environmentally-sensitive) polymers offer a drug delivery platform that can be utilized to deliver the proteins at a controlled rate and in a stable and biologically active form (8,9). The uniqueness of smart polymers lies in their nonlinear response triggered by a very small stimulus which causes a significant macroscopic alteration in their structure and properties. They are also referred as 'intelligent polymers' since these materials are able to sense a small change in the

surrounding environment and respond to it in a noticeable manner, and have the ability to regain their original shape/state upon removal of the stimulus. The attractiveness of smart polymer-based delivery systems is enhanced by their features such as reduced dosing frequency, improved safety profile, and therapeutic effectiveness.

1.2. Smart Polymers

Smart or the stimuli sensitive polymers are characterized by an abrupt (and hence, nonlinear) change in their physical properties in response to small environmental triggers. These transitions in smart polymers can be reversible and include changes in their solvent interactions (swelling/shrinking), conductivity, physical state, shape, and solubility, among others. The major advantages of smart polymer-based injectable delivery systems include ease of preparation and administration, prolonged release of incorporated drug, maintenance of desired drug-therapeutic levels with a single dose, site specific/localized delivery, reduced side-effects, increased stability of incorporated drugs during formulation, storage and release, and the most importantly, improved patient compliance and reduction in follow-up care (7,10).

1.3. Classification of Smart Polymers

The types of stimuli that elicit the responses from smart polymers can be broadly categorized as: a) physical, b) chemical and c) biochemical (11). The physical stimuli include temperature, electric/magnetic/electromagnetic fields, presence of mechanical stress or strain, and ultrasound waves as illustrated in figure 1. The chemical stimuli comprise of the shifts in pH, presence of certain chemicals or ions while the biochemical stimuli include presence of biological molecules such as enzymes and ligands, etc. Such triggers could be internal, external, single or combination of two or more stimuli (8,11,12). In the recent past, temperature and phase sensitive polymer-based delivery systems have been the focus of major investigations for protein

therapeutics. The application of smart polymers which respond to light, ultrasound, magnetic and electric fields is rather limited and very few studies have been reported for their use as parenteral protein/peptide delivery systems. Though these delivery systems are useful in controlling the release of incorporated proteins; their non-biodegradable nature, need of surgical procedure for implantation and explantation, possibility of infection, and their cost limit their application.

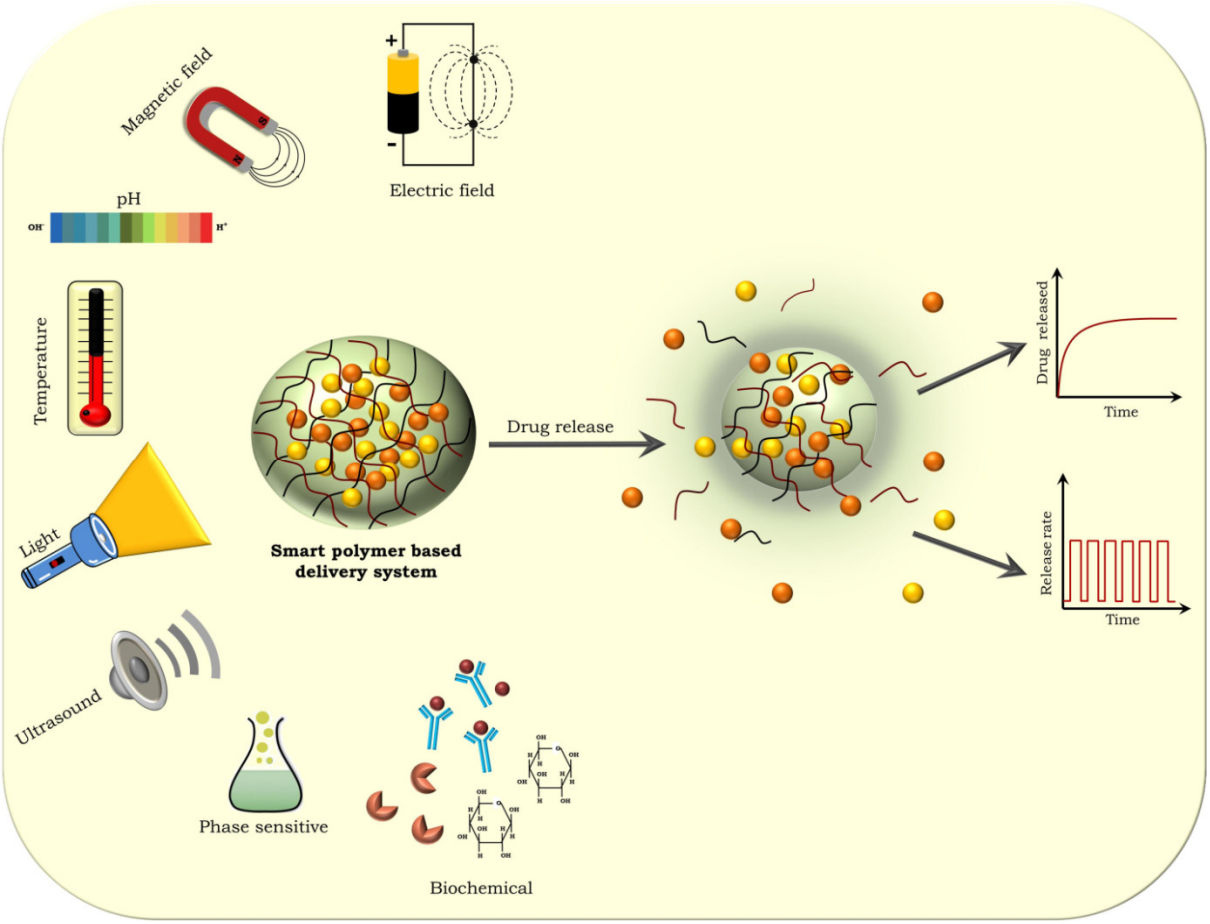

Figure 1. Various stimuli controlling the drug release from smart polymer based delivery systems

1.3.1. Temperature sensitive/thermosensitive polymers

These polymeric delivery systems exhibit sudden changes in their physical state in response to small changes in temperature. The aqueous thermosensitive polymer solutions which exhibit this temperature-dependent reversible sol/gel transitions have been studied and used extensively in past decade for protein delivery due to their unique and fascinating properties such

as ability to undergo sol-gel transitions near body temperature and controlling the release rate of incorporated biologics while maintaining their physicochemical stability and biological activity (14). Depending on their 'critical solution temperature', these polymers exist in two different phases. Jeong and co-workers (15) have defined the **'**sol phase' as a fluid, whereas the 'gel phase' is a non-flowing state that maintains its structural integrity. These polymers are further subdivided into negatively (reverse), positively temperature sensitive, and thermoreversible according to their phase response to the temperature change (16).The aqueous polymer solutions are monophasic systems at certain temperatures and exhibit phase separation above a specific temperature known as Lower Critical Solution Temperature (LCST) (17). At this temperature, the interactions between polymer and water molecules become thermodynamically unfavorable as compared to water/water or polymer/polymer interactions, leading to phase separation due to the dehydration of solvated polymer chains. Some amphiphilic polymers undergo self-assembly, forming micelle like structures, and form gel due to energetically favorable polymer/polymer interactions (18). This phase separation depends on the ratio of hydrophilic to hydrophobic moieties in the polymer, and the polymer/solvent interactions (18,19), and is an energy driven phenomenon which changes depending on the entropy or enthalpy of the system (18,20). The major additives which can affect the phase transition behavior include salts, surfactants, and co-solvents (19). This thermoresponsive nature of polymers offers an attractive and promising strategy which makes these polymers suitable for controlled drug delivery of many proteins and peptides. The commonly used thermosensitive polymers include poly(N-isopropylacrylamide) (poly(NIPAAm), Poly(N,N-diethylacrylamide (PDEAAm), Pluronics®, Tetronics®, and PLGA-PEG-PLGA (ReGel®) (16,21). Thermosensitive polymer-based delivery systems offer advantages such as the avoidance of organic solvents, ease of preparation and administration,

site-specific delivery, ability to deliver both hydrophilic and hydrophobic drugs, reduced systemic toxicity, and sustained drug release (22). Though temperature is one of the easiest external stimuli to apply, some of the challenges associated with these delivery systems include low mechanical strength of the gel leading to disruption of depot with potential of dose dumping, gradual lowering of pH of delivery system microenvironment due to presence of acidic degradation products of the polymers, instability of proteins and peptides in the presence of acidic by-products causing formation of immunogenic moieties, and finally, the biocompatibility of the delivery system in some of the cases. Some analytical techniques which are routinely used for the characterization of thermosensitive polymers are mentioned in table 1.

1.3.2. Phase-sensitive polymers

Formulations containing phase sensitive polymers have been widely studied for controlled delivery of proteins (36). The phase sensitive delivery system usually comprises of a water insoluble polymer dissolved in an organic solvent (phase), and the drug molecules are usually dispersed/dissolved in the organic solvent. The critical constraints for the application of this delivery system include the biodegradability of the polymer and toxicological properties of the employed organic solvent system. Since most of the organic solvents are poorly tolerated at the site of injection, selecting a nontoxic solvent is essential (37). After administration/injection of the delivery system into the body, the organic solvent dissipates into the aqueous phase and water penetrates into the polymer matrix leading to polymer precipitation as a consequence of the phase separation (9,38). Thus, a depot is formed at the site of injection from which incorporated drug can be released slowly for longer durations (38,39). The drug release depends on the rate of phase inversion, as well as the morphology of the depot (40).

Table 1. Polymer properties and their evaluation methods

Polymer Property	:	**Analytical Methods**
Structure and Molecular weight	:	Nuclear Magnetic Resonance (NMR) (23), Fourier Transform Infrared Spectroscopy (FT-IR) (14,24,25), Gel Permeation Chromatography (GPC) (26)
Micelle formation, Critical micelle concentration (CMC), Critical micelle temperature (CMT)	:	Transmission Electron Microscopy (Cryo-TEM) (27), NMR (^{1}H and ^{13}C-NMR) (23), Dynamic Light Scattering (27), Dye solubilization method (23,28), Fluorescence Spectroscopy (Pyrene probe method) (29)
Cloud point	:	Ultraviolet Spectroscopy (UV), Static Light Scattering (30)
Sol gel transition temperature	:	Tube Inversion method (31)
Rheology/ viscosity	:	Rheometer (32)
Hydrogel internal/surface structure	:	Confocal Microscopy (30), Scanning Electron Microscopy (SEM) (30)
Swelling and in vitro hydrolytic degradation of polymer hydrogels	:	GPC (33), Differential Scanning Calorimetry (DSC) (34), FT-IR (34)
In vitro biocompatibility of polymer, and polymer extracts	:	Cell viability assay (31)
In vivo biocompatibility	:	Histological analysis of tissue surface in contact (35)

Various factors such as polymer molecular weight, its composition (hydrophobic/hydrophilic chains), depot size, drug loading affect the drug release. Poly (D, L-lactide) (PLA), poly (D, L-lactide-co-glycolide) (PLGA), poly (ε-caprolactone) are the most widely studied phase-sensitive polymers, while N-methyl-2-pyrrolidone (NMP), dimethyl sulfoxide (DMSO), glycofurol, triacetin, ethyl acetate, benzyl benzoate (BB), benzyl alcohol (BA) are the commonly used solvents (7,41). These delivery systems offer many advantages including high protein loading, simple manufacturing procedures, and inherent extended release

feature. The major problems associated with phase sensitive delivery systems include burst release and instability of incorporated proteins due to the presence of organic solvents. It has been reported that the burst release can be controlled by modulating solvent composition, polymer concentration, whereas protein stability can be improved by adding proteins in the form of dry powders along with stabilizers prior to administration (7). An alternate approach of adding emulsifying agents along with bioactive molecules has also been investigated to improve the drug stability (42).

1.3.3. Chemosensitive polymers

Chemosensitive polymers respond to a chemical stimulus, which includes changes in pH, concentration of ions, enzymes, and ligands. The pH-sensitive polymers are polyelectrolytes containing either acidic (e.g. carboxylic groups), or basic (ammonium groups) on their surface, and are capable of accepting or donating protons in response to external pH change (9,10). Though many pH responsive polymers are used to deliver proteins and peptides, most of these polymers are suitable for oral drug delivery.

The glucose sensitive polymeric delivery system is of particular interest for controlled delivery of insulin. These delivery systems can be based on glucose oxidase (GOD) responsive polymers or simple competitive binding of glucose. In case of GOD responsive insulin delivery, the enzyme (GOD) is usually immobilized on the pH sensitive polymer surface/membrane with insulin. The mechanism of insulin release involves conversion of glucose to glucuronic acid by GOD causing reduction in overall pH of the system, which in turn triggers a change in polymer geometry/swelling leading to the release of adsorbed insulin molecules (43). In this self-regulated insulin delivery system, polycationic, polyanionic or erodible membranes are used which respond differently to glucose oxidase induced change in pH (16). In case of competitive

binding method, glycosylated insulin moieties are adsorbed on a carbohydrate binding polymer such as Concanavalin A (Con A), and compete with incoming glucose molecules for binding. As the glucose concentration increases, it competes with and eventually displaces glycosylated insulin from Con A surface (44). Number of glycosylated insulin derivatives with different binding affinities to Con A have been studied in order to manipulate the release of immobilized insulin in response to different glucose levels (16). Con A cross-linked glucose sensitive sol gel phase reversible delivery systems have also been studied for insulin delivery. Though this type of delivery systems holds a great promise in self-regulating the insulin release, the slow response time, long restoration time after removal of the stimulus, and the immunogenic nature of con A warrant the application of better biocompatible glucose sensitive molecules (16). A glucose responsive boronic acid based system has also been evaluated for controlled release of insulin to overcome the limitations of enzyme based components (45).

1.3.4. Light-sensitive/photosensitive polymers

These polymers display phase transition in response to exposure to light and have attracted great attention since the stimulus can be imposed with extreme accuracy and precision and is easy to manipulate. Light sensitive smart polymers are partly water soluble, biodegradable, and biocompatible (7). These polymers can be sub-classified on the basis of the wavelength of the light that can trigger the phase transition response (16). The hydrogels of the polymers sensitive to light in UV region undergo swelling due to increased osmotic pressure in response to ionization induced by UV radiation, while in absence of this stimulus the gel collapses. Visible light sensitive gels are usually prepared by incorporating photosensitive molecules/chromophores. Therefore, the phase transition behavior of polymer depends on absorbance of light energy by chromophores, which is then dissipated as heat in the

surroundings, which in turn leads to heating/swelling on polymer chains. The process is considered fast as compared to UV sensitive polymer gels (46). Additionally, visible light sensitive polymers are comparatively easy to manipulate, safe and inexpensive as compared to their UV light sensing counterparts (16). Some photo-responsive polymers have been studied for in vitro release of bovine serum albumin (BSA) and lysozyme (7). The limitations of light sensitive polymers include slow response of hydrogels to stimulus (light), and an inconsistent response due to leaching out of non-covalently bound chromophores during swelling or deswelling (16).

1.3.5. Ultrasound sensitive polymers

Considerable research has been done to exploit the use of ultrasound waves for controlled delivery of proteins using both bio-erodible and non-erodible polymer depots. Lavon and Kost (47) have investigated a non-erodible ethylenevinylacetate (EVAc) copolymer matrix to regulate the protein release in response to ultrasound radiation. The mechanism of enhanced protein release includes convection generated by cavitation without alteration in the polymer structure and morphology, and is a useful stimulus for enhancing the drug delivery from diffusion dependent non-bioerodable systems. The precise physical characteristics of polymers that respond to ultrasound is difficult to determine, but the factors that influence the drug release involve ultrasound frequency, structure and size of pores of polymer matrix, polymer degradation rate, and the properties of drug incorporated. While these systems have potential of offering highly tunable protein release, the lack of biocompatible and biodegradable ultrasound sensitive polymers can potentially hamper their widespread applications.

1.3.6. Magnetic field sensitive polymers

This type of delivery system usually consists of a polymer matrix embedding small magnetic beads and the biotherapeutic protein/peptide of interest. Under the influence of external magnetic field, the small magnetic beads oscillate within the matrix, leading to drug release from the matrix. Such release of the incorporated drugs depends on number of factors including magnetic strength, orientation and position of magnetic beads, the amplitude and frequency of external magnetic field, as well as the mechanical properties of the polymer matrix (48). Hsieh et al., (49) reported the protein release from the polymeric delivery system modulated and controlled by application of external oscillating magnetic field. Multiple studies have been reported the use of polymer implants/matrices embedded with magnetic beads to achieve optimum controlled insulin release both in vitro and in vivo (10). Alginate spheres embedded with magnetic beads, and alginate/chitosan microcapsules containing magnetic nanoparticles have been evaluated for controlled delivery of insulin (50,51). While affording a better control over the drug release profile, these delivery systems are often plagued with issues of biocompatibility, need of surgical implantation/explantation, and subsequent potential patient compliance issues.

1.3.7. Electric field sensitive polymers

Electric field responsive/electroresponsive polymers change their physical state in response to small change in electric current. Usually, these polymers contain ionisable groups which are sensitive to pH. The electric current causes increase/decrease in the local pH which leads to disruption of hydrogen bonding between polymer chains, causing polymer swelling/deswelling or degradation and finally drug release. Various cationic, anionic or neutral molecules can be delivered using different amplitudes of current. An electroresponsive polymer

matrix prepared using poly(ethyloxazoline)-poly(methacrylic acid) has been reported for protein delivery (52). In this approach, a pulsatile release of incorporated protein was seen due to the erosion of polymer matrix/hydrogel using a well-regulated electric stimulus. Drug can be incorporated into the electroresponsive polymer and injected subcutaneously to form a depot, followed by application of a low electric current (well-tolerated by human) to release the drug in pulsatile manner. The mechanism of release is reported to be due to the transportation of counter ions and water molecules in the polyelectrolyte gel matrix. These gels of poly(dimethylaminopropylacrylamide) (PDMAPAA) have been evaluated for pulsatile insulin delivery in vivo (53). Another important mechanism of drug release from electro-responsive polymers involves forced convection of drug upon polymer swelling/deswelling (54). The drug release from these types of gels can be changed by modulating the electric current. Responsive hydrogels made up of chondroitin sulfate have been explored for the delivery of various proteins and peptides, where the macromolecules get released upon application of electric field (55). Another type of electric field responsive hydrogel made up of hyaluronic acid shown the release of glutamic acid and tyrosine when the electric current is "switched off." In this type of delivery system, small amino acids can diffuse easily through the pores of the swollen hydrogels in absence of electric current via diffusion, but cannot diffuse out when the gel shrinks under the influence of electric current (55). The major advantage of this type of delivery system is a simple control of drug release in a constant/pulsatile manner by modulating the external electric field. Though it seems to be a promising approach, its in vivo application should be assessed with extreme care. The important constraint that has to be considered while designing this type of delivery system includes the critical selection of electric current which will be sufficient to trigger the drug release without stimulating the nerve endings in the surrounding tissue.

1.3.8. Mechanical stress/strain sensitive polymers

The delivery systems formulated from mechanical stress/strain sensitive polymers respond to the external stress/compressive force and release the incorporated drug from the polymer matrix. After removal of the external force/stress the matrix regains its original shape/volume reducing the release. Though this type of delivery system has a potential to be used for controlled delivery of various small and large molecules, very few finding have been reported regarding the use of mechanical stimuli-sensitive delivery systems. Alginate hydrogel implants were tested for their ability to deliver vascular endothelial growth factor (VEGF) in a pulsatile manner upon mechanical stimulation both in vitro and in vivo (56).

1.3.9. Antigen-responsive polymers

This type of delivery system is fabricated by grafting specific antigen and corresponding antibody to the polymer chains. The antibody-antigen binding leads to the crosslinking between the polymer chains forming a three dimensional gel network. The release of incorporated protein is based on the competitive binding between the polymer-bound and free antigen present in the release medium, causing changes in the hydrogel shape, size, or crosslinking. The polyacrylamide based semi interpenetrating network (IPN) hydrogels have been studied for the pulsatile delivery of a model protein, hemoglobin (57). The most important property of this IPN is that the hydrogel shows a shape-memory behavior, which is solely dependent on the concentration of free antigen, and consequently the hydrogel swelling and protein release. Therefore, the protein release can be controlled by a change in antigen concentration (57).

1.3.10. Multiple-stimuli responsive polymers

While a single stimulus would restrict the practical application of smart polymers, multi-stimuli responsive polymer-based drug delivery platforms are receiving heightened interest as

controlled delivery systems (58), since these multiple responsive polymers establish a better control over the drug release profile and duration. Al-Tahami and Singh (7) have summarized some recent patents describing the use of multiple-stimuli sensitive polymers for the delivery of proteins for prolonged period. A pH/temperature-sensitive injectable pentablock copolymer hydrogel has already been used for insulin delivery in vitro and in vivo (59). This dual responsive pH/ temperature sensitive copolymers overcome the limitations of both temperature and pH sensitive polymers, like clogging of needle during injection, reduction in the development of acidic conditions due to degradation of polymer chains etc. Additionally, cationic polymer chains can form reversible complex with anionic proteins/peptide at physiological pH by ionic interactions leading to sustained release, and also help in reducing initial burst release (60). Even though these multiple stimuli sensitive systems have certain advantages over single stimulus, there complicated structure, and different degradation rates make the formulation optimization difficult. The number of factors to be fine-tuned while developing such delivery systems include injectability, gel/depot strength after incorporation of drugs, interaction with incorporated proteins/peptides, interaction with surrounding tissues, and finally not the least, biodegradability, and biocompatibility.

1.4. Biocompatibility of the Delivery Systems

In the development of increasing number of new polymers for controlled delivery systems, 'biocompatibility' is the key prerequisite they have to fulfill for their safe use. Local skin/tissue compatibility is an essential parameter in their in vivo application. Non-biodegradable implantable polymeric materials need surgical procedures for their implantation and explantation, and extended exposure to these polymers may cause chronic inflammation of the surrounding tissue, as well as tissue damage. The foreign body reaction caused by implants

presents a great risk and inconvenience to the patients and is one of the most important reasons for their low patient acceptance. Onuki et al., (61) has described various types of foreign body reactions towards the implants and ways to overcome them. Since biocompatibility of a delivery system is an essential feature to be considered during formulation, the correct choice of a biocompatible material can minimize the untoward body reactions, thereby improving the durability of the formulation. International Standard ISO-10993 has prepared a guideline for testing the biocompatible nature of materials for medical applications using both direct and indirect contact approaches (62).

Biodegradable polylactic acid (PLA), and PEG based polymers and copolymers are of great technological interest, and are commonly used in many biomedical devices due to their biocompatible nature. PLA degrades by non-enzymatic hydrolysis of ester bonds, and the degradation products are further transformed into non-toxic moieties which are easily eliminated by the body. Though the polymer is biodegradable, it does not mean that it is non-toxic and biocompatible. There are number of in vitro and in vivo tests used to determine the biocompatibility of these polymers. The commonly used methods for determination of in vitro biocompatibility include, a cell viability assay, while for in vivo biocompatibility evaluation, tissue inflammatory reaction upon administration of the polymeric material is visualized (14,31,35,63,64). The in vitro cytotoxicity tests such as agar diffusion test, filter test, and MTT assay are very effective methods for biocompatibility evaluation; however, an MTT assay is much more sensitive than other tests. MTT (3-(4,5-dimethylthiazol-2-yl)-2,5-diphenyltetrazolium bromide) cell viability assay is the most popular and widely used assay for in vitro biocompatibility testing for many years. Ignatius and Claes (65) have explained a procedure to determine the in vitro cytotoxicity of polymers and their extracts or degradation

products. For this, the polymers are extracted in PBS by incubating at 37 and 70°C. Since degradation rate of polymers is greater at higher temperatures, the extracts prepared at 70°C mimics the long-term effects of the delivery system. To exclude the effect of pH on the cell viability, pH neutralized extracts are usually prepared and are incubated with cells for a specific duration. After incubation, the cell viability is assessed by mitochondrial succinate dehydrogenase activity using MTT. Since only live cells can metabolize MTT into purple formazan crystals, the results are indirectly correlated with the number of viable cells after polymer treatment. Though this is widely accepted method for cytotoxicity evaluation, it does not reflect the actual effect of reduced pH due to polymer degradation. The reduced pH may cause several acute or chronic inflammatory reactions in the surround tissue after implantation, and hence, it is very essential to evaluate the biocompatibility of the delivery system in vivo.

A series of inflammatory events that occur after implantation of PLA and PLGA poly (DL, lactide-co-glycolide) polymeric delivery systems in vivo have been described by Shive and Anderson (66). Though degradation rate varies according to the nature of the polymeric delivery system, the presence of depot initiates a series of inflammatory events in the surrounding tissue after injection, and the severity of the foreign body reaction determines the biocompatibility of the polymer. For an ideal delivery system, the polymer should cause minimal inflammation for short duration, and tissue damage should be reversible without formation of any scar tissue or necrosis.

1.5. Various Stages of Drug Release from Controlled Delivery System

An important factor that has to be studied during development of a controlled delivery system is the different stages of drug release. Most of the polymeric controlled delivery systems usually follow a triphasic or sigmoidal release pattern (67-73), which can be divided into

following stages: a) fast initial burst release as a result of quick diffusion of drug molecules located at the surface, b) slow release for days/weeks where drug is released in controlled fashion, c) rapid release/secondary burst release due to polymer degradation, and sometimes a fourth phase which is characterized by a slow release observed after secondary burst, usually as a result of depletion of drug content. This sigmoidal release pattern is not desirable in most of the situations except in case of vaccine immunizations (74), where the triphasic release pattern mimics the traditional boosting regimes.

The release pattern of controlled delivery system usually comprises of a characteristic phenomenon, called as "initial burst release," which usually reduces the effective lifetime of the delivery system. It has been reported that, in case of many controlled release formulations, immediately upon placement in the release medium, an initial large bolus of drug is released before the actual release starts (75,76). This is a short-term phenomenon compared to the entire release process, but affects the overall release duration, therapeutic efficacy and safety profile of the incorporated drug molecules. Since the burst occurs in a very short period as compared to the entire release process, it was not explored in detail earlier, and never considered as an essential part during mathematical modeling of the release. But, recently this phenomenon has been noticed and widely explored. Researchers are trying to understand the mechanisms of burst release and ways to prevent it using various approaches (75). There are number of publications in which this key issue is addressed (69,77-80). Though the burst release is favorable in some cases (81), it is considered as an undesirable effect, and has to be taken into consideration while designing a controlled delivery system.

Studies reported that the initial burst release occurs due to the presence of drug molecules located close to the surface of the delivery system. For example, in case of insulin-loaded

microspheres, initial burst release was noticed due to the presence of insulin molecules in vicinity of microsphere surface (3,82), and it eventually reduced the overall release duration from microspheres. Strategies tried to lower the initial burst release include, non-uniform drug loading in the polymer matrices (83), changing the hydrophilic or hydrophobic content of the polymeric delivery system (35,84), increasing the size, or reducing the solubility of the drug molecule (2) to name a few. However, sometimes these additional steps involved in the formulation process could potentially result into reduction in drug loading and might increase the overall cost of the formulation.

1.6. Delivery of Proteins and Peptides

Most of the protein/peptide drugs are administered via invasive routes and need multiple injections. Though the conventional routes have been tried for the delivery of proteins and peptides their delivery is still difficult and challenging. Various strategies have been developed to overcome the barriers for protein delivery via oral route, but their fragile nature, delicate structure and degradation by various enzymes in the gastrointestinal tract limits the application of oral route. Other routes such as buccal, nasal, rectal, vaginal, ocular, and transdermal have also been tried for delivery of proteins with limited success (85). The primary reason is their low bioavailability, mostly due to the poor permeability through the mucosa and skin tissue (36). Therefore, parenteral route is the most preferred route for delivery of proteins and peptides.

Thus, before even it can be considered as a candidate for treatment, its complex biochemical and biological properties should be taken into consideration. Proteins usually comprise of higher order of structures to elicit their biological response, and any alteration in their primary/secondary/tertiary or quaternary structure greatly influences their activity. The structure of protein is divided into primary (amino acids sequence), secondary (α-helix, β-sheets,

β-turns, random coils), tertiary (folding into three dimensional structure), and quaternary (spatial arrangement of its subunits) structure (86). Due to the relatively poor stability, the formulation and storage conditions greatly hamper their higher order structures. Disruption of these structures leads to the loss of their biological activity, and sometimes increases immunogenic potential. Thus, is very crucial to maintain the highly organized structure of protein for proper activity and functionality (87). The partially unfolded protein undergoes precipitation/aggregation reactions and is able to provoke immune response. It also increases its rate of clearance from the body leading to reduced efficacy, and subsequently repeated administration becomes inevitable (88).

These problems related to protein instabilities can be divided into two major categories namely; a) instabilities during formulation, and b) during storage and administration (89). It has been reported that the harsh manufacturing conditions, use of organic solvents, high temperatures, agitation, presence of detergents, and hydrophobic surfaces could risk the chemical and structural integrity of proteins (44). Even after administration, proteins get hydrated, remain hydrated, and get exposed to various physiological conditions (pH, temperature, enzymes) for long duration. This type of prolonged exposure to various stress conditions can adversely affect their effective half-life in body. Some of the degradation reactions proteins can undergo include deamidation (asparagine and glutamine residues), peptide bond hydrolysis (aspartic residues), β-elimination and disulphide bond reshuffling (cysteine residues), and oxidation (cysteine and methionine residues) (90). Protein aggregation is an important issue usually encountered during almost all stages during formulation and development of proteins and peptides. It is reported that there are more than 20 diseases caused as a result of partial/abnormal protein aggregation (91). The key factors contributing towards protein aggregation include, moisture (92-94), temperature

(95,96), pH (96), shaking (97), presence of hydrophobic surfaces (98), organic solvents (99), and free-drying/ freeze-thawing procedures (100,101).

Therefore, to get a clinically viable formulation, researchers have tried to overcome the difficulties with protein degradation and aggregation in the delivery systems, which would finally result into a product having an intact structural integrity and biological activity of the incorporated protein (90). The primary focus of protein formulation development should be not only minimizing the degradation reactions, but also avoiding the causes of these reactions. One way to overcome these difficulties associated with protein stability is to add stabilizers (102), polyethylene glycol (103,104), non-ionic surfactants (105), inorganic bases (magnesium hydroxide) (106,107), or divalent ions (zinc) (108). Another way is to decrease the formation of harmful degradation products of controlled release polymeric delivery systems which is one of the crucial factors affecting protein degradation/aggregation (90). The third approach would be 'PEGylation', i.e. modifying the protein by covalently conjugating with nontoxic and non-immunogenic polyethylene glycol (PEG), which would help to improve the protein stability and retention time in blood as well as reduces the proteolytic degradation (109,110).

1.7. Techniques of Protein Stability Evaluation

Some of techniques used to monitor protein/peptide stability include calorimetry (Differential Scanning Calorimetry), chromatography (High Performance Liquid Chromatography, Size Exclusion Chromatography), gel electrophoresis (Native/SDS-Polyacrylamide Gel Electrophoresis), mass spectroscopy (Matrix Assisted Laser Ionization/Desorption-Time of Flight), rheology and microscopy (111). These methods mainly focus on physicochemical characterization, such as presence of secondary structural components of protein (α helix, β sheets, and random coils), association state, folding/unfolding, molecular

weight and structural integrity. Additionally, the biological activity of a protein can be evaluated directly using various protein-specific bioassay procedures or indirectly by determining its pharmacodynamic activity (2-4,31,35,64). Some of the commonly used techniques are discussed below.

1.7.1. Circular dichroism spectroscopy (CD)

Circular dichroism spectroscopy is one of the most widely used techniques for structural determination of protein. 'Circular dichroism' is defined as "the unequal absorption of left-handed and right-handed circularly polarized light" (112). The clockwise/counter-clockwise rotation of the wave helps in determining the structure of a molecule (112). This effect usually takes place when a chromophore itself is optically active (chiral), covalently linked to a chiral molecule, or is placed in an asymmetric environment (113). The far UV region in CD spectra gives an idea about the structure of the backbone of the protein, and can be directly correlated to the relative composition, and changes in secondary structure of protein (2-4,31,35,64). At the same time, the near UV CD spectra can be used to estimate the presence of aromatic residues present on the surface of a protein and further can help in identifying its association state. A characteristic CD spectrum is usually observed depending on the alignment of the chromophores in the polypeptide backbone. The negative bands at 208 and 222 nm, and a positive band at 193 nm arise specifically due to the presence of α-helical structure of protein, while anti-parallel β-sheets show a negative band at 218 nm and a positive band at 195 nm (114). The presence of random coils shows a positive band at 212 nm, and a negative band around 195 nm (115). Thus, every protein has specific percentage of α-helix, β-sheet, or random coils content, and therefore it is a widely accepted method for determination of any change in the secondary structure of protein under various stress conditions during formulation or storage. For tertiary structure

analysis, near-UV CD spectra provide the useful information, and arise from the presence of aromatic residues like tryptophan, tyrosine and phenylalanine on protein surface (116). Thus, even if the protein has well defined secondary structure but showing inadequate near-UV CD signal indicates that it is not folded correctly. Thus, a well-defined band in near UV region is also considered as a good indication that the protein in folded in a well-defined structure (115).

1.7.2. Differential scanning calorimetry (DSC)

DSC has a long history in understanding protein energetics, and is one of the important techniques in evaluation of folded/unfolded state of proteins with respect to change in temperature. The primary sequence of amino acids is a driving force for interactions between amino acids, between protein and solvent, and is mainly governed by thermodynamics, and there is a delicate balance between the thermodynamic parameters and protein folding. The protein structure in folded state is usually stabilized by ~80-120 kJ/mol (20-30 kcal/mol) (117), and DSC aids to determine the heat capacity of protein solution (C_p) as a function of temperature. The melting temperature (T_m), also known as midpoint temperature, is also a good indicator of folding/unfolding state of protein. Assuming a two-state transition, T_m is defined as a temperature at which the half of the protein molecule is in unfolded state (118). Thus, during denaturation of protein in response to temperature, the transition shows a sharp endothermic peak with T_m at the center and maximum in C_p. The area under the transition peak gives the information about the transition enthalpy (ΔH), and is correlated with the content of secondary structure of a protein. Thus, T_m indicates the thermostability of a protein and it is observed that, higher is the T_m; more thermodynamically stable is the protein. Therefore, proteins with higher T_m are less prone to unfolding/denaturation (118).

1.7.3. High performance liquid chromatography (HPLC)

Reversed-phase high performance liquid chromatography (RP-HPLC) is a well-established tool used in the analysis of proteins and peptides and their degradation/aggregation products. It separates proteins/peptides depending on their affinities towards the stationary phase and mobile phase. The RP-HPLC experimental system for proteins/peptides usually consists of an *n*-alkylsilica-based sorbent and an organic solvent such as acetonitrile containing an ionic modifier (e.g. trifluoroacetic acid, TFA) (119). This is a widely used technique for protein and peptide separation since it separates the complex mixtures easily at picomolar/femtomolar concentrations and can be collected for further characterization. It is a versatile and reliable technique used for detection of both covalent and non-covalent aggregates as opposed to Size Exclusion Chromatography (SEC-HPLC) which detects the presence of aggregates based on size (111).

1.7.4. Polyacrylamide gel electrophoresis (PAGE) and sodium dodecyl sulfate-PAGE (SDS-PAGE)

One dimensional polyacrylamide gel electrophoresis (PAGE) is another simple method which provides information about the molecular size, purity, and presence of protein aggregates. In native PAGE, the rate of protein migration depends on the size, charge, shape of the molecule, and pore size of the gel matrix, under the influence of an external electrical field. Gel electrophoresis under denaturing conditions (in the presence of SDS, without a reducing agent such as 2-mercaptoethanol), separates the protein only depending on its size (120), and does not dissociate the covalent disulfide bonds, and therefore can be used to distinguish between the covalent/non-covalent protein aggregates (121).

1.7.5. Matrix assisted laser desorption ionization time-of-flight mass spectrometry (MALDI-TOF MS)

MALDI-TOF MS, an analytical method, has been first described in 1988 (122), which essentially estimates the molecular weight of proteins accurately up to 100 kDa from picomolar amount of sample (123). This technique can be used to identify proteins and their degradation products without prior chromatographic separation, helps to determine higher orders protein structures, is highly sensitive, and requires minimal sample for analysis (124,125). The important constituent of this analysis is matrix molecules of organic nature. The role of matrix material is crucial and aids in co-crystallization of the analyte, absorbs energy from the strong laser pulse thereby protecting analyte, and expels analyte into gas phase, and helps in ionization of the analyte. The matrices are usually aromatic compounds containing carboxylic acid functional groups such as several cinnamic acid derivatives, sinapinic acids and 2,5-dihydroxybenzoic acid (122).

1.8. Diabetes Mellitus and Insulin

Diabetes mellitus is cited as one of the most challenging health problems in the 21st century. More than four million patients in the United States use insulin for the treatment of diabetes mellitus (126). World Health Organization defines diabetes mellitus as “A metabolic disorder of multiple etiologies characterized by chronic hyperglycemia with disturbances of carbohydrate, fat and protein metabolism resulting from defects in insulin secretion, insulin action or both” (127). It is a growing health concern around the globe in spite of the employment of newer treatment regimes. It is characterized by absolute or relative (type 1 or 2) deficiency in insulin secretion/response resulting in hyperglycemia. Insulin, a polypeptide hormone, decreases the level of glucose in blood and regulates the metabolism of glucose, fat and proteins, thus

helping to achieve proper glycemic control. Despite the fact that insulin is discovered almost 90 years ago, clinicians have been still challenged to achieve euglycemia in their patients using injectable insulin formulations.

Human insulin (~6000 Da) consists of 51 amino acid residues divided into two chains; chain A contains 21 amino acids, while chain B has 30 amino acids (128). Though there is species variation in the primary structure of insulin, the folding of two chains and its three-dimensional conformation is reported to be same. The A chain forms two anti-parallel α helixes, and an additional α-helix, a turn and a β-sheet is formed by B chain (128). The isoelectric point (pI) of insulin is ~5.4 (129), and therefore it carries a positive charge below pI, while, above the pI it carries net negative charge (130). The chemical stability of insulin is a function of pH, and around pH 4 it forms covalent dimers, while undergoes minimum hydrolytic degradation near pH 6.5 (131). Depending on the concentration and pH, insulin forms dimers and in presence of divalent cations it self-associates to form hexamers. The self-association is an important phenomenon since the hexameric state provides insulin stability. It is known that the metal bound insulin hexamers usually exist in three different states, namely T_6, T_3R_3, and R_6 conformations. In solution state these states are in equilibrium and can be shifted from one another in the presence of some additives such are phenols, inorganic anions etc. (132). It has been reported that insulin monomers associate with zinc by co-ordinate bonds, and this association is very important for storage, and secretion of insulin (133). The zinc coordinated hexamer is a physiological form of insulin, and is stored in the body in this form in storage granules (134). Increasing the number of zinc ions (more than 4/hexamer) adversely affects insulin stability by causing peptide link cleavage (131), and therefore, the zinc/insulin hexamer ratio during formulation should be closely monitored. The availability of insulin molecules in the

body depends on the dissociation of its hexameric state, and its rate of diffusion from the site of administration into the blood. Thus, its availability can be varied by changing its solubility and in turn association state.

In healthy individuals, physiological insulin secretion has two phases; basal secretion, wherein the pancreas secrete a constant low level of insulin into the circulation throughout the day, and stimulated secretion, where the pancreas respond to food intake by secreting large bolus of insulin to maintain normoglycemia (135). The basal insulin which is secreted at a rate of 0.5-1U/h throughout the day and between meals, accounts for ~50% of the total daily output, and plays a major role in preventing long-term diabetic complications (136,137). Basal insulin secretion does not shut-off hepatic glucose production and provides adequate substrate for cerebral glucose metabolism (138). In a normal non-diabetic individual the stimulated insulin levels up to 60-80 μU/ml can be observed within few minutes after ingestion of a meal. This increased insulin secretion leads to disposition of glucose and various nutrients mainly into muscle and to a slight extent into liver. Therefore, type 1 diabetic patients with absolute deficiency of insulin completely rely on basal-bolus insulin regimen for maintaining their blood glucose levels. This regimen attempts to replicate the normal insulin secretion profile and comprises of multiple injections of rapid acting insulin before each meal to mimic prandial insulin secretion, and an additional injection of intermediate/long acting insulin before bedtime to mimic basal insulin secretion. This repeated insulin administration gives rise to numerous complications and the pain from multiple daily injections adversely affects the quality of life of patients. Therefore, from a patient compliance perspective, to avoid the discomfort and inconvenience associated with multiple daily injections, alternate administration routes have been explored.

Various inhalation insulin preparations (Exubera®, AERx® insulin) (139,140), nasal sprays (Nasulin™) (141), and oral insulin spray (Oralin™) (142) have been used to relieve pain and discomfort experienced by patients due to repeated injections. However, due to the absence of the controlled delivery feature, these systems do not offer a prolonged insulin release. Insulin pumps are extensively tried due to their ability to offer improved glycemic control as compared to daily injections (143). Almost every feasible route for insulin administration has been tested with limited success and the subcutaneous route still remains the principal route of administration. The two long acting basal insulin analogues, Lantus® (Insulin Glargine), and Levemir® (Insulin detemir) have become available in recent years to achieve adequate glycemic control (144-146). Though these analogues are known to achieve good glycemic control, and lower the incidence of fasting hypoglycemia efficiently (147); they do not completely eliminate the risk of nocturnal/fasting hypoglycemia (148). In view of these shortcomings, attempt have been made to fabricate an ideal basal insulin therapy, which will essentially provide a constant, peak-free, prolonged and continuous insulin supply after subcutaneous administration, eliminating the risk of fasting hypoglycemia.

1.9. Controlled Delivery of Insulin

Controlled delivery of insulin using in situ gel forming delivery systems can be an effective strategy which could provide continuous low basal insulin level, and partly alleviate the pain felt by multiple injections (35). Such insulin delivery is also critical in reducing the long-term micro and macro vascular complications of diabetes (3). Several researchers have focused on the development of injectable thermosensitive copolymeric delivery systems for the delivery of insulin at a controlled rate and in response to the physiological need (35,59,149). These delivery systems with varying hydrophilic/hydrophobic content can alter the rate of insulin

release. The major advantage of these delivery systems is absence of organic phase which hampers the delicate protein structure (4,149-151). Additionally, the biodegradable and biocompatible nature of the copolymers, as well as simplicity of administration of the delivery system makes them attractive candidates for sustained drug delivery. Some of the biodegradable thermosensitive copolymers investigated include, poly(D,L-lactide-co-glycolide)-poly(ethylene glycol)- poly(D,L-lactide-co-glycolide) PLGA-PEG-PLGA (149), a mixture of pH/temperature-sensitive poly(β-amino ester)-poly(ε-caprolactone)-poly(ethylene glycol)-poly(ε-caprolactone)-poly(β-amino ester), PAE-PCL-PEG-PCL-PAE pentablock copolymer (150), chitosan/glycerophosphate complex (151). Even though these polymeric systems have many advantages, the issues such as high initial burst release, relatively short release duration of the incorporated drug, and incomplete release make their development difficult. The high initial burst release of insulin often leads to hypoglycemia and is considered as the major barrier in achieving good glycemic control. Hence the delivery system which shows a relatively flat/peak-less time action profile could limit the peak induced hypoglycemia. Some of the approaches that have been tried in order to reduce the initial burst of insulin, to control the release duration, and stabilization of insulin are PEGylation of insulin, addition of zinc salts, ethanol and/or glycerol, hydroxypropyl-β-cyclodextrins (HP-β-CD), sugars, salts, cationic polyelectrolyte and nonionic and ionic surfactants to insulin (3,152-159). A combination approach of two or more delivery systems such as nanoparticle/microsphere or microsphere/hydrogel has also been tried to control and prolong the release behavior of various proteins (160-163).

1.10. Chitosan as Protein Stabilizer

Chitosan is a linear polysaccharide, made up of randomly distributed α-(1-4)-linked D-glucosamine (deacetylated unit) and N-acetyl-D-glucosamine (acetylated unit) (164). The

structure of chitosan is presented in figure 2. Chitosan is obtained by partial deacetylation of chitin under alkaline conditions (164,165). It is reported as a biocompatible and biodegradable positively charged polymer with minimum immunogenic potential and also possesses low cytotoxicity (166).

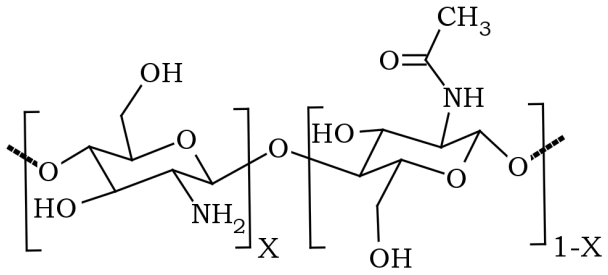

Figure 2. Chemical structure of chitosan

It is a well-known gene delivery vector and has been reported as a safe and promising material for controlled drug delivery (164,166,167). It has been widely used for encapsulating number of drugs and biological substances by simple and nontoxic procedures (168-171). It has been reported that chitosan interacts with peptides/proteins and imparts a stabilizing effect on the proteins (168,172-174). The pH and temperature of both chitosan and peptide are important factors need to be considered while preparing the chitosan-protein drug delivery systems (175).

1.10.1. Chitosan based polyelectrolyte complexes for drug delivery

When the oppositely charged polymers/polyelectrolytes are mixed together in solution, they self-assemble due to the presence of electrostatic interactions to form a 'polyelectrolyte complex.' According to the IUPAC Compendium of Chemical Terminology 2007, the polyelectrolyte complex is "Neutral polymer-polymer complex composed of macromolecules carrying charges of opposite sign causing the macromolecules to be bound together by electrostatic interactions." Polyelectrolyte complexes have been used as non-viral gene carriers (176-181), drug carriers (182-184), bioseparation (185), and multilayer/films (186-189).

Chitosan has an ability to form specific complexes with polyanions of various types which involve electrostatic and dipole-dipole interactions, hydrogen and hydrophobic bonds (190). The positively charged amino groups on chitosan (C2 position in glucopyranose unit) can interact with negatively charged groups (carboxylic acids) on polyanions electrostatically, to form polyelectrolyte complexes (191). The pka value of chitosan is reported to be ~6.3-6.5, thus, in acidic pH most of the amino groups on chitosan are in protonated form and hence can form complexes with various polyanions near this pH range (192,193). It has been reported that the polyelectrolyte complex formation depends on number of factors such as the degree of ionization of cationic and anionic polymers, in turn, pH and ionic strength of the solutions, the concentration of the polyelectrolytes, their mixing ratio, nature of ionic groups and their charge density, temperature, as well as polymer chain flexibility (191).

1.10.2. Chitosan for insulin delivery

Chitosan and its derivatives have been widely used for delivery of insulin via various routes including oral (194-199), nasal (200-203), and buccal (204). Chitosan based injectable microparticles have also been investigated for the delivery of insulin (3,172,205,206). In case of chitosan-insulin nanoparticles, the formulation pH and insulin loading played important role (207), and it has been reported that, pH had the major impact on the conformational as well as chemical stability of incorporated insulin (131).

1.11. Statement of Problem

The objective of the proposed research was to develop a controlled release polymeric formulation based on chitosan-zinc-insulin complex incorporated into thermosensitive polymer, which can deliver insulin continuously over three months to meet basal insulin requirement after a single subcutaneous injection. The delivery system is also expected to eliminate the initial burst

release of insulin, and preserve its stability during release and storage. Additionally, the delivery system should be biodegradable and biocompatible in vitro and in vivo.

To achieve this goal we took a dual approach:

- We utilized the self-association property of insulin to form hexamers in the presence of Zn^{+2}. Hexameric insulin is less soluble and highly stable.
- The second approach is to restrict diffusion of a large chitosan-zinc-insulin complex through the inner gel passage/pathway of the polymer gel matrix.

Chitosan has abundant positive charge due to the presence of primary amine groups on its surface, and insulin carries negative charge at pH > pI (5.4). Therefore, complexes can be formed under optimized conditions by electrostatic interactions between positively charged chitosan and negatively charged insulin. By incorporating the chitosan-zinc-insulin complex in the thermosensitive polymeric delivery system, the rate of insulin release can be controlled. We hypothesize that the novel approach of utilizing the combination of distinctive properties of insulin such as self-association in presence of zinc, their ability to interact electrostatically with chitosan and subsequent addition of the chitosan-zinc-insulin complex into thermosensitive polymer solution would circumvent the problems associated with insulin burst release and stability, while providing controlled release of insulin at basal level over long duration. The chitosan-zinc-insulin complexes were designed characterized by ionic interactions between chitosan and insulin, and the schematic is presented in figure 3.

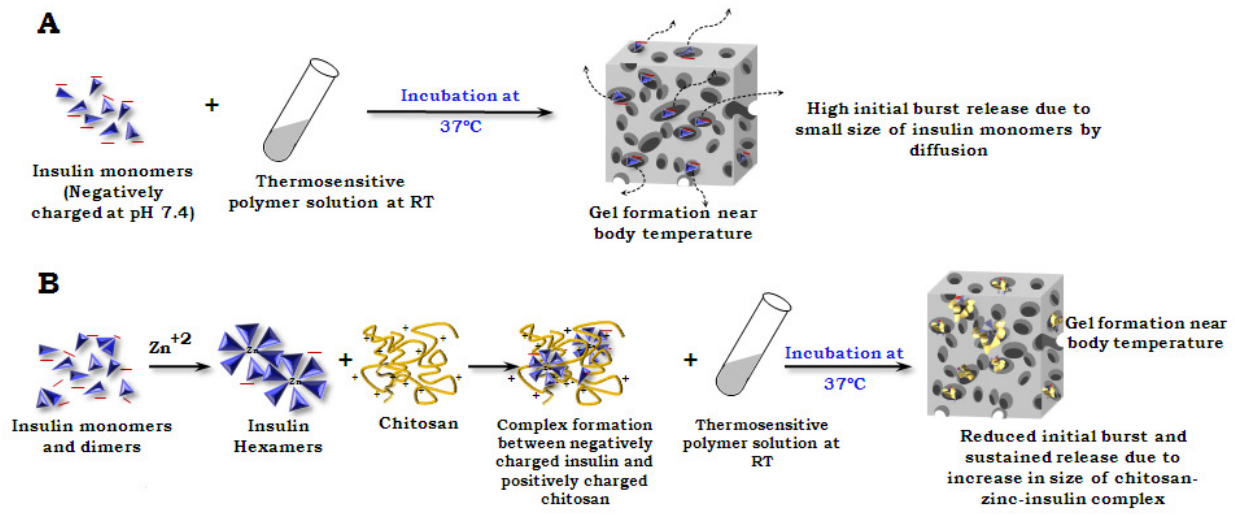

Figure 3. Schematic representation comparing the release behavior of (A) insulin loaded, and (B) chitosan-zinc-insulin complex loaded thermosensitive polymeric delivery system

We propose the following specific aims to test our hypothesis and to accomplish the above stated goals:

- **Synthesis and characterization of triblock thermosensitive copolymer, and study of hydrolytic degradation of polymer in presence of various molecules**
  - ♦ To synthesize thermosensitive Polylactic acid-Polyethylene glycol-Polylactic acid (PLA-PEG-PLA) triblock copolymer with 1500-1500-1500, and 1600-1500-1600 chain lengths (4500, and 4700 Da, respectively).
  - ♦ To characterize the synthesized copolymers for structure, molecular weight and polydispersity using Nuclear Magnetic Resonance (NMR), and Gel Permeation Chromatography (GPC), and tube inversion method.
  - ♦ To study the hydrolytic degradation of copolymer A and B using Nuclear Magnetic Resonance (NMR), and Gel Permeation Chromatography (GPC), and Scanning Electron Microscopy (SEM).

- To study the effect of various model molecules on hydrolytic degradation of copolymer A, and to study in vitro release of incorporated molecules from the delivery systems.

• Study the effect of various formulation parameters on release profile of insulin

- To study the effect of polymer concentration, insulin loading, and zinc addition on in vitro release of insulin from the thermosensitive polymeric delivery system.
- To determine the stability of insulin released in vitro.

• Study the effect of addition of chitosan on insulin release and stability

- To evaluate the effect of addition of chitosan on stability of insulin by UV, fluorescence and CD spectroscopy, and to prepare the delivery system and investigate the effect of chitosan on the in vitro release of insulin from the thermosensitive polymeric delivery systems.
- To optimize the delivery system to achieve a controlled, and predictable release of insulin for approximately three months at basal level.
- To investigate the stability of insulin released from the delivery systems in vitro.
- To investigate the stability of insulin during storage at 37°C and 4°C, as well as to investigate the stability of insulin in the polymeric delivery systems during in vitro release.

The instrumental techniques used for stability analysis include:

- Circular Dichroism (CD), Differential Scanning Calorimetry (DSC), Native Polyacrylamide Gel Electrophoresis (PAGE)/ Sodium Dodecyl Sulfate-PAGE (SDS-PAGE), Matrix Assisted Laser Desorption/Ionization-Time of Flight (MALDI-TOF) Mass Spectroscopy, and High Performance Liquid Chromatography (HPLC).

- **Study in vivo release, and bioactivity of insulin released from the delivery systems, and the biocompatibility of the delivery systems in vitro and in vivo**
    - ♦ To study the in vivo absorption, release profile and bioactivity of insulin released from thermosensitive gel depots in streptozotocin induced diabetic rat model.
    - ♦ To study the in vitro biocompatibility by MTT (3-(4,5-dimethylthiazol-2-yl)-2,5-diphenyltetrazolium bromide) cell viability assay.
    - ♦ To study the in vivo biocompatibility by histological analysis of tissue-delivery system interface using light microscopy.
    - ♦ To study the immunogenic potential of insulin released in vivo using an indirect ELISA.

Accomplishing the above specific aims will result in a biodegradable polymeric delivery system which can deliver adequate basal insulin continuously over three months after a single subcutaneous injection with minimal initial burst release, and could partially relieve patients from multiple daily injections, thus improving patient compliance. Figure 4 is a pictorial representation depicting the events following subcutaneous administration of chitosan-zinc-insulin complex loaded thermosensitive delivery system in vivo. It included the formation of depot at the site of injection, polymer degradation and dissociation of the chitosan-zinc-insulin complex into insulin monomers, and finally absorption of insulin monomers into systemic circulation to elicit the pharmacological response.

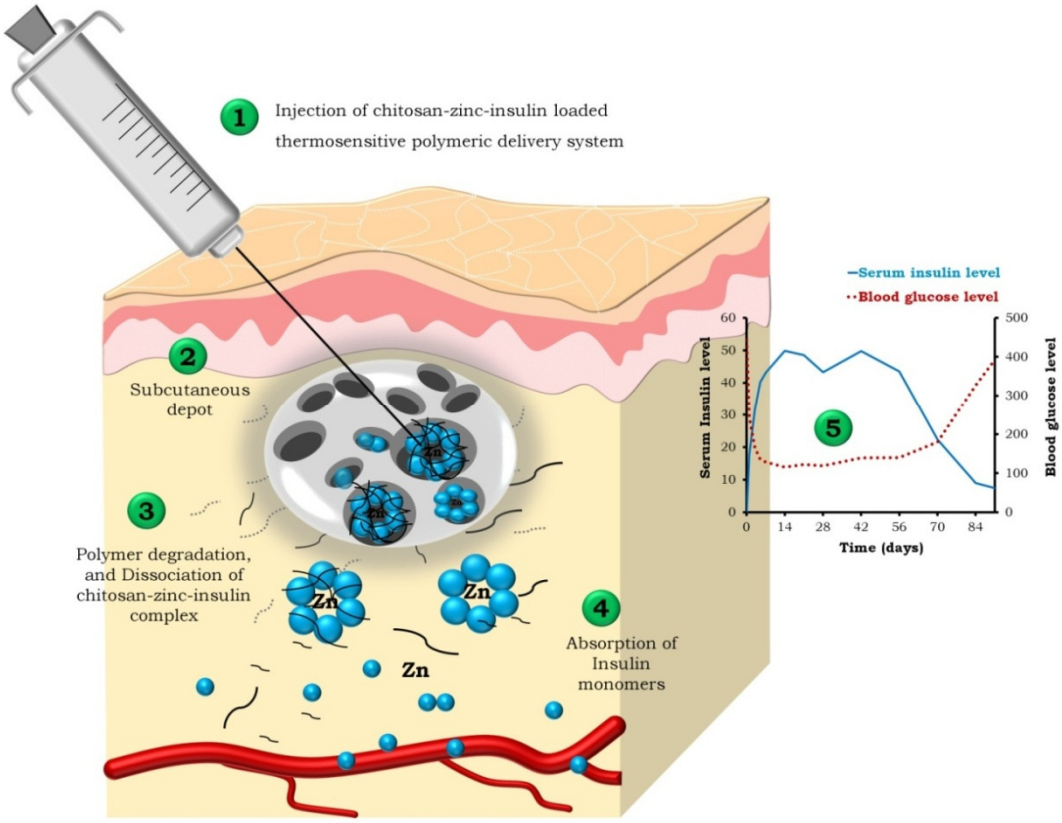

Figure 4. The events following subcutaneous administration of chitosan-zinc-insulin complex loaded thermosensitive delivery system in vivo

2. MATERIALS AND METHODS

2.1. Materials

The list of materials used in this study is presented in table 2.

Table 2. Materials used and their source

Materials	:	Source and location
Human recombinant insulin (Incelligent SG)	:	Millipore Corporation, (GA, USA)
Polyelthylene glycol (1500 Da)	:	Sigma Aldrich Co., (MO, USA)
D,L-lactide	:	Alfa Aesar, (MA, USA)
Stannous octoate	:	Pfaltz and Bauer Inc., (CT, USA)
MicroBCA protein assay kit	:	Pierce Biotechnology Inc., (IL, USA)
MTT	:	Sigma Aldrich Co., (MO, USA)
Dimethyl sufoxide	:	Calbiochem, (USA)
Nembutal (Pentobarbital Sodium)	:	Lundbeck, (IL, USA)
10% Neutral buffered formalin	:	Richard-Allan Scientific, (MI, USA)
Glucometer	:	Bayer Contour® Glucometer, (IN, USA)
Streptozotocin	:	Enzo Life Sciences, (NY, USA)
OmniPur®Acrylamide:Bis-acrylamide	:	EMD Chemicals, (NJ, USA)
OmniPur Ammonium persulphate (APS)	:	EMD Chemicals, (NJ, USA)
Tetramethylethylenediamine (TEMED)	:	Promega Corporation, (WI, USA)

(Continued)

Table 2. Materials used and their source (Continued)

Materials	:	Source and location
Sodium dodecyl sulphate (SDS)	:	Promega Corporation, (WI, USA)
PlusOne Tris	:	Amersham Biosciences, (Uppasala, Sweden)
Seeblue® plus protein marker	:	Invitrogen Corp., (CA, USA)
Chitosan	:	Sigma Aldrich Co., (MO, USA)
Acetonitrile	:	Sigma Aldrich Co., (MO, USA)
Triacetin	:	Sigma Aldrich Co., (MO, USA)
Human Embryonic Kidney (HEK293) cell line	:	American Type Culture Collection (ATCC), (MD, USA)
α-cyano-4-hydroxycinnamic acid	:	Sigma Chemical Co., (MO, USA)
Ketoprofen	:	Medisca, (NY, USA)
Rat immunoglobulin (IgG)	:	Santa Cruz Biotechnology, (CA, USA)

2.2. Animals

Male Sprague-Dawley rats weighing 180-200 g were obtained from Harlan Laboratories Inc., USA. Rats were housed in a temperature controlled facility maintained at 12 hour light-dark cycle in North Dakota State University Department of Pharmaceutical Sciences animal care facility. All animal experiments were performed according to the guidelines by NDSU Institutional Animal Care and Use Committee (IACUC). The experimental protocol was approved by IACUC (Protocol #A10054).

2.3. Methods

2.3.1. Synthesis and characterization of thermosensitive polymers

The synthesis and characterization of copolymer poly(lactic acid)-poly(ethylene glycol)-poly(lactic acid) (PLA-PEG-PLA) triblock copolymer used in this study has been reported by Al-Tahami K (84). The two copolymers with 1500-1500-1500 (4500 Da, copolymer A), and 1600-1500-1600 (4700 Da, copolymer B) chain lengths were synthesized by the ring opening polymerization of D, L lactide, catalyzed by stannous octoate, using polyethylene glycol (PEG 1500 Da) as an initiator. The scheme of synthesis is described in figure 5. Briefly, D, L lactide was charged into the three-necked flask containing pre-dried PEG (MW 1500 Da). To the molten reactants, stannous octoate (0.03% w/w) was added, and the reaction was carried out under nitrogen atmosphere at 120°C for 12 h to prepare the copolymer. The crude product obtained after polymerization was dissolved in ice cold water at 5-8°C, and reheated to 80°C for purification. To remove the unreacted monomers, impurities and to improve the purity of the synthesized copolymer the dissolution and reheating steps were repeated. The purified aqueous copolymeric solution was freeze-dried to remove the residual water content.

The synthesized copolymer was characterized by ^{1}H and ^{13}C NMR spectrometry and Gel Permeation Chromatography (GPC) in order to determine the structure, number average molecular weight, and molecular weight distribution (Polydispersity Index, PDI).

2.3.1.1. Proton and ^{13}C nuclear magnetic resonance (NMR)

The chemical structure of the synthesized polymer was determined by proton and carbon NMR using deuterated chloroform ($CDCl_3$) as a solvent. Tetramethylsilane (TMS) signal was used for calibration and its signal was taken as the zero chemical shift. Varian spectrometer operated at 400 MHz and 25°C was used for the measurements. The signals corresponding to

chemical groups such as -CH and -CH_3 of LA and -CH_2 of ethylene glycol in ^{1}H-NMR were integrated and used to calculate the number average molecular weight (M_n) of the polymer. The presence of PLA and PEG blocks were confirmed by the ^{13}C NMR spectra.

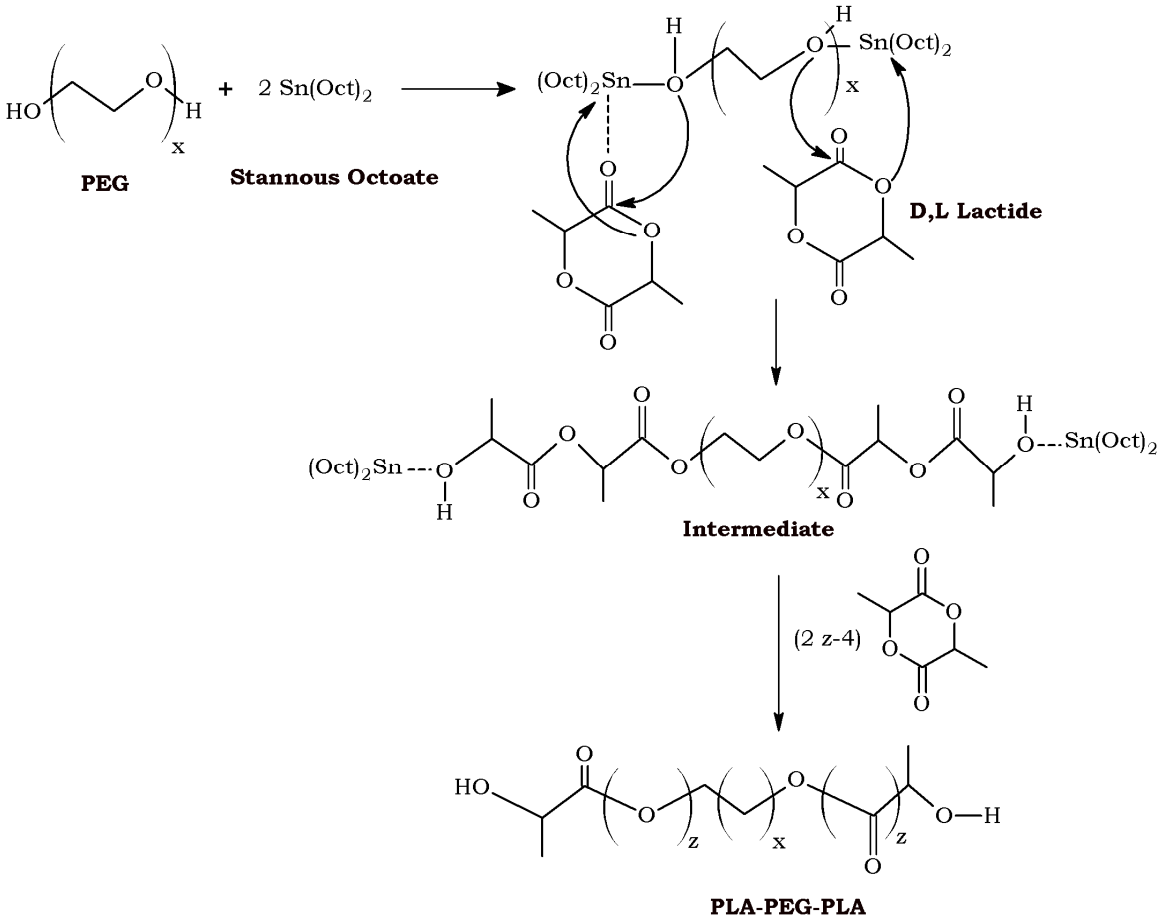

Figure 5. Scheme of synthesis of PLA-PEG-PLA triblock copolymer by ring opening polymerization reaction (84)

2.3.1.2. Gel permeation chromatography (GPC)

The number average molecular weight (M_n) and weight average molecular weight (M_w), as well as molecular weight distribution (polydispersity index, PDI) of the synthesized copolymers were determined using Gel Permeation Chromatography (GPC) (Waters 515, Milford, MA). Waters 2410 refractive index detector, and two Styragel® HR4E and HR5E columns (Milford, MA) were used. The analysis was based on the calibration using polystyrene

standards and tetrahydrofuran (THF) as a carrier solvent at 30°C with a flow rate of 1 mL/min and sample volume 100 µl.

2.3.1.3. Phase inversion of aqueous copolymer solutions

Aqueous solutions of triblock copolymers A and B at various concentrations were prepared (10, 15, 20, 25, 30, 35, 40% w/w) at 4°C. The vials containing aqueous copolymer solutions were equilibrated at 10°C by immersing in a temperature controlled water bath before the start of the experiment. The temperature of the water bath was raised at 2°C/step, and the phase transition temperatures of the sol (flow) to gel (no flow) of these solutions were noted by inverting the vials horizontally after keeping the sample at constant temperature for 10 min (208).

2.3.1.4. Morphology of polymeric delivery systems determined by scanning electron microscopy (Cryo-SEM)

Thermosensitive nature of the delivery system was studied by visualizing the surface morphologies. To visualize the surface morphology of copolymer solution maintained at room temperature (25°C), small amount of copolymer solution was mounted on a brass mount with an excess amount on the surface, and the mount was immersed into liquid nitrogen immediately to flash freeze the solution. The frozen sample was cut with a sharp, cold scalpel to obtain a clean surface, and visualized immediately (0 min), and at 5 min after sublimation using JEOL JSM-6490LV High-performance variable pressure SEM with a laser beam (15kV acceleration voltage) under low vacuum, and at 1500x magnification. Sublimation under low vacuum (35Pa) helped to remove the frozen layer of water from surface. To determine the thermosensitive behavior of the delivery system, aqueous copolymer solution (30%w/w) was injected into a tube, and incubated at body temperature (37°C) allowing it to form gel. The entire tube was immersed

into liquid nitrogen to flash freeze the hydrogel, and to avoid the ice crystal formation during freezing, as well as to minimize the alteration in gel structure. The delivery system surface was cut with the cold scalpel, and visualized under SEM.

2.3.2. Hydrolytic degradation and drug release behaviors of the delivery systems

The delivery systems were investigated for mass loss to study the time dependent hydrolytic degradation of the PLA-PEG-PLA copolymers. Proton NMR and GPC were used to determine the reduction in molecular weight during hydrolytic degradation.

2.3.2.1. Mass loss of polymer hydrogels during hydrolytic degradation

PLA-PEG-PLA copolymer based delivery systems (30 and 40 %w/w) were injected into the polypropylene tubes using 25G needle, incubated at body temperature and allowed to form gels. A pre-warmed phosphate buffered saline (PBS, pH 7.4, 10 ml) was added to each tube as release medium. At predetermined time intervals, the release medium was decanted, the hydrogels were freeze-dried, weighed and the % mass loss was calculated. The effect of PLA chain length, and polymer concentration on the mass loss was studied.

2.3.2.2. Hydrolytic degradation of copolymer determined by proton NMR

The freeze dried copolymer residues obtained at particular time points were dissolved in deuterated chloroform ($CDCl_3$), and proton NMR spectra was recorded on Varian Spectrometer (400 MHz), as per the procedure described earlier. The proton NMR signals were integrated and the ratio of lactic acid (LA) to ethylene glycol (EG) moieties was used to determine the degradation behavior.

2.3.2.3. Hydrolytic degradation of copolymer determined by GPC

GPC was used to evaluate the change in molecular weight, and molecular weight distribution of copolymers during hydrolytic degradation. The freeze dried copolymer residues obtained at 0, 30, 60, and 90 min were dissolved in tetrahydrofuran (THF), and analyzed using GPC (Waters 515, Milford, MA). The GPC experiment was carried out as per the procedure described previously.

2.3.2.4. In vitro release of incorporated molecules from the delivery systems

The in vitro release and degradation behavior of the delivery systems in presence of three different molecules was studied in detail. Aqueous solutions of thermosensitive copolymer A were prepared at a concentration of 30% w/w by stirring at 4°C. The copolymer solutions were examined for injectability by passing through 25 G needle. The model molecule (i.e. BSA, risperidone, or insulin) was dispersed into the aqueous copolymer solutions at room temperature, and homogenized at 8000 rpm for 30 seconds. The formulations (1ml) were injected in a tube and were allowed to form gels by incubating at 37°C. PBS (pH 7.4, 10 ml) was added slowly over the gel depot as release medium, and the entire assembly was incubated at 37°C in a water bath. The release medium was replaced periodically for the entire study period, and the amount of protein released was quantified by Pierce Micro BCA™ protein assay kit, according to the manufacturer's instructions (209). Agilent 1120 compact LC system was used to determine the amount of risperidone released (210). An Agilent Eclipse Plus C18 column (4.6 x 150 mm, 5 µm, Agilent, Santa Clara, California) was used, and risperidone analysis was performed using isocratic elution. The mobile phase consisted of methanol and ammonium acetate buffer (10 mM, pH 5.5) in the ratio of 85:15 at a flow rate of 1mL/min. Run time was 5 min and absorbance was monitored continuously at 280 nm. EZChrom Elite™ 3.3.2 software (Agilent, Santa Clara,

CA, USA) was used for data acquisition and analysis. The concentration correction was performed according to the method described by Hayton and Chen (211).

2.3.2.5. Mass loss of polymer hydrogels during in vitro release

The delivery systems prepared for in vitro release studies were also evaluated for percent mass loss. At predetermined time intervals, the release medium was removed, and the delivery systems were freeze-dried, weighed and the mass loss was calculated.

2.3.2.6. Hydrolytic degradation determined by proton NMR

The freeze dried formulation residues obtained at particular time points were mixed with $CDCl_3$, and proton NMR spectra was recorded.

2.3.2.7. Hydrolytic degradation determined by GPC

The change in molecular weight and its distribution of copolymer during in vitro release was determined using GPC. The freeze dried residues obtained at 0, 30, 60, and 90 min, were dissolved in THF, and were analyzed using GPC as per the procedure described earlier.

2.3.2.8. Morphology of polymer hydrogels visualized using SEM

The morphology and pore size of the drug loaded delivery systems were visualized using cryo-SEM. The delivery system containing insulin, risperidone or BSA were prepared, injected into polypropylene tubes, and incubated at 37°C to form gel. The in vitro release study was carried out as per the procedure described earlier. At 30 and 60 days, the release medium was decanted, and the delivery system was flash frozen by immersing in liquid nitrogen. The surface of the delivery system was cut with the cold scalpel, and was visualized under low vacuum (35Pa), 15kV acceleration voltage, and 1500x magnification. Approximately 200 pores were measured for their size.

2.3.2.9. Effect of molecular modification of insulin by chitosan, and zinc on in vitro release

The formulations were prepared by dispersing insulin, zinc-insulin, chitosan-zinc-insulin complexes in aqueous copolymer A (30% w/w) solutions at room temperature. In vitro release study was performed as described earlier, and the effect of molecular size and solubility on the in vitro release profile insulin was investigated.

2.3.2.10. Effect of chitosan on pH of release medium during hydrolytic degradation

The effect of addition of a cationic copolymer on pH of the release medium was investigated. Chitosan solution (0.2% w/v, pH 6.8) was mixed with the aqueous solution of copolymer A (30% w/w) at room temperature. One ml of the delivery system was injected in a tube and allowed to form gel at 37°C. Pre-warmed PBS (10 ml) was added as a release medium, and the pH of release medium was monitored during hydrolytic degradation for ~70 days.

2.4. Formulation of Delivery Systems for Insulin and In Vitro Release

The in vitro release profile of insulin was governed by various factors including concentration of the copolymer, addition of zinc, and insulin loading in the delivery systems. It has also reported that the polymeric delivery system at 40% w/w copolymer concentration reduced the initial burst release of insulin, and exhibited best fit for zero order release (84). Zinc addition (5:1 zinc ions: insulin hexamer) further helped to reduce the initial burst release and the release was prolonged for two months. For this reason, these previously studied delivery systems (copolymer concentrations: 30, and 40% w/w, and zinc: insulin hexamer ratio: 5:1) were utilized in preliminary studies. Formulations were prepared by dispersing insulin alone or zinc-insulin in aqueous copolymer solutions. The injectability of formulations was tested by passing through 25 G needle. The effect of zinc and polymer concentration (30 % w/w and 40 %w/w) on in vitro release profile of insulin at 60 mg insulin loading from the thermosensitive delivery system was

studied. To study the effect of insulin loading on in vitro release, copolymer concentration was fixed at 30% w/w, since it was difficult to inject the formulations at increased insulin loading and higher polymer concentration (40% w/w) from 25 G needle. Therefore, insulin was incorporated at different doses (60, 80 and 100 mg zinc-insulin) into the thermosensitive delivery system (30% w/w), and in vitro release study was performed. The delivery system compositions are listed in table 3.

Table 3. Delivery system compositions for in vitro release

Formulations	**Zinc:Insulin hexamer**	**Insulin loading**	**PLA-PEG-PLA**
I	-----	60 mg	30% (w/w)
II	5:1	60 mg	30% (w/w)
III	-----	60 mg	40% (w/w)
IV	5:1	60 mg	40% (w/w)
V	-----	60 mg	30% (w/w)
VI	5:1	60 mg	30% (w/w)
VII	5:1	80 mg	30% (w/w)
VIII	5:1	100 mg	30% (w/w)

(Mean ± SD, n=4)

For in vitro release study, an aliquot of 1 ml of the formulation was injected into the polypropylene tube and transferred to 37°C water bath for 2 minutes to form a gel. Twenty milliliters of pre-warmed PBS (pH 7.4) was added to the tube as release medium, and the tube was incubated in shaking water bath maintained at 37°C and 35 rpm for the entire study duration. Five milliliters of the release medium was withdrawn periodically and replaced with the same amount of fresh PBS. The amount of insulin released was determined by MicroBCA protein

assay kit. To ensure that the entrapped insulin is released in its native form, CD, native PAGE, SDS-PAGE and MALDI-TOF MS were performed.

2.4.1. Circular dichroism spectroscopy (CD)

J-815 CD Spectrometer (Jasco, Tokyo, Japan) was used to record the CD spectra. The released samples of insulin were filtered, and scanned in near-UV region (250-300 nm) in order to determine the tertiary structure, while far-UV CD (200-250 nm) spectra were used to investigate the changes in the secondary structure of released insulin during in vitro release. Five scans at a scan rate of 5 nm per min were recorded at 25°C using a quartz cuvette (0.1 cm path length). To remove the background interference, fresh PBS (pH 7.4) was scanned in the same range, and freshly prepared insulin solution was used as standard. Spectra manager®2 software (Jasco, Tokyo, Japan) was used for spectrum analysis. The molar ellipticity was calculated using the following equation:

$$\text{Molar Ellipticity } (\Theta) = \left(\frac{\Theta}{C}\right) \text{x } l$$

[θ: Ellipticity in mdeg; C: Concentration of insulin in mmol/L; l: Path length of the cell (0.1 cm)]

2.4.2. Polyacrylamide gel electrophoresis (Native and SDS-PAGE)

Native polyacrylamide gel electrophoresis (Native PAGE) was performed on Bio-Rad Mini-Protean tetra-cell electrophoresis (Hercules, CA) system. Native PAGE was performed to determine the presence of aggregates of insulin during in vitro release. The in vitro released samples of insulin were mixed with loading buffer (62.5 mM Tris-HCl, pH 6.8, 40% glycerol, 0.01% w/v bromophenol blue) before loading onto the polyacrylamide gel consisting of separating (12.5%) and stacking gel (5%). Fresh insulin solution was used as a standard, and the gels were ran at 100 V in tris-glycine buffer, then stained with Coomassie blue, and then

destained. Pre-stained protein marker (SeeBlue plus 2 Prestained Standard) was used to analyze the insulin band. In case of higher molecular weight bands, the covalent or non-covalent nature of insulin aggregates was assessed using non reducing SDS-PAGE. SDS-PAGE under non-reducing conditions helps to dissociate non-covalent aggregates. In SDS-PAGE analysis, samples collected during in vitro release studies at various time points were incubated with equal volume of SDS-PAGE sample loading buffer, and then resolved through the polyacrylamide gel at constant voltage (100V) for ~90 min. The molecular weights of the detected bands were compared with fresh insulin as well as with the pre-stained protein marker.

2.4.3. MALDI-TOF mass spectroscopy

Primary structural integrity of the insulin released from polymeric delivery system was evaluated using MALDI-TOF Mass Spectrometry. MALDI-TOF experiments were carried out using a Bruker MALDI TOF II-MS (Bruker Daltonics Inc., Billerica, MA) combined with a solid state smart-beam laser operated at a frequency of 200 Hz. A standard protein/peptide mixture kit (Bruker Daltonics) was used for the external calibration of the instrument before use. The sample was prepared as follows; The matrix solution was prepared by dissolving 10 mg of α-Cyano-4-hydroxycinnamic acid in 1 ml mixture of acetonitrile/1% TFA water (v/v = l:l). Twenty microliters of released insulin sample was mixed with 90 µl of matrix solution, and 2 µl of the final solution was placed on the MALDI-sample plate, air dried at room temperature, and analyzed in the Positive Reflectron mode. FlexAnalysis® software was used for data analysis.

2.5. Chitosan-Zinc-Insulin Complex Formation, Dissociation, and Effect of Chitosan on Insulin Stability

Since pH is one of the important factors in determining the complex formation between zinc-insulin and chitosan, the relationship between pH of the overall system and transmittance

was studied in our preliminary studies. Zinc-insulin-chitosan complexes were prepared at increasing chitosan to zinc-insulin weight ratio (1:1, 2:1, 4:1, 8:1) at different pH conditions, and the % transmittance of the overall system was recorded as a function of change in pH using UV/Vis spectrophotometer (UV-1601, Shimadzu, Japan). The complexes were centrifuged and the amount of insulin entrapped was determined. The amount of insulin entrapped was calculated by measuring the difference between the total amount of insulin added and the amount of non-associated insulin in the aqueous supernatant after complex formation. For this purpose, the formed chitosan-insulin complex was centrifuged at 10000 rpm for 30 min at room temperature, and the amount of unassociated insulin in the supernatant was measured using Pierce Micro BCA™ protein assay reagent kit (209).

The formation of complex between insulin and chitosan was visualized using gel retardation assay (native PAGE) and the dissociation of complex was characterized using SDS PAGE. Chitosan-zinc-insulin complexes were prepared at various ratios by mixing zinc-insulin with chitosan solutions (1:1, 1:2, 1:4, 1:8, 1:16 and 1:32 weight ratio), and incubated for 20 minutes at room temperature. The complexes were mixed with a loading dye before loading and native gel electrophoresis was performed as described earlier.

The structural changes in the insulin during complex formation with chitosan were assessed by Fluorescence and Circular Dichroism (CD) Spectroscopy, and Differential Scanning Calorimetry (DSC).

2.5.1. Fluorescence spectroscopy

Chitosan solution (0.0666 mg/ml, pH 6.8) was added to insulin solution (1 mg/ml, pH 6.8), at increasing amount (1:1, 1:2, 1:4 v/v) and the effect of chitosan on the fluorescence property of insulin (tyrosine/phenylalanine fluorescence) was recorded using Fluoromax-4

Spectrofluorometer (Horiba Scientific, New Jersey, NJ), with a 200 µl capacity quartz cell. The excitation/emission slit width was set at 5 nm, and the excitation wavelength was fixed at 280 nm to excite tyrosine and phenylalanine residues, and the emission spectra were collected in the range of 295-400 nm.

2.5.2. Circular dichroism spectroscopy (CD)

Chitosan solution (pH 6.8) was mixed with to zinc-insulin solution at increasing weight ratios (1:1, 1:2, 1:4, 1:8, 1:16 v/v) and the changes in the secondary structure (200-250 nm) of insulin upon addition of chitosan were determined using CD spectroscopy. The scan rate of 5nm/min was used, and all spectra were recorded at 25°C with a quartz cuvette (0.1 cm path length). To remove the background interference, fresh PBS (pH 7.4) was scanned in the same range, while freshly prepared insulin solution was used as standard. Spectra manager 2 software (Jasco, Tokyo, Japan) was used for spectrum analysis, and molar ellipticity was calculated as described earlier.

2.5.3. Differential scanning calorimetry (DSC)

The change in association state of zinc-insulin and its thermostability of insulin after addition of chitosan was investigated using DSC. The change in the unfolding temperature of insulin and zinc insulin after the addition of chitosan was recorded using Nano-DSC (TA Instruments, DE, USA). Before loading into the cells, samples and reference buffer (PBS, 10 mM, pH 7.4) were degassed under vacuum. Data was collected by scanning the samples from 10 to 110°C at a scan rate of 1°C/min. The reference scan (buffer scan) was subtracted from sample scan during the data analysis. All data analysis was performed using Nanoanalyze® software provided with the instrument. The transition curve was fitted using two-state scaled model following the “pseudo” V’ant Hoff method.

2.6. Stability of Insulin, Zinc-Insulin, and Chitosan-Zinc-Insulin Complex in Presence of Lactic Acid

Insulin alone, zinc-insulin, and chitosan-zinc-insulin complexes were incubated with the lactic acid which is the major end product of copolymer degradation, and the stability of insulin was investigated using titrimetric analysis, and DSC. Chitosan-zinc-insulin complexes were prepared by mixing 200 mg of chitosan with 1 ml of 60 mg/ml zinc-insulin hexamer solution in water at pH 7.4. A 1 ml aliquot of the solution containing this complex was titrated against 5 ml of 40 mg/ml of lactic acid (total theoretical lactic acid content in 1 ml of final formulation). The zinc-insulin complex without addition of chitosan was used as a control and the change in pH of final solution was measured using a calibrated pH meter. The zinc-insulin complex without addition of chitosan was used as a control and the change in pH of final solution was measured using a calibrated pH meter. To confirm the stability of insulin after addition of lactic acid, diluted titrates from the above experiment was subjected to analysis by DSC.

2.7. Formulation of Chitosan-Zinc-Insulin Complex Loaded Thermosensitive Copolymer Delivery System, and In Vitro Release

The formation of chitosan-zinc-insulin loaded thermosensitive polymeric formulations is presented in figure 6. The details about the composition of the delivery systems prepared are in table 4. The formulations were tested for their injectability, and thermosensitivity, and in vitro release study was performed as per the procedure described earlier. Briefly, 1 ml formulation was injected into a polypropylene tube and allowed to form gel by incubating in a water bath at 37°C. Upon gel formation, pre-warmed PBS was added slowly to the tubes as release medium, and the entire assembly was kept in a reciprocating water bath maintained at 37°C and 35 rpm. The released medium was removed and replaced periodically, and the amount of insulin released

was quantified by Pierce Micro BCA™ protein assay reagent kit. The concentration correction was performed according to the method described by Hayton and Chen (211).

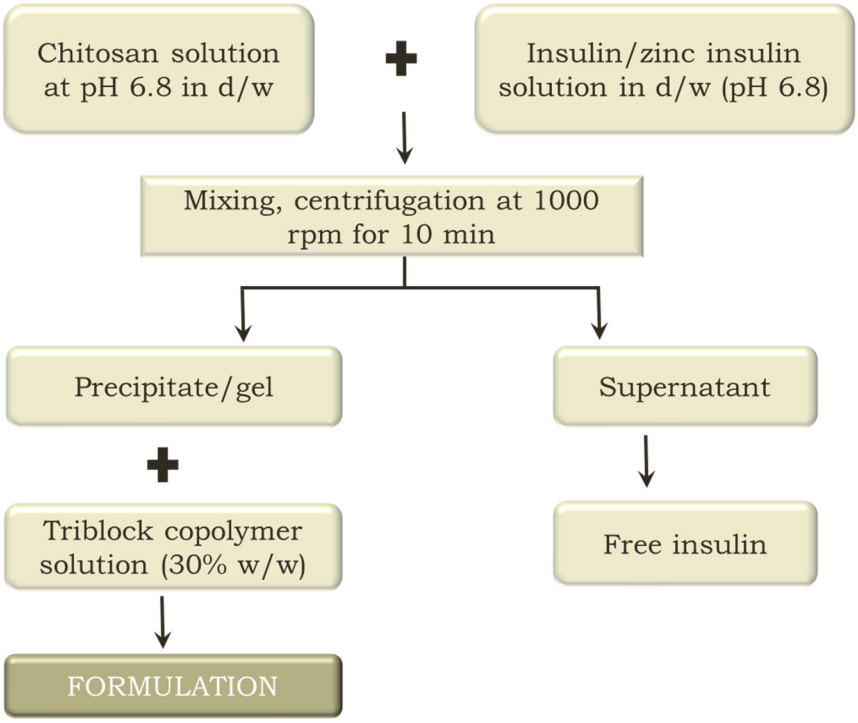

Figure 6. Scheme of formulation of chitosan-zinc-insulin complex loaded thermosensitive delivery system

Table 4. Polymeric formulations of insulin

Formulation	PLA-PEG-PLA	Insulin	Zinc:Insulin Hexamer	Chitosan (w/v)
A	30% (w/w)	5 mg	----	----
B	30% (w/w)	5 mg	4:1	----
C	30% (w/w)	5 mg	----	0.2%
D (Blank)	30% (w/w)	5 mg	4:1	0.2%

(N=4, mean ± SD)

2.7.1. Optimization of the delivery systems at higher insulin loading, in vitro release, and stability of insulin released in vitro

The delivery systems were optimized for higher insulin loading (30, 45, and 60 mg), and the effect of increasing amount of chitosan was also studied. Chitosan (50 kDa) solution in 1% acetic acid (0.2 and 0.4 % w/v of the total delivery system) was mixed with zinc-insulin (4:1 zinc to insulin hexamer) at an optimized pH (~6.8), and incubated at room temperature for 15 min. Zinc acetate was used as a source of zinc. Table 5 describes the formulation parameters for various insulin preparations studied. Insulin, zinc-insulin or chitosan-zinc-insulin complexes were incorporated into the thermosensitive polymeric delivery system (30% w/w), and 1 ml formulation was injected into a 50 ml tube using a 25 G needle. The delivery system was incubated in a reciprocating bath maintained at 37°C. After the solutions were transformed into gels, 30 ml of pre-warmed phosphate buffered saline (pH 7.4) was added as a release medium. During the release study, the tubes were incubated in a reciprocating water bath maintained at 37°C with mild shaking (35 rpm). Ten milliliter samples were removed from the media at specific time points, and replaced periodically with fresh buffer to maintain the sink condition. The released samples were then centrifuged and the amount of insulin released was determined using micro BCA protein assay. Delivery system without insulin was used as a blank control for absorbance correction. The amount of insulin released was obtained from the standard curve and corrected for sample removal as described earlier. The effect of chitosan and insulin amount on in vitro release of insulin was also studied.

The stability of in vitro released insulin was determined by the aforementioned analytical techniques.

Table 5. Polymeric formulations of insulin

Formulation	PLA-PEG-PLA	Insulin	Zinc: Insulin Hexamer	Chitosan (w/v)
A	30% (w/w)	30 mg	----	----
B	30% (w/w)	30 mg	4:1	----
C	30% (w/w)	30 mg	----	0.2%
D	30% (w/w)	30 mg	4:1	0.2%
E	30% (w/w)	30 mg	4:1	0.4%
F	30% (w/w)	45 mg	4:1	0.2%
G	30% (w/w)	45 mg	----	----
H	30% (w/w)	45 mg	4:1	----
I (Blank)	30% (w/w)	----	----	----
J	30% (w/w)	60 mg	4:1	0.2%
K	30% (w/w)	60 mg	----	----
L	30% (w/w)	60 mg	4:1	----
M (Blank)	30% (w/w)	----	----	----

(Mean ± SD, n=4)

2.7.1.1. Circular dichroism spectroscopy (CD)

The released samples of insulin were filtered, and scanned in near, and far UV regions in order to determine the 2° and 3° structures to investigate the changes in the secondary structure of insulin after incubation at 37°C for ~3 months. The detailed procedure can be found in section 2.3.2.1. The secondary structure analysis was performed using Spectra Manager 2 software and the percentages of α helix, β sheets, and random ordered structures were determined.

2.7.1.2. Differential scanning calorimetry (DSC)

Insulin released from the delivery systems containing insulin alone, zinc-insulin, and chitosan-zinc-insulin complex at day 7, 30, and 60 were analyzed for their thermostability using DSC. The released samples were filtered, degassed, and DSC analysis was performed to determine the calorimetric measurements including midpoint transition temperature (T_m) and the calorimetric enthalpy (ΔH). All data was analyzed using Nanoanalyze software, and fitted with two-state scaled model.

2.7.1.3. Polyacrylamide gel electrophoresis (Native and SDS-PAGE)

The released samples of insulin from formulations D and H, at day 15, 30, 45, and 60, were analyzed using PAGE and SDS-PAGE to determine the presence and nature of insulin aggregates during release.

2.7.1.4. High performance liquid chromatography (HPLC)

The chemical stability of in vitro released insulin was assessed by RP-HPLC (3,212), and the chromatographic conditions used are presented in table 6.

2.7.1.5. MALDI-TOF mass spectroscopy

Primary structural integrity of the insulin released from various polymeric formulations was evaluated using MALDI-TOF MS. Freshly prepared insulin solution was used as control, and the details about the procedure are in section 2.4.3.

2.7.2. Stability of insulin in delivery system during release

In this study, polymeric formulations containing chitosan-zinc-insulin complex were injected into a tube using 25 G needle at room temperature and incubated in a water bath at 37°C in order to transform the solutions into hydrogels. Pre-warmed PBS (pH 7.4) was added as

dissolution medium and replaced periodically similar to release study for the entire release duration (~60 days). At predetermined time points, the gel depot was collected after decanting the supernatant. Insulin remaining inside the gel depot was extracted using 1:1 (v/v) mixture of acetonitrile and PBS with a mild shaking for ~15 min. the samples were then centrifuged at 5000 rpm for 20 min. The stability of insulin was determined using MALDI-TOF MS and HPLC.

Table 6. Chromatographic conditions for insulin analysis

Chromatographic conditions	**:**	**Details**
System	:	Agilent 1120 compact LC system
Column	:	Zorbax-SB reversed-phase C18 column (4.6x150 mm, 5μm)
Elution	:	Gradient
Mobile phase A	:	0.1% v/v TFA in water
Mobile phase B	:	0.1% v/v TFA in acetonitrile
Mobile phase composition	:	75:25 (A:B) to 50:50 (A:B)
Flow rate	:	1 ml/min
Injection volume	:	25 μl
Run time	:	20 min
Detector	:	UV
Detection wavelength		280 nm
Retention time	:	9.8 min
Data acquisition and analysis		EZChrom Elite 3.3.2 software (Agilent, Santa Clara, CA)

2.7.3. Stability of insulin in delivery system during storage

The effect of zinc and chitosan on the stability of insulin in the polymeric delivery systems during storage at 4°C and 37°C was also investigated. The polymeric delivery systems containing chitosan-zinc-insulin complex were stored at 4°C and 37°C for 60 days. Insulin was extracted from the polymeric gel using acetonitrile-PBS (1:1) at predetermined time points, and the stability of insulin inside the polymeric formulations was determined using HPLC and MALDI-TOF MS. The stability of insulin in the presence of zinc and chitosan was compared with that of fresh insulin and insulin control (insulin incubated in PBS at similar conditions).

2.7.4. In vivo absorption and bioactivity of insulin

The North Dakota State University Institutional Animal Care and Use Committee (IACUC) approved the animal study protocol and experiments. Eight weeks old male Sprague-Dawley rats weighing 180-200 g were used to study the in vivo absorption and bioactivity of the recombinant human insulin (rH) released from the delivery systems. Rats were housed in a temperature controlled facility maintained at 12 h light-dark cycle, and allowed free access to food and water. The rats were acclimatized to the housing conditions one week before the study initiation. A single dose of freshly prepared streptozotocin (STZ, 55 mg/kg body weight) dissolved in ice cold citrate buffer (pH 4.5) was injected intraperitoneally to the rats to induce diabetes. Post-injection, rats were provided with 5% sucrose solution to counteract the potential risk of hypoglycemia caused by massive insulin release under the influence of STZ. Rats were monitored daily, and one week after STZ injection, blood glucose levels were measured. The rats with fasting blood glucose levels >200 mg/dl were considered diabetic and retained in the study. The diabetic rats were divided into 8 different groups (6 animals/group), and assigned to the treatments randomly. An additional group of non-diabetic rats was used as control. The

formulations were injected as a single subcutaneous dose at the back neck region of rats using 25 G needle. The treatment groups were injected with the polymeric delivery systems (500µl) containing either insulin alone, zinc-insulin or and chitosan-zinc-insulin complexes at two different doses. Assuming the daily basal insulin requirement of ~18-24 IU (~0.4-0.5 IU/kg/day; total dose: ~30 and 45 IU/kg for 90 days), two doses were selected to provide a continuous basal level of insulin. Groups I and II were injected with the thermosensitive delivery system containing insulin alone at a dose of 30 and 45 IU/kg, groups III and IV with zinc-insulin (30 and 45 IU/kg), and group V and VI with chitosan-zinc-insulin complex at a dose of 30 and 45 IU/kg. Group VII was treated with single dose of insulin (2 IU/kg) dissolved in PBS (pH 7.4) subcutaneously; while STZ treated animals without treatment (group VIII) were used as a negative control. After the initial week, blood sampling was performed on a weekly basis until three months using tail vein puncture. At the end of the study period, an intravenous injection of pentobarbital (150 mg/kg) was used to euthanize the rats.

2.7.4.1. Quantification of serum insulin levels using enzyme linked immunosorbent assay (ELISA)

Insulin levels were measured by sampling blood from the tail vein of rats at pre-determined time points after overnight fasting. Serum was collected after centrifuging the blood samples at 4°C at 3000 rpm for 15 min, and stored at -20°C. Mercodia Human Insulin ELISA kit was utilized to determine the of serum insulin (rH) levels (213).

2.7.4.2. Determination of blood glucose levels

The pharmacodynamic activity of insulin released from the delivery systems was estimated from blood glucose levels. After overnight fasting, blood was withdrawn from tail vein of rats, and the fasting blood glucose levels were measured by the glucose oxidase method using

a glucometer (Bayer CONTOUR blood glucose monitoring system, IN), and expressed in milligrams per deciliter (mg/dl).

2.7.4.3. Body weight determination

The change in the body weight of rats before and after induction of diabetes, as well as after insulin treatment was noted daily for the first week, and further monitored on weekly basis during entire study duration.

2.7.4.4. Detection of anti-insulin (rH) antibodies

The rat serum samples were collected after 1, 2 and 3 months of treatment and were subjected to ELISA. For detection of anti-human insulin antibodies in rat serum an indirect ELISA was performed (214). Briefly, ELISA plate was coated with 800 ng/ml insulin in coating buffer (carbonate buffer, 50 mM, pH 9.6, 100 µl/well), and kept overnight at 4°C. Plates were incubated with a blocking agent [3% bovine serum albumin (BSA)], at 37°C for 1 h. The plates were washed with PBS containing 0.02% tween 20 (PBST) followed by addition of diluted rat serum and again incubated at 37°C for 1 h. The plates were washed again with PBST, and 1:5000 diluted goat anti-rat-IgG-Horseradish Peroxidase conjugated secondary antibody was added, followed by incubation at 37°C for 2 h. Substrate solution (tetramethylbenzidine, TMB) was added at the end of incubation, and the plates were further incubated for 20 min at 37°C. Sulfuric acid (0.5 M) was used to stop the reaction, and the optical density was recorded at 450 nm using a microplate reader. Rat IgG were used as a control.

2.7.5. Biocompatibility of the delivery systems

The in vitro biocompatibility of the delivery systems was determined by a cell viability assay, while for determination of in vivo biocompatibility, histology of implanted skin tissue was studied after injection of the delivery system.

2.7.5.1. In vitro biocompatibility of the delivery systems

In vitro biocompatibility of the thermosensitive polymeric delivery system with and without chitosan was quantitatively assessed using a standard MTT cell viability assay. This assay was aimed to evaluate the effect of polymer extracts, and their degradation products on the cell viability in vitro. The detailed procedure is described previously (64). Briefly, the aqueous solutions of thermosensitive polymer (30% w/w, 500µl) with/without chitosan were prepared, injected in a tube, and allowed to form gels by incubating at 37°C in water bath. The polymeric hydrogels were extracted into PBS (10 ml, pH 7.4) at 37 and 70°C by incubating for 10 days. The extracts were diluted with growth medium, added to the Human Embryonic Kidney (HEK293) cells and incubated for 24, 48 and 72 hours. Percent cell viability was calculated considering the cell viability of untreated cells (growth medium only) as 100%. For comparison purposes cells treated with PBS (without polymer), 2% DMSO, and chitosan were used.

2.7.5.2. In vivo biocompatibility of the delivery systems

The in vivo biodegradability and biocompatibility of the delivery system with and without chitosan was evaluated after injecting 500 µl of the delivery system subcutaneously into the upper neck area of rats. The appearance of gel lump was monitored regularly by visual examination. At 1, 7, 30 and 90 days post-injection, rats were euthanized, and the subcutaneous tissue surrounding the injection site was excised and examined visually for the presence of any delivery system residue. For assessing the biocompatibility of the delivery system, the excised

hydrogel-contacting subcutaneous tissue was fixed in 10% neutrally buffered formalin at room temperature, sectioned (5 μm thickness), and processed for histological analysis. The skin sections were stained with hematoxylin eosin (H&E) and examined under the light microscope for any inflammatory reactions.

The collagen deposition near the injection site was visualized by staining the skin sections with Gomori's trichrome stain, and the collagen density and its appearance at the injection site were compared to that of normal skin tissue using ImageJ 1.45 software (NIH, MD).

2.7.6. Statistical analysis

For statistical analysis, a single factor ANOVA was performed using Minitab 16 statistical software (Minitab Inc., PA). A p-value of less than 0.05 was considered to be significant. Serum insulin levels were plotted against time and the bioavaialability of insulin was determined based on the area under the curve (AUC) data calculated by linear trapezoidal rule (215). The concentration versus time profile was used to determine maximum serum concentration (C_{max}) and corresponding time at which maximum concentration is reached (T_{max}) for the solution group (Insulin in PBS: 2 IU/kg SC).

3. RESULTS

A series of PLA-PEG-PLA copolymers of different molecular weights, and PEG/PLA block ratios were synthesized and studied for insulin delivery by Al-Tahami (84). The most promising copolymers in terms of release duration and rate among them were PLA-PEG-PLA with chain lengths 1500-1500-1500, and 1600-1500-1600 (molecular weights 4500, and 4700 Da), and hence were used in our further studies.

3.1. Synthesis and Characterization of Thermosensitive Copolymer

PLA-PEG-PLA triblock copolymers A and B, with molecular weights of 4500, and 4700 Da, respectively, were synthesized by ring opening polymerization reaction using PEG (an initiator), and D, L lactide. The synthesis and characterization of PLA-PEG-PLA triblock copolymer used in this study has been reported by Al-Tahami (84) however, some essential properties were re-determined for reproducibility. The structure of the copolymer is presented in figure 7.

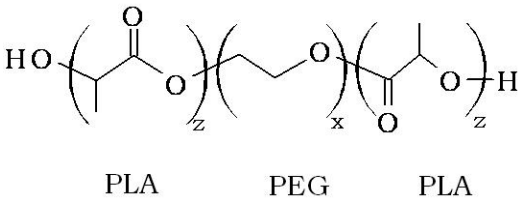

Figure 7. Structure of polylactic acid-polyethylene glycol-polylactic acid (PLA-PEG-PLA) triblock copolymer

3.1.1. Proton and ^{13}C nuclear magnetic resonance (NMR)

The proton and ^{13}C NMR spectra of the synthesized copolymer are presented in figures 8 and 9. The proton NMR spectrum was similar to the reported spectrum of PLA-PEG-PLA (84). The signals corresponding to -CH (methine) of LA at 5.20, $-CH_3$ (methyl) of LA at 1.55, $-CH_2$ (methene) of PEG at 3.65, and -OH of LA at 2.35 ppm were observed and shown in figure 8. To

determine the number average molecular weight, the peaks corresponding to -CH of LA, $-CH_2$ of PEG and $-CH_3$ of LA at 5.2, 3.65 and 1.55 ppm, respectively, were used and the calculation details can be found in the work of Jeong et al (23). The ^{13}C NMR spectrum (figure 9) showed the presence of the groups, -C=O, -CH and $-CH_3$ in the PLA block at 170, 69.4 and 17 ppm, respectively, while $-CH_2$ group in PEG block was found at 71 ppm. The NMR spectra confirmed the structure of the synthesized copolymer.

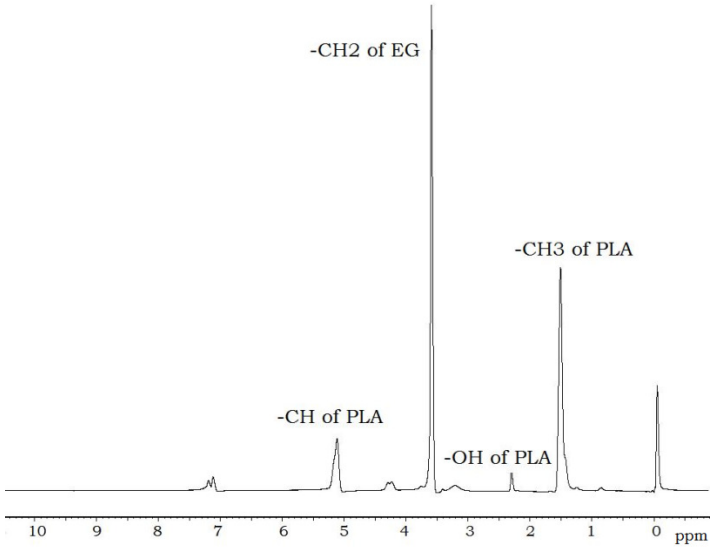

Figure 8. Proton NMR spectrum of triblock copolymer PLA-PEG-PLA

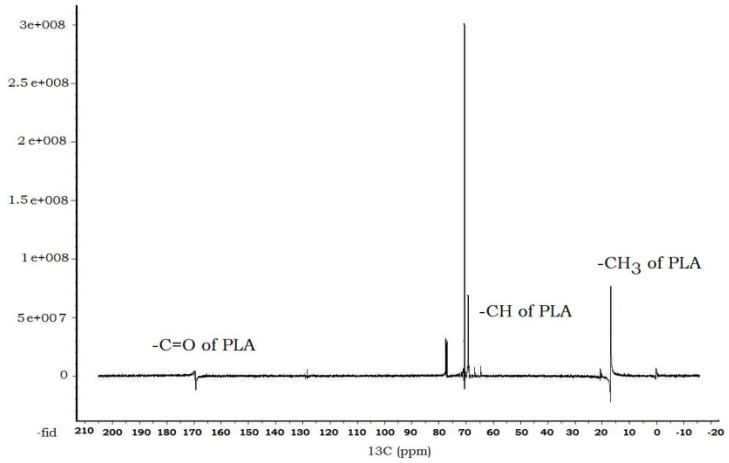

Figure 9. ^{13}C NMR spectrum of triblock copolymer PLA-PEG-PLA

3.1.2. Gel permeation chromatography (GPC)

The number average molecular weight (M_n), weight average molecular weight (M_w) and molecular weight distribution of the synthesized copolymers determined by GPC is presented in table 7. A representative chromatogram from GPC analysis is shown in figure 10. The retention times for triblock copolymer A and B were found to be ~17.3, and 18 min, respectively, with a unimodal GPC trace, and the PDI was found to be 1.11. The characteristics of the copolymer determined by GPC and NMR are summarized in table 7.

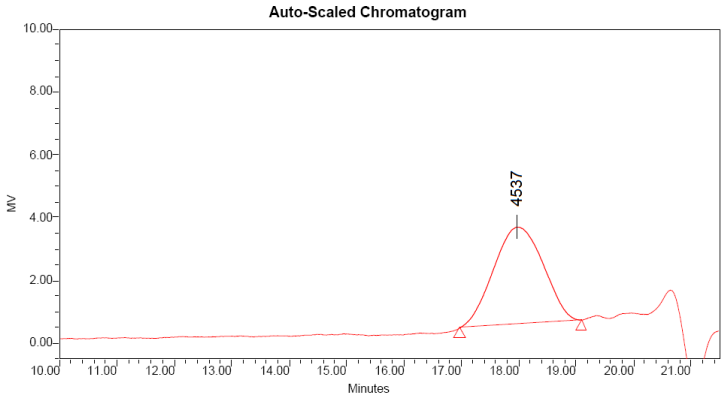

GPC Results

	Retention Time	Mn	Mw	MP	Mz	Mz+1	Polydispersity
1	17.957	4344	4865	4537	4051	4476	1.119945

Figure 10. GPC chromatogram for triblock copolymer PLA-PEG-PLA (1500-1500-1500)

Table 7. Characteristics of copolymer PLA-PEG-PLA

NMR			**GPC**		
Copolymer	Mn^a	Retention Time	Mn^b	Mw^c	Polydispersity^d (Mw^c/Mn^b)
PLA-PEG-PLA	4480	17.957	4344	4865	1.119
PLA-PEG-PLA	4720	17.353	4917	5408	1.1

Mn^a : Number average molecular weight determined by NMR
Mn^b : Number average molecular weight determined by GPC
Mn^c : Weight average molecular weight determined by GPC
^{d} Polydispersity index determined by GPC

3.1.3. Phase inversion of aqueous copolymer solutions

The phase behavior of aqueous copolymer solutions is an essential property involved in the design of thermosensitive polymer based drug delivery systems. The sol-gel transition of the triblock copolymer was determined by tube inversion method and the phase diagram is presented in figure 11. At lower concentration (10 % w/w), copolymer solutions did not turned into gel form but, when the concentration of the copolymer was increased to 15-40% w/w, the aqueous copolymer solutions existed in three distinct phases namely sol, gel and precipitate in the temperature range of 15-65°C. It existed in 'sol phase' below the lower critical solution temperature (LCST), and above LCST, it existed in the 'gel form'. When the copolymer concentration was increased from 15 to 30% w/w and higher, sol-gel transition temperature reduced by ~8-10°C, and gel-sol transition temperature increased by ~14-16°C. As the temperature increased above the upper critical transition temperature (UCST), the polymer precipitated. The thermosensitive nature of the polymeric delivery system is presented in figure 12.

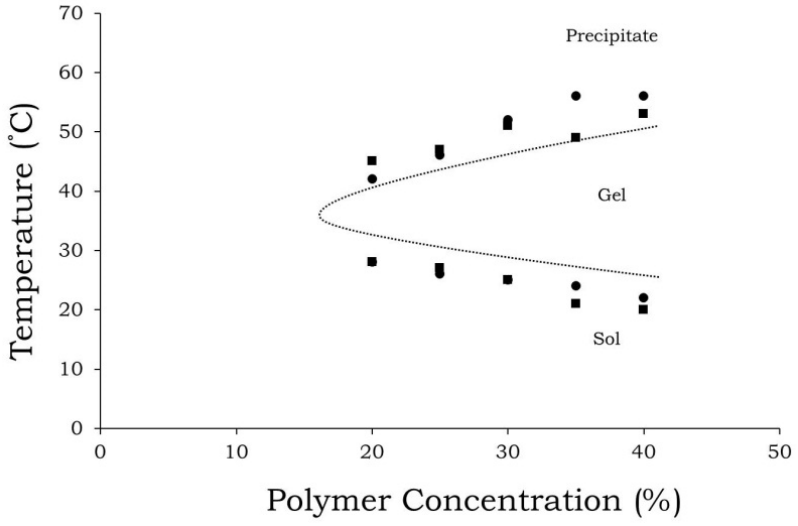

Figure 11. Sol-gel transition of triblock copolymer PLA-PEG-PLA aqueous solutions (1500-1500-1500 (●), and 1600-1500-1600 (■) copolymers)

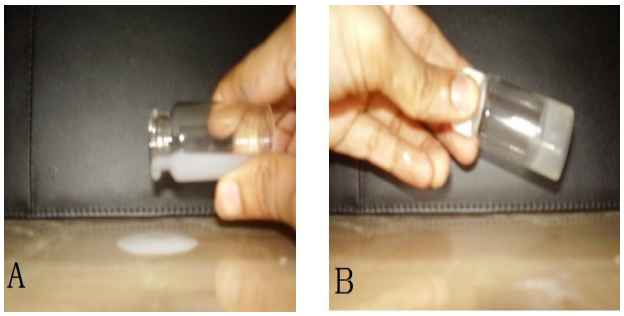

Figure 12. Thermosensitive nature of the delivery system at room temperature (A) and body temperature (B)

3.2. Morphology of Polymeric Delivery System Determined by Cryo-SEM

Freshly cut surface morphologies of the delivery systems maintained at room temperature (25°C) and body temperature (37°C) visualized using cryo-SEM are presented in figure 13. The delivery systems showed a marked difference in their appearance. The freshly cut surface of copolymer solution maintained at 25°C did not show any particular three dimensional surface characteristics (figure 13 A and B). According to the approach orientation of the scalpel blade, the delivery surface showed striations oriented along the cut surface. On the other hand, freshly cut surface of the delivery system maintained at body temperature showed presence of three dimensional structures consisting of two distinct domains. The polymer rich portion was observed as dense white area, while the water filled pores were observed as dark empty spaces (figure 13C).

3.3. Hydrolytic Degradation of the Copolymers

3.3.1. Mass loss of polymer hydrogels during hydrolytic degradation

The total mass loss in the delivery systems containing copolymer A (1500-1500-1500), and copolymer B (1600-1500-1600) at specific time points during hydrolytic degradation is presented in figure 14. It was observed that the copolymer with higher PLA chain length (1600-1500-1600) degraded slower, and a significant ($P<0.05$) difference in the percent mass loss was

observed until 30 days as compared to the copolymer with smaller PLA chains. The effect of polymer concentration on the mass loss was studied and the data is presented in figure 15. The delivery system showed significant difference ($P<0.05$) in mass loss for ~45-50 days, however, after that both the hydrogels degraded at similar rate.

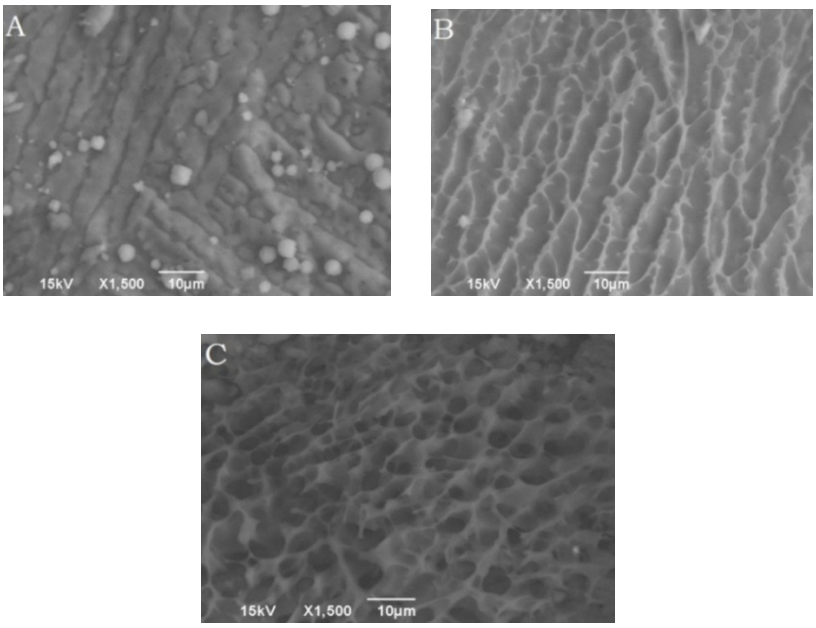

Figure 13. Cryo-SEM images visualizing the morphologies of freshly cut surfaces of the polymeric delivery systems maintained at 25°C at 0 min (A) and 5 min (B) after sublimation, and at 37°C (C), 5 min after sublimation

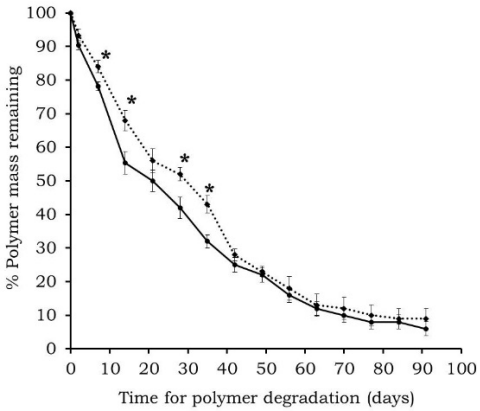

Figure 14. Effect of PLA chain length on in vitro hydrolytic degradation of 30% w/w delivery system (●) copolymer A (1500-1500-1500) and (♦) copolymer B (1600-1500-1600) (n=4, mean ± SD, *: significant at $p<0.05$)

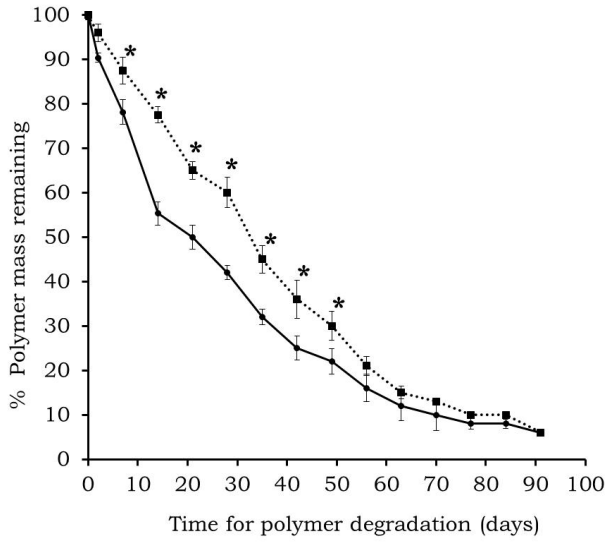

Figure 15. Effect of polymer concentration on in vitro hydrolytic degradation (●) 30% w/w, and (■) 40% w/w copolymer A containing delivery systems (n=4, mean ± SD, *: significant at $p<0.05$)

3.3.2. Hydrolytic degradation determined by proton NMR

Figure 16 summarizes the changes in the relative amount of LA and EG content of the copolymers (A and B) after degradation in PBS (pH 7.4) at 37°C. The change in the peak height of $-CH_3$ of PLA (1.55 ppm) and $-CH_2$ of PEG (3.65 ppm) in proton NMR spectra was used to evaluate the content of lactide (LA) and ethylene glycol (EG), respectively. No significant difference in the content of residual polymers was noticed until ~45 days of degradation. However, a significant increase ($P<0.05$) in the peak height of $-CH_3$ of LA and corresponding reduction in the EG signal at 3.65 ppm was observed in case of both the delivery systems at days 60 and 90. The effect of concentration of copolymers on degradation profile was also evaluated by studying the change in LA/EG ratio, and is presented in figure 17. The results indicated that there was gradual increase in LA content, but the copolymer concentration did not significantly ($p>0.05$) affect the LA/EG ratio during entire degradation period.

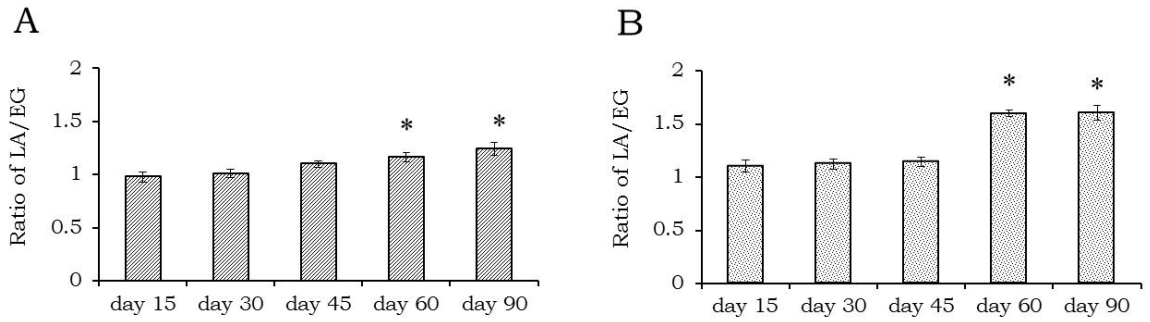

Figure 16. Effect of PLA chain length on hydrolytic degradation
A) Copolymer A (1500-1500-1500), and B) Copolymer B (1600-1500-1600)
(n=4, mean ± SD, *: significant at $p<0.05$)

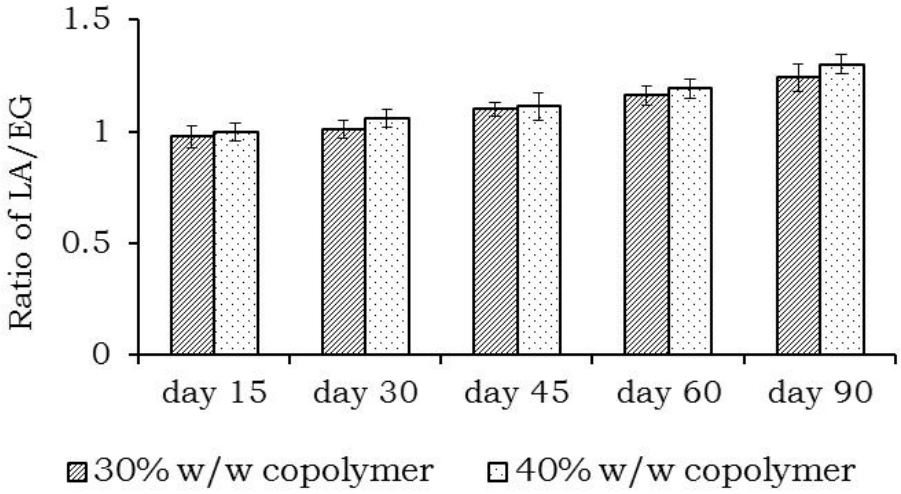

Figure 17. The change in LA/EG ratio of copolymer A (1500-1500-1500), during hydrolytic degradation at 30% and 40% w/w concentration
(n=4, mean ± SD)

3.3.3. Hydrolytic degradation determined by GPC

The results of GPC for hydrolytic degradation of copolymer A are summarized in table 8. The GPC trace of copolymer A was unimodal initially, with a bell-shaped peak near 17.9 min (RT), which was attributed to the similar molecular weight (Mw) of the copolymer. During hydrolytic degradation, a slight increase in RT (18.05 min) was observed after 30 days, with a bimodal GPC chromatogram. The delivery systems showed a noticeable degradation after 30 days of incubation at 37°C in PBS (pH 7.4), and at the end of 60 days copolymer was completely

degraded into smaller segments (RT_1: 18.19 and RT_2: 20.83). At the end of 90 days no peak corresponding to original polymer was detected.

Table 8. Molecular weight of the polymer PLA-PEG-PLA (4500 Da) remaining after hydrolytic degradation in PBS, pH 7.4 at 37ºC

Sample	Time	M_n (1)	RT	PDI	M_n (2)	RT	PDI
	0 days	4344	17.957	1.119	----	----	----
Copolymer A	30 days	3177	18.054	1.283	335	20.812	1.214
(1500-1500-1500)	60 days	2673	18.190	1.152	200	20.836	1.160
	90 days	----	----	----	188	20.92	1.163

3.4. Effect of Various Molecules on In Vitro Release Behavior of Delivery Systems

In vitro release behaviors of small protein insulin, large hydrophilic protein BSA, and a small hydrophobic molecule, risperidone from the polymeric delivery system containing 30% w/w PLA-PEG-PLA is presented in figure 18. The polymer degradation pattern of hydrogels in presence of these different molecules was studied using NMR, and GPC, while the gel morphology was visualized using Cryo-SEM.

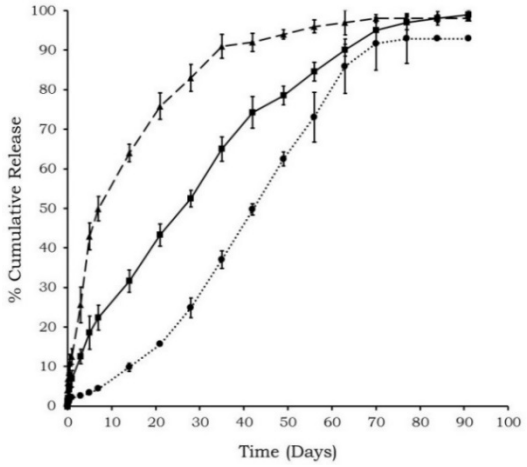

Figure 18. In vitro release profiles of (●) risperidone, (▲) BSA, and (■) insulin released from 30% w/w copolymer A containing delivery systems (n=4, mean ± SD, drug loading: 0.3% w/v)

The HPLC chromatogram of freshly prepared risperidone solution showed retention time (RT) at 2.16 min. The release profile of risperidone showed that only 2.13±0.047% of the total risperidone incorporated into the delivery system was released in day 1. It was observed that only 10% of the total risperidone was released in 15 days, and the overall release period lasted for approximately 77 days. While BSA showed high initial burst release (13.54±0.89%), followed by insulin (7.32±3.1%). BSA was released rapidly and completely in ~42 days including a fast release phase observed up to 7 days, followed by a slow release phase for 42 days. Insulin was released over 70 days in a controlled manner after an initial burst release. The correlation coefficients for BSA, insulin, and risperidone were 0.76, 0.86, and 0.98, respectively, for zero order release kinetics.

3.4.1. Mass loss of polymer hydrogels during in vitro release

It was observed that the hydrophobicity of the incorporated molecule affected the mass loss in hydrogels. Figure 19 shows the degradation of copolymer A in presence of various molecules. The delivery system containing BSA degraded faster as compared to risperidone, and insulin containing delivery systems, and the mass loss was significantly higher ($p<0.05$) until 45 days of release.

3.4.2. Hydrolytic degradation of polymer hydrogels determined by proton NMR

Figure 20 shows the change in the relative amount of LA and EG content of the copolymer after degradation in PBS (pH 7.4) at 37°C in presence of risperidone, BSA and insulin. In case of BSA containing delivery system the ratio of LA and EG increased to 1.4 after 30 days of degradation, indicating preferential loss of hydrophilic PEG segments. The delivery systems containing insulin and risperidone showed gradual increase in LA/EG ratio. The residual

polymer appearance was visually compared and it was noted that the BSA loaded delivery systems appeared more porous.

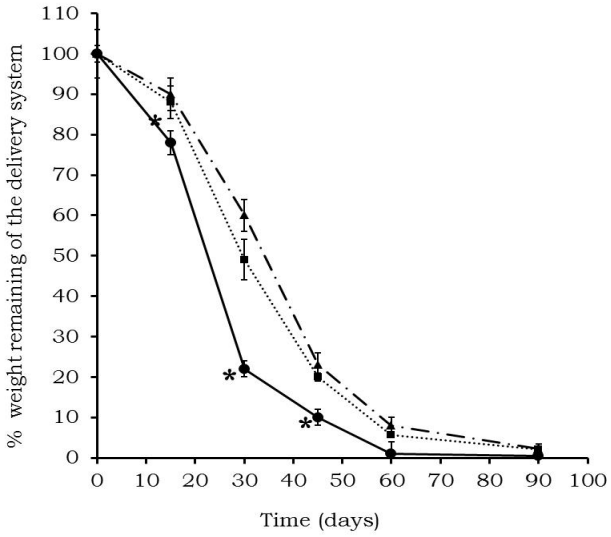

Figure 19. Weight loss of the delivery system during in vitro release of (●) BSA, (▲) risperidone, and (■) insulin, from 30% w/w copolymer A containing delivery systems (n=4, mean ± SD, *: significant at $p<0.05$)

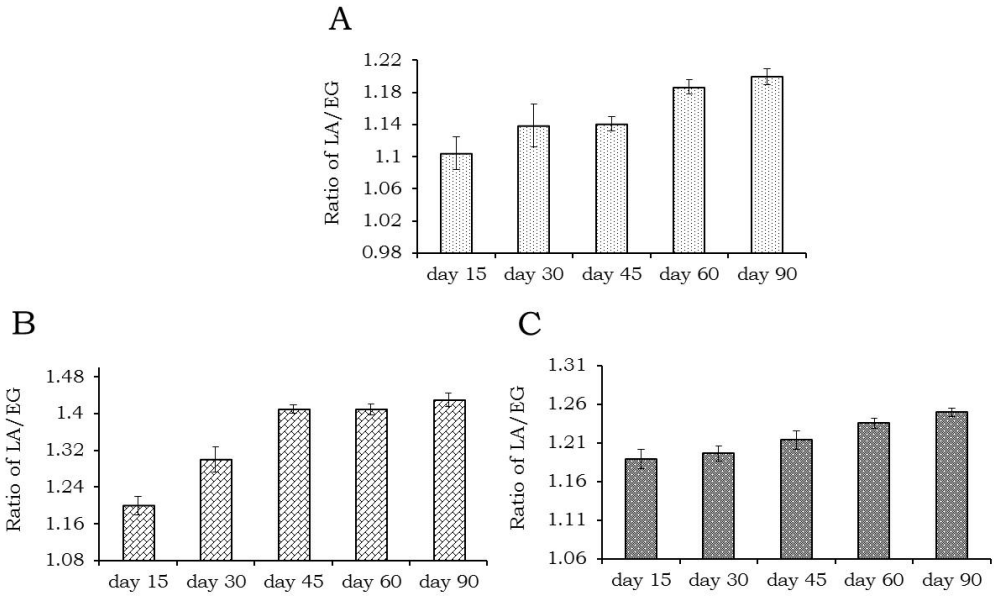

Figure 20. The change in LA/EG ratio of the polymer containing (A) zinc-insulin + polymer, (B) BSA + polymer, and (C) risperidone + polymer, during in vitro release

3.4.3. Hydrolytic degradation determined by GPC

GPC helped to determine the change in molecular weight of copolymer during hydrolytic degradation. GPC results of polymer alone, and loaded with BSA, insulin, and risperidone analyzed over the release duration are summarized in table 9. The drug loaded delivery systems showed noticeable degradation after 30 days of in vitro release. As the degradation proceeded, the chromatogram showed a bimodal distribution, and a reduction in molecular weight (M_n) of polymer illustrated by an increase in retention time (RT) was observed. Increase in the polydispersity index (PDI) observed indicated that the rate of degradation was faster in case of polymeric delivery system containing BSA as compared to that of insulin or risperidone. The reduction in molecular weight was rapid after 30 days of incubation, and at the end of 60 days, most of the polymer was hydrolyzed into smaller segments indicated by corresponding increase in RT. At the end of 90 days, no peak corresponding to original polymer was detected, while increase in polymer degradation products with RT near 20 min was noticed.

3.4.4. Morphology of the delivery system determined using Cryo-SEM

Figure 21 (A-F) shows the morphology of the delivery systems after incorporation of insulin, BSA, and risperidone. It was observed that the size of pores formed in the delivery system was dependent on the type of drug incorporated. Table 10 shows the average size of pores formed in the delivery systems at various drug loading. By the end of day 30, the hydrogel containing BSA showed significantly larger ($p<0.05$) pores (3.95±1.45 μm) than insulin (2.53±0.93 μm), or risperidone (0.96±0.26 μm) loaded hydrogels as shown in figure 21 (C, E and G). At the end of 60 days, pore size increased irrespective of drug loading and no significant difference was observed in the mean pore size (figure 21 D, F, and H).

Table 9. Molecular weight of the polymer PLA-PEG-PLA (4500 Da) remaining after hydrolytic degradation in PBS, pH 7.4 at 37ºC

Sample	**Time**	**M_n (1)**	**RT**	**PDI**	**M_n (2)**	**RT**	**PDI**
Polymer + Insulin	0 days	344	17.957	1.119	----	----	----
	30 days	3157	18.047	1.285	317	20.649	1.150
	60 days	2073	18.086	1.291	258	20.751	1.351
	90 days	----	----	----	200	20.84	1.161
Polymer + Risperidone	0 days	4344	17.957	1.119	----	----	----
	30 days	2567	18.095	1.164	----	----	----
	60 days	1902	18.175	1.32	200	20.839	1.159
	90 days	----	----	----	208	20.81	1.158
Polymer + BSA	0 days	4344	17.957	1.119	----	----	----
	30 days	2431	18.030	1.288	225	20.653	1.168
	60 days	----	----	----	307	20.715	1.230
	90 days	----	----	----	----	----	----

Table 10. Average size of pores formed in the delivery systems loaded with different molecules

Incorporated molecules	**Day 30 (average pore size, n=200)**	**Day 60 (average pore size, n=20)**
Blank (Polymer only)	2.17 ± 0.41 μm	10.84 ± 1.68 μm
Risperidone	0.96 ± 0.26 μm	9.67 ± 2.81 μm
Zinc-Insulin	2.53 ± 0.93 μm	12.58 ± 2.55 μm
BSA	3.95 ±1.45 μm	15.31 ± 3.66 μm

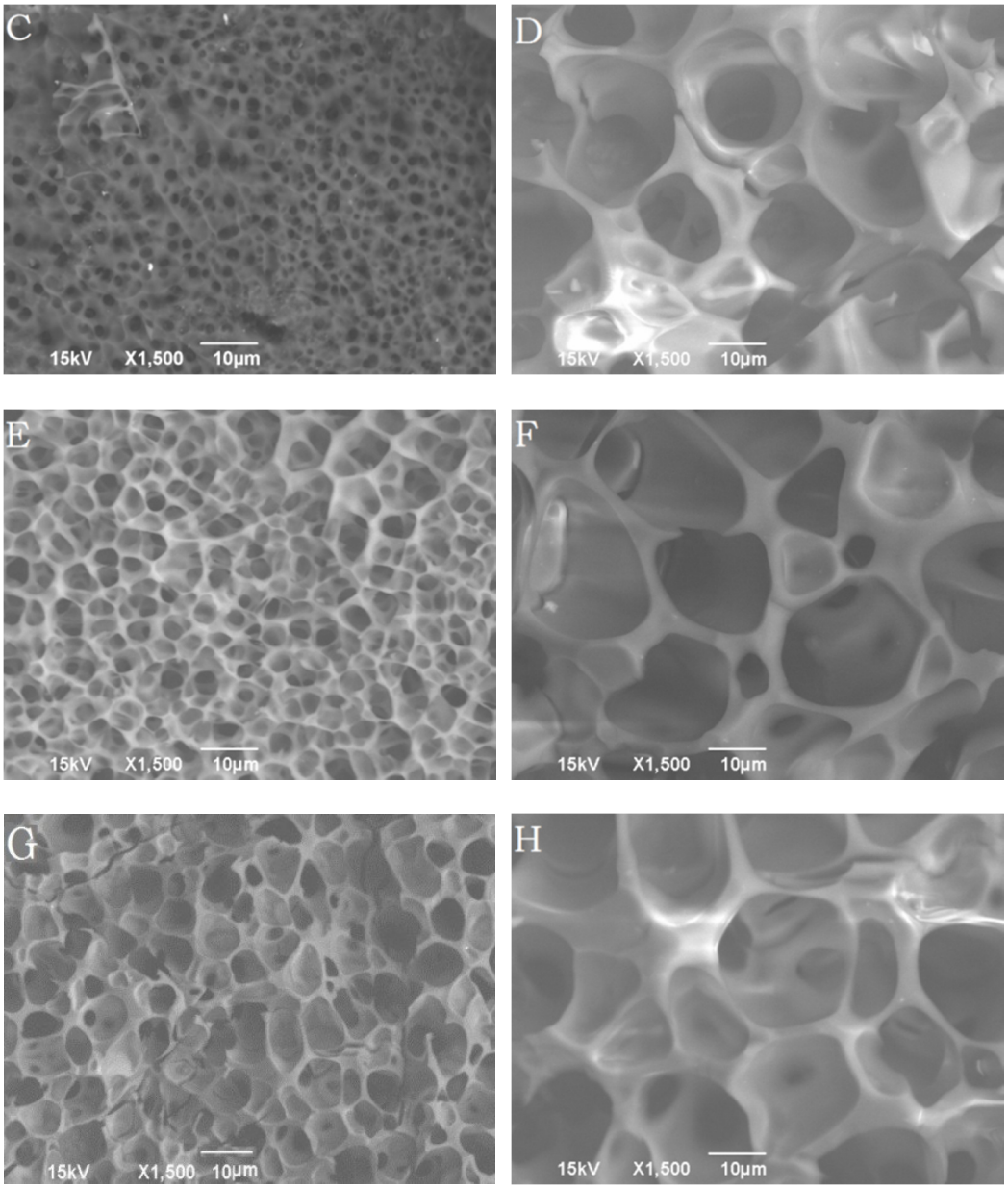

Figure 21. Cryo-SEM images of porous morphology of freshly cut surfaces of the polymeric delivery systems loaded with risperidone (30 and 60 days) (C-D), insulin (30 and 60 days) (E-F), and BSA (30 and 60 days) (G-H) maintained at body temperature (5 min sublimation)

3.5. Effect of Increasing Molecular Size on In Vitro Release Behavior of Thermosensitive Polymeric Delivery Systems

The effect of molecular size and solubility on the in vitro release profile of delivery system was studied using insulin, zinc-insulin and chitosan-zinc-insulin complexes. The in vitro

release profile is presented in figure 22. It was observed that the rate of release of insulin monomers was faster as compared to zinc-insulin hexamers or chitosan-zinc-insulin complexes. Insulin containing formulations showed highest initial burst release (14.21±0.51%), followed by zinc-insulin (9.23±1.25%), and chitosan-zinc-insulin complexes (8.87±1.5%). The delivery system containing chitosan-zinc-insulin complex showed higher correlation coefficient (r^2=0.983), followed by zinc-insulin (r^2=0.95), and insulin alone (r^2=0.884), respectively, for zero order release kinetics.

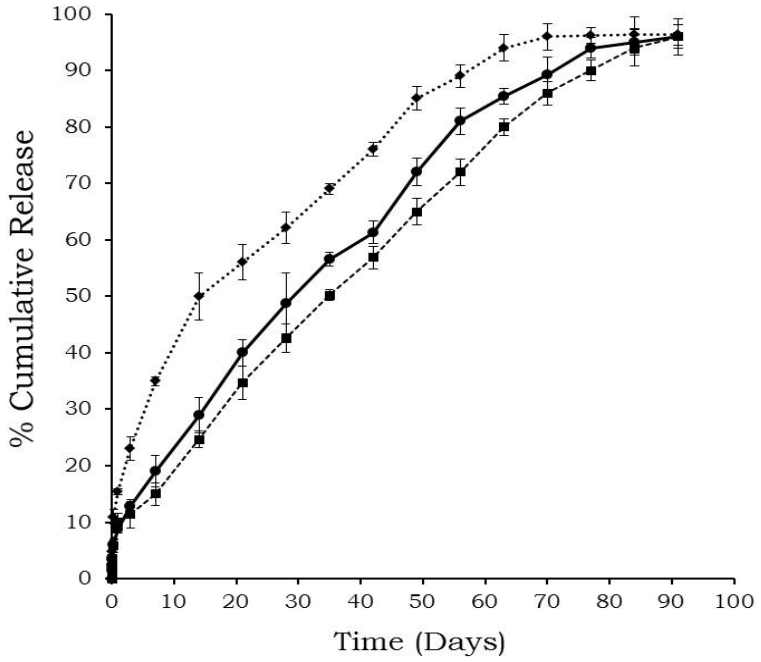

Figure 22. In vitro release profiles of (♦) insulin, (●) zinc-insulin, and (■) chitosan-zinc-insulin complex released from 30% w/w copolymer A containing delivery systems (n=4, mean ± SD, drug loading: 0.3% w/v)

3.6. Effect of Chitosan (Cationic Polymer) on pH of Release Medium During Hydrolytic Degradation

The change in pH of the delivery system during hydrolytic degradation in presence and absence of a cationic polymer, chitosan is presented in figure 23. It was observed that the

delivery system containing copolymer A alone showed gradual reduction in pH, and the pH dropped rapidly after ~40 days of incubation, and at the end of 70 days, it reached to ~4.5. In contrast, the delivery system containing chitosan resisted the change in pH for ~45-50 days, and then pH reduced gradually over the period of 70 days. However, the pH of the release medium still remained higher as compared to the delivery system without chitosan.

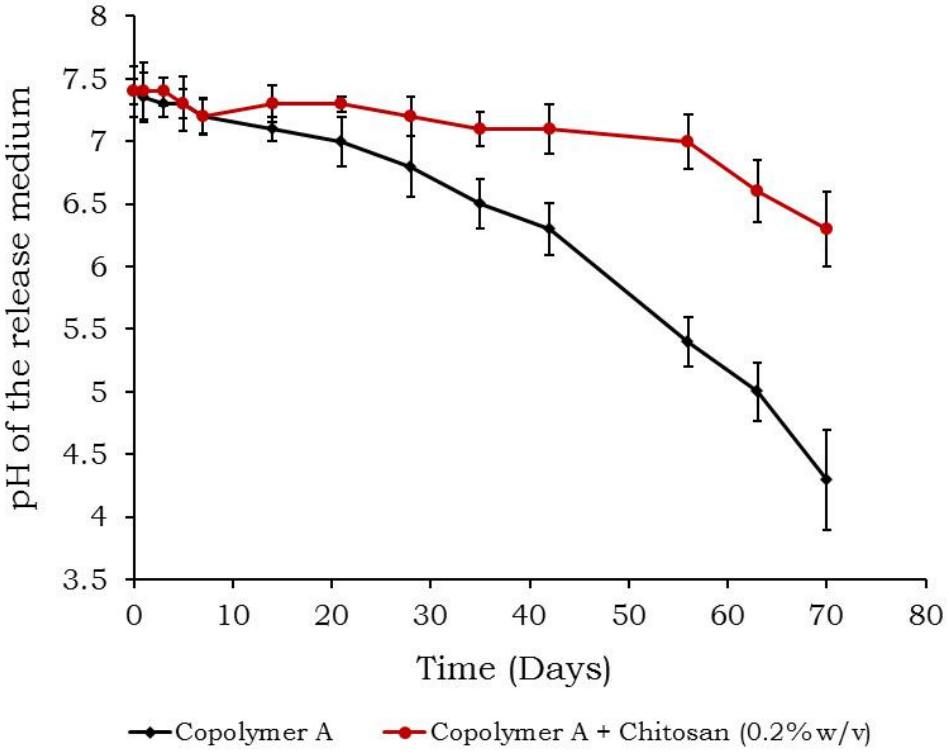

Figure 23. Change in the pH of the release medium during hydrolytic degradation of copolymer A (♦) copolymer alone, and (●) copolymer A + Chitosan (n=4, mean ±SD)

3.7. Preparation of Polymer Formulations for Insulin, In Vitro Release, and Stability

The polymeric formulations containing insulin, or zinc-insulin were easily injectable through 25 G needle at room temperature and formed gel in ~30 sec upon incubation at body temperature.

3.7.1. Effect of polymer concentration, zinc addition and insulin loading on in vitro release of insulin released in vitro

Figures 24 and 25 show the release profiles of insulin alone and in presence of zinc at 60 mg loading. We found 11.45±2.3%, and 10.28±1% initial burst release of insulin from formulations containing insulin alone in 30% and 40% w/w polymeric systems. While, 7.64±0.96%, 5.41±3.3% burst release of insulin was observed from formulations containing zinc-insulin, in 30% and 40% w/w polymeric delivery systems, respectively. In addition to reduced initial burst release, zinc also helped control the release of insulin from the delivery system for ~84 days. The delivery system containing insulin alone showed poorly controlled release and only 70-75% of the total insulin loading released from delivery system at the end of three months. It was observed that increasing polymer concentration from 30 to 40 % w/w (formulations I-III, and II-IV) improved the correlation coefficients for zero order for insulin, and zinc-insulin.

The release kinetics is listed in table 11. The insulin loading in the delivery system was selected to meet the basal insulin requirement (0.5-1 IU/h corresponding to 0.5-1mg/day) for two to three months. We used the release kinetics equations as follows: zero order ($M_t/M_\infty = k\,t$), First order $\ln[(M_t/M_\infty)] = kt$, and Higuchi $(M_t/M_\infty) = kt^{0.5}$, where (M_t/M_∞) is the fractional release of the loaded protein, k is a kinetic constant, and t is the release time.

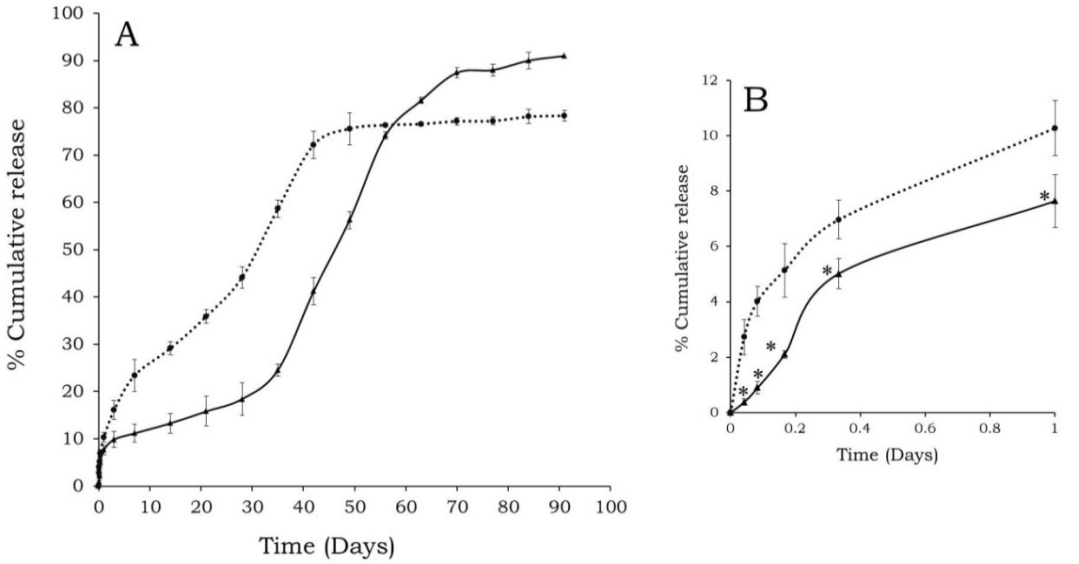

Figure 24. In vitro release of insulin from 30% w/w thermosensitive polymeric delivery system (A), (●) 60 mg insulin alone and (▲) 60 mg zinc-insulin, and initial burst release (B) of insulin from the formulations
(n=4, mean ± SD, *: significantly lower at p<0.05)

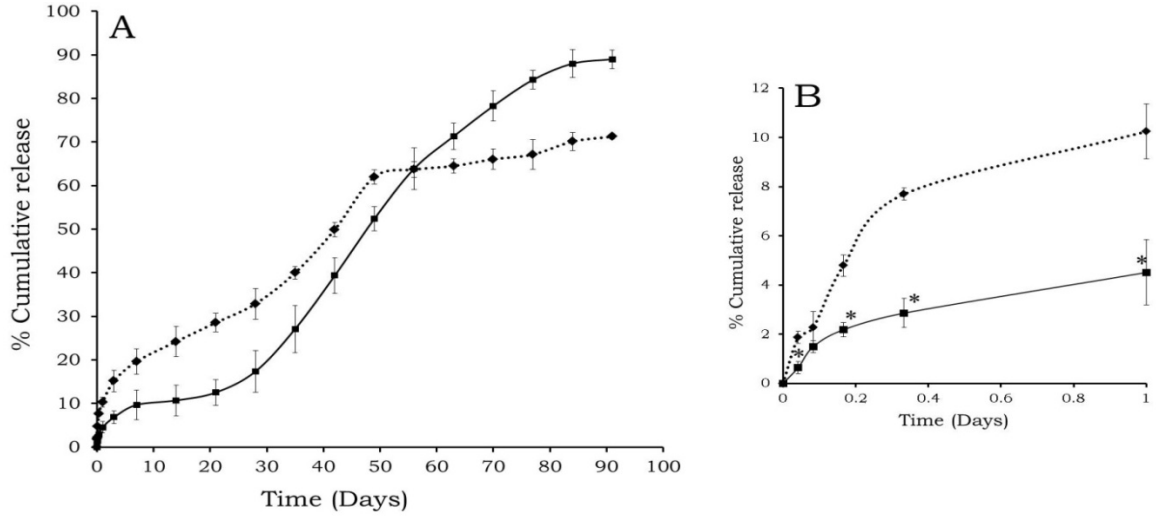

Figure 25. In vitro release of insulin from 40% w/w thermosensitive polymeric delivery system (A), (♦) 60 mg insulin alone and (■) 60 mg zinc-insulin, and initial burst release (B) of insulin from the formulations
(n=4, mean ± SD, *: significantly lower at p<0.05)

Table 11. Release kinetics of insulin from formulations

Formulations	Insulin loading	Zero order (r^2)	Higuchi (r^2)
I	60 mg	0.88	0.94
II	60 mg	0.91	0.82
III	60 mg	0.90	0.91
IV	60 mg	0.93	0.87
V	60 mg	0.86	0.92
VI	60 mg	0.90	0.89
VII	80 mg	0.88	0.80
VIII	100 mg	0.83	0.77

Since zinc addition significantly reduced the initial burst release of insulin at 60 mg drug loading, the effect of zinc addition (1:5 insulin hexamer: zinc ions) on insulin release from the thermosensitive delivery systems was determined at higher insulin loading (80 and 100 mg insulin). The release profile of insulin from all formulations is presented in figure 26. The in vitro release study showed that the addition of zinc to insulin lowered the initial burst release in comparison to formulation without zinc, even at higher protein loading. The results indicate that the protein loading played a major role in controlling the release. There was no significant difference in initial burst release (7.00±0.41, 7.91±0.15, and 8.33±0.12 %) from formulations containing 60 mg insulin alone, and 60, 80 and 100 mg zinc-insulin, respectively. Compared to the large burst release (~10.4%) from formulation containing insulin alone, addition of zinc significantly ($p<0.05$) reduced the initial burst release to a relatively low level. After the initial burst an extended lag period was observed where a negligible amount of insulin was released

from the delivery system. In case of all formulations a sudden increase in the release rate (secondary burst release) was observed after ~25-35 days. A consistent and complete release of insulin was expected due to the progressive degradation of the delivery system, but it was observed that as the insulin loading was increased from 60 to 100 mg, only 68-70% of the total insulin loading was released. As the amount of insulin was increased in the delivery system from 60 to 80 and 100 mg, it reduced the correlation coefficient for zero order release (R^2: 0.90, 0.88, 0.83).

3.7.2. Stability studies of insulin released in vitro

The stability of in vitro released insulin was determined by CD, PAGE/SDS-PAGE, and MALDI-TOF MS.

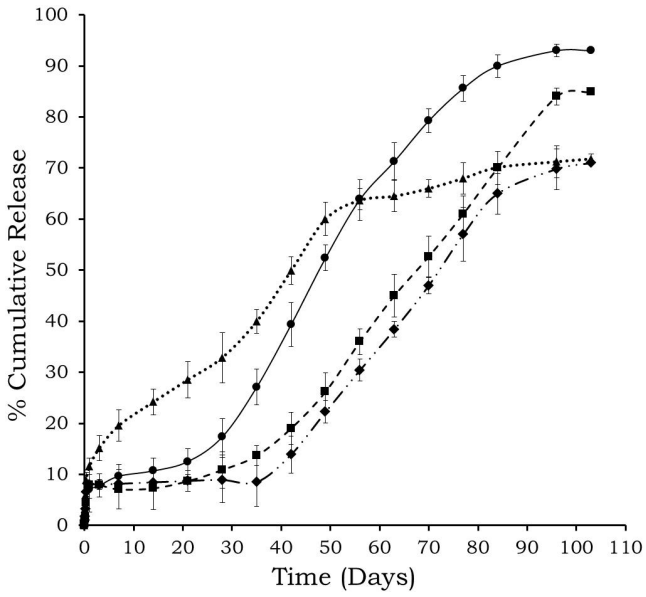

Figure 26. Effect of insulin loading on in vitro release profile of insulin from 30% w/w polymeric delivery system (▲) 60 mg insulin alone, (●) 60 mg zinc-insulin, (■) 80 mg zinc-insulin, and (♦) 100 mg zinc-insulin (n=4, mean ± SD)

3.7.2.1. Circular dichroism spectroscopy (CD)

The representative far UV-CD spectra of insulin released at various time points from delivery systems containing zinc-insulin are presented in figure 27A. The CD spectra in far UV

region showed presence of two characteristic minima at 208 and 222 nm indicating the secondary structure of insulin was preserved up to 42 days. An increase in random coils and reduction in α-helix and β-sheets (reduction in the minima at 208 and 222 nm) in secondary structure of released insulin was observed after ~56 days from all formulations as compared to fresh insulin. The secondary structure analysis of released samples of insulin is presented in table 12. During tertiary structure analysis it was observed that the tyrosyl signal at 278 nm in near UV-CD spectra was increased in the initially released samples of insulin. The results indicated that the increased in the intensity is noticed when insulin is in the form of hexamers, but eventually the signal intensity reduced and was comparable to that of fresh insulin (figure 27B). Thus insulin was released in the form of hexamers initially, and as the release duration proceeded, they dissociated into dimers and hexamers.

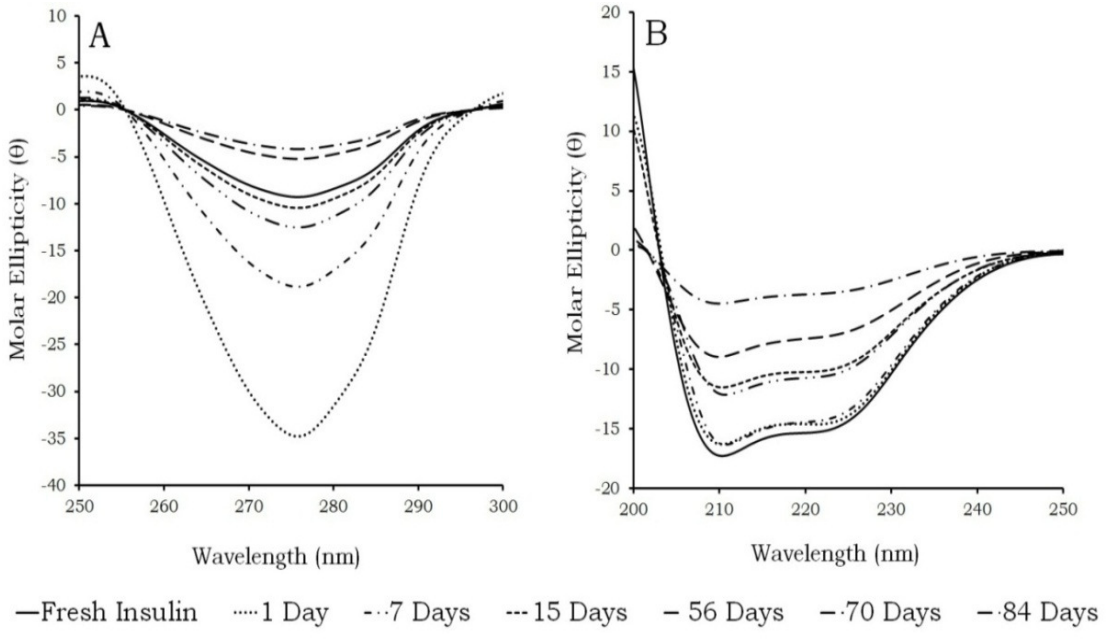

Figure 27. Far UV-CD (A) and near UV-CD (B) spectra of insulin released from formulation containing 60 mg zinc-insulin in 30% w/w polymeric delivery system

Table 12. Secondary structure analysis of insulin released from formulations

Formulations	Insulin loading	Days	α Helix	β Sheets	β turns	Random Coils
Fresh Insulin in PBS	---	---	39±1	16±2	21±2	24±4
A (Insulin alone)	60 mg	30	18±2	6±1	47±3	29±3
		60	9±2	8±1	44±1	39±2
B (Zinc-insulin)	60 mg	30	35±2	20±4	22±1	23±2
		60	20±3	9±1	41±2	30±2
C (Zinc-insulin)	80 mg	30	25±3	15±3	40±4	20±3
		60	12±3	6±2	47±6	35±2
D (Zinc-insulin)	100 mg	30	38±1	10±3	22±3	30±2
		60	10±2	12±2	46±5	32±3

(n=4, mean ± SD)

3.7.2.2. Polyacrylamide gel electrophoresis (Native and SDS-PAGE)

Freshly prepared sample of insulin showed a band at 6 kDa in native PAGE. Representative gel images for native PAGE and SDS-PAGE for released samples of insulin from formulation containing zinc-insulin are presented in figure 28A and B. We found higher molecular weight bands at 12 and 36 kDa, initially (released samples of 7 days) in native PAGE experiments along with a strong presence of insulin monomers at 6 kDa. These higher molecular weight bands indicated the presence of insulin dimer aggregates (~ 12 kDa) or hexameric insulin (36 kDa). Though monomeric insulin band was found during native PAGE analysis, the insulin released from formulations was in the form of mixture containing dimers/hexamers. The covalent or non-covalent nature of aggregates can be determined using SDS-PAGE under non-reducing conditions, since it dissociates non-covalent aggregates. A single band corresponding to

6 kDa was observed in SDS-PAGE experiments under non-reducing conditions. The formulation without zinc also showed a single band around 6 kDa indicating that no dimerization occurred during formulation of the delivery system. No additional bands were observed below 6 kDa in both SDS-PAGE and native PAGE experiments.

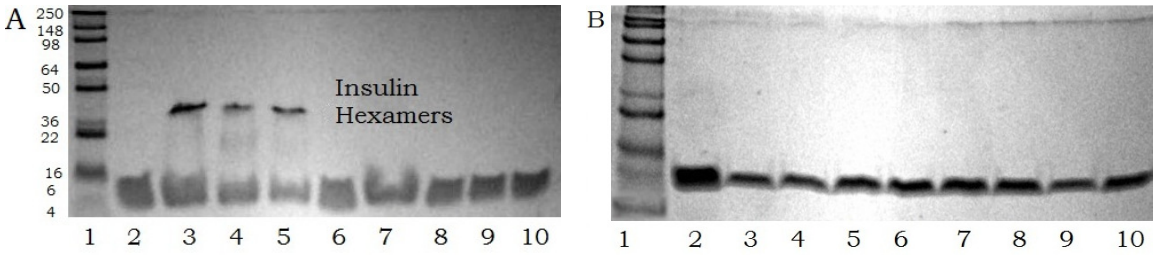

Figure 28. Native PAGE (A) and SDS-PAGE (B) analysis of insulin released (lane 1: molecular marker, lane 2: fresh insulin and lanes 3-10: insulin released at day 1, 3, 7, 14, 28, 42, 56, and 77 days from zinc-insulin containing polymeric delivery system)

3.7.2.3. MALDI-TOF mass spectroscopy

The MALDI-TOF MS helped to detect the chemical stability of released insulin from the delivery systems containing zinc-insulin and the results are presented in figure 29. Fresh insulin shows peak at ~5808 Da. A single peak corresponding to native insulin was observed corresponding to a molecular mass of $(M+H)^+$ 5808.477 Da. No major degradation products were detected in MALDI-TOF analysis till one month in vitro release. Some degradation products were observed in the released samples after two months. The released sample of insulin showed the presence of a peak corresponding to native insulin along with a small peak at 2907.95 Da along with some unidentified peaks.

3.8. Chitosan-Zinc-Insulin Complex Formation, Dissociation, and Effect of Chitosan Addition on Insulin Stability

To reduce the initial burst release from the delivery system, and to reduce the diffusion of insulin monomers from the polymeric delivery system, chitosan-zinc-insulin complexes were

prepared. The complexes were incorporated into the thermosensitive polymeric delivery system and the effect of chitosan and zinc addition on initial burst release, in vitro release profile of insulin as well as stability was observed. Since insulin is stable in the pH range of 5-8, complex formation between insulin and chitosan was characterized using turbidimetry (preliminary studies) at a pH range of 5 to 8. After addition of chitosan to insulin, a gradual increase in the transmittance was observed, and plateau appeared at pH ~6.5-6.8. Above pH 6.8, since both insulin (isoelectric point 5.4) and chitosan bear opposite charges, large insoluble complexes were observed indicated by increased turbidity and subsequent precipitation. It was also noted that the insulin/chitosan complex formation took place in the pH range of 6.5-6.8 irrespective of the chitosan concentration. The entrapment efficiency was found to be ~70-76%.

The results of gel retardation assay and SDS-PAGE are depicted in figure 30. It was observed that when the chitosan: insulin weight ratio was increased to 4:1; most of the protein was retained in the gel wells indicated by the disappearance of band at 6 kDa (figure 30A). After incubation of chitosan-insulin complex with an anionic surfactant SDS it was noted that insulin was released from the complex and a band corresponding to fresh insulin was observed at (6 kDa) (figure 30B).

3.8.1. Fluorescence spectroscopy

The fluorescence property of insulin (tyrosine/phenylalanine fluorescence) was studied after addition of insulin to chitosan solutions at increasing weight ratios and the spectra is presented in figure 31. The fluorescence spectra of insulin in presence of increasing amount of chitosan indicated no shift in the $\lambda_{emission}$ for tyrosine/phenylalanine of insulin. It was observed that chitosan does not show any fluoresce when excited at 280 nm. But insulin molecules excited at 280 nm showed the fluorescence spectra collected at wavelength between 295-395nm (λ_{em}). It

was noted that even after addition of increasing amount of chitosan to insulin there was no shift in the λ_{em} appeared due to tyrosine/phenylalanine residues. These results suggested that there is no change in the tertiary structure of insulin in presence of chitosan at the concentrations tested. This further substantiates that the 3-D structure of insulin is conserved during complex formation with chitosan.

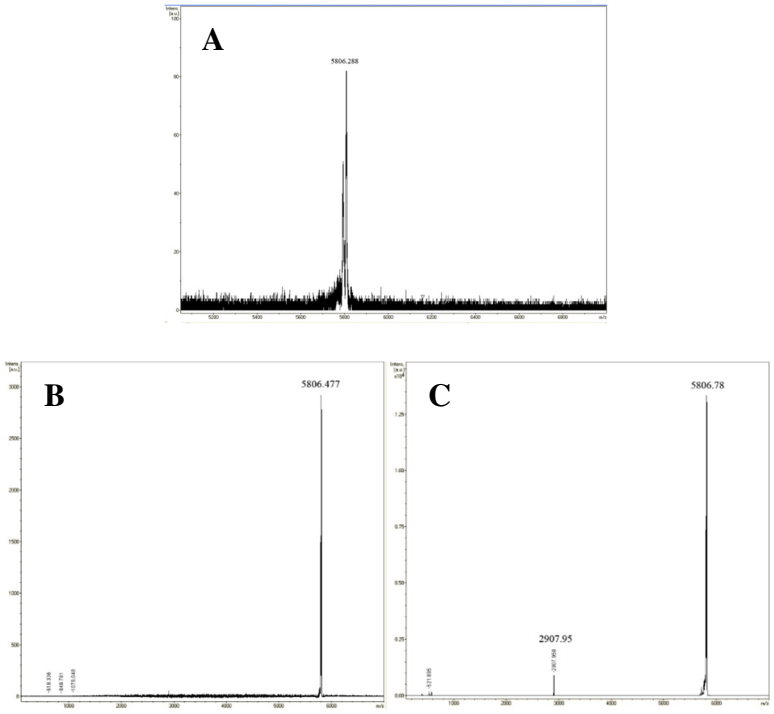

Figure 29. MALDI-TOF mass spectra of fresh insulin (A), insulin released from the polymeric delivery system containing zinc-insulin at 1 and 2 months (B and C)

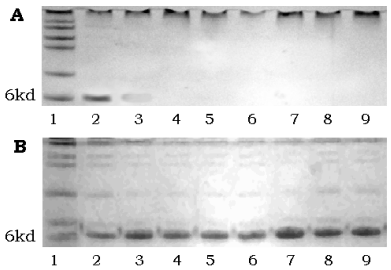

Figure 30. Gel retardation assay (native PAGE) (A), and SDS-PAGE (B) for insulin-chitosan complexes (lane 1: molecular marker, lane 2: fresh insulin, lanes 3-9: insulin: chitosan 1:0.5, 1:1, 1:2, 1:4, 1:8, 1:16 and 1:32 w/w)

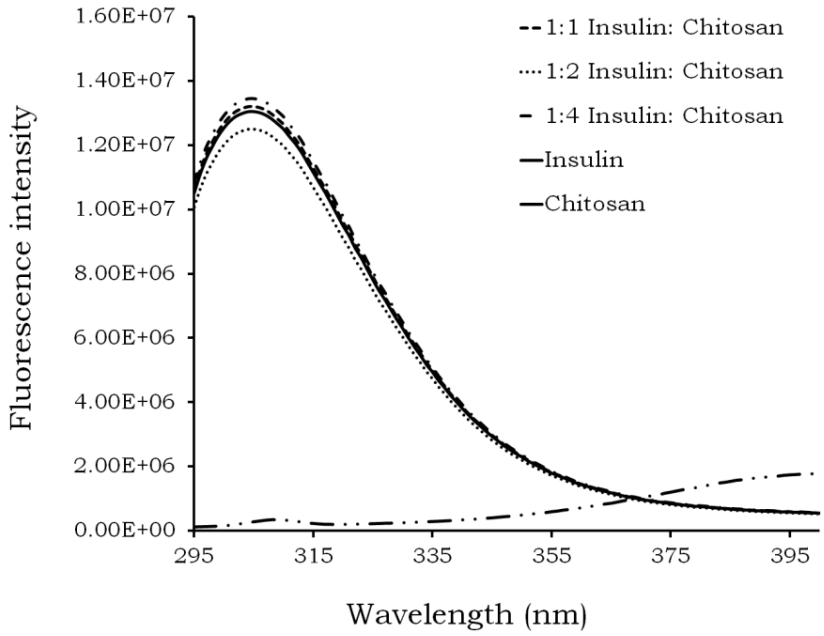

Figure 31. Fluorescence spectra of insulin after addition of chitosan (insulin: 1 mg/ml, pH 6.8, chitosan: 0.0666 mg/ml, pH 6.8)

3.8.2. Circular dichroism spectroscopy (CD)

The change in the secondary structure of insulin in the presence of chitosan was determined by CD spectroscopy and the results are presented in figure 32. Fresh insulin shows the presence of 2 distinct minima at 208 and 222 nm in far UV-CD region. This is due to the presence of α helix in the structure of insulin. After addition of chitosan to insulin at increasing weight ratios and incubating for 20 min, it was observed that there was no shift in the minima observed at 208 and 222 nm, but, a very small reduction in the CD signal intensity was observed with increased chitosan concentration.

3.8.3. Differential scanning calorimetry (DSC)

DSC also helped to study the structural changes in insulin after addition of chitosan. DSC spectra of insulin in presence of zinc, and chitosan are presented in figure 33. Fresh insulin showed two distinct transitions at 68.0±2.1°C (T_{m1}) and 82.4±1.41°C (T_{m2}). This biphasic

denaturation was observed due to the presence of dimers and hexamers present. Further increase in T_m and ΔH (90.3±0.79°C, and ~11.6 KCal/mol) was observed after addition of chitosan to zinc-insulin compared to zinc-insulin (84.5±1.2°C, and ~9.89 KCal/mol). At increasing the chitosan amount in the complex analyzed with DSC showed that the T_m reached to a maximum value of 90±0.8°C. Since addition of chitosan solution (0.066 mg/ml) to insulin solution (1 mg/ml) at a ratio of 1:2 v/v (1:15 w/w) showed stabilizing effect on zinc-insulin indicated by increased T_m which reached to a maximum value of 90.3°C, this or higher weight ratio was used during formulating the delivery system containing chitosan-zinc-insulin complex.

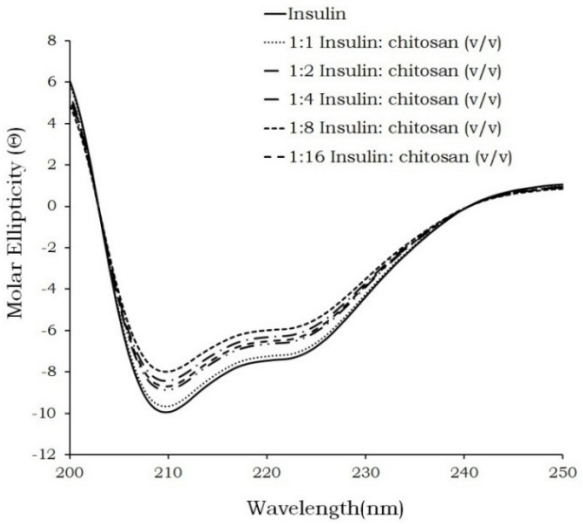

Figure 32. Far UV-CD spectra of insulin after addition of chitosan (insulin: 1 mg/ml, pH 6.8, chitosan: 0.0666 mg/ml, pH 6.8)

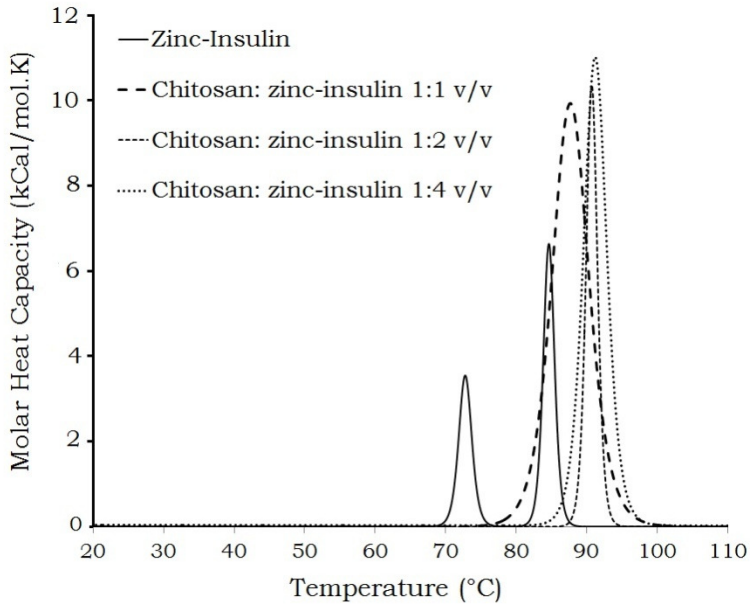

Figure 33. DSC thermograms of zinc-insulin after addition of chitosan (insulin: 1 mg/ml, pH 6.8, chitosan: 0.0666 mg/ml, pH 6.8)

3.8.4. Stability of insulin, zinc-insulin and chitosan-zinc-insulin complex in presence of lactic acid

Figure 34 represents the thermostability of insulin, zinc-insulin, and chitosan-zinc-insulin complexes in presence of lactic acid. It was noticed that presence of lactic acid completely destroyed the insulin structure, and reduced the thermostability of zinc-insulin indicated by shift in T_m to 60 and 79°C, respectively for insulin monomers and hexamers (figure 34A). But, it did not significantly affect insulin in the form of chitosan-zinc-insulin complex (figure 34B). These results indicate the additional stabilizing effect of chitosan on protein structure. Chitosan also possesses good buffering ability which might have resisted the major pH change in the microenvironment of the delivery system (figure 35).

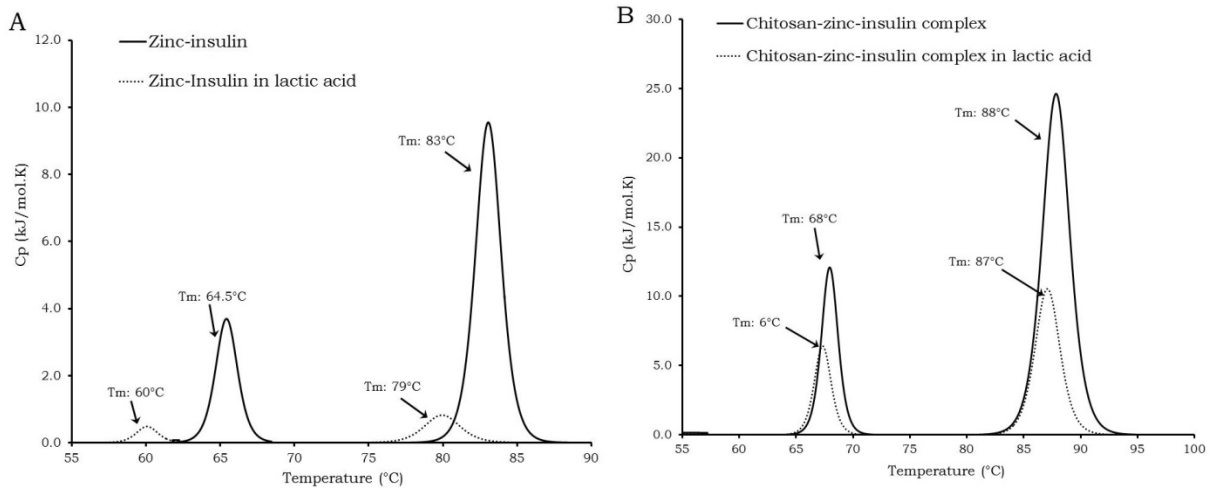

Figure 34. DSC thermograms of zinc-insulin (A) and chitosan-zinc-insulin (B) complex incubated with lactic acid

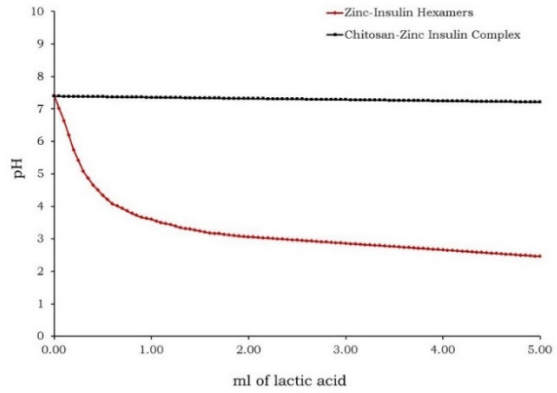

Figure 35. Buffering ability of chitosan-zinc-insulin complex

It was observed that the chitosan could effectively resist the change in the pH by lactic acid, which is generated by degradation of the thermosensitive polymer, even in the highly unlikely scenario of complete, instantaneous degradation of polymer in the delivery system.

3.9. Formulation of the Delivery System Containing Chitosan-Zinc-Insulin Complex and In Vitro Release

The amount of free insulin present in the supernatant was ~18-20% of the total loading. The formulations were injectable through 25 G needle at room temperature without clogging the

needle, and showed rapid conversion from sol to gel within ~ 50 sec near body temperature. The effect of addition of chitosan on in vitro release of insulin at low protein loading (5 mg) was evaluated in our initial studies. Figure 36A represents the release profile of insulin alone, zinc-insulin, chitosan-insulin and chitosan-zinc-insulin complex from thermosensitive polymeric delivery systems (30% w/w). The formulation containing chitosan-insulin and zinc-insulin showed reduction in the initial burst release as compared to formulation containing insulin alone. It was observed that chitosan-zinc-insulin complex helped to reduce the initial burst release, with minimal secondary burst and controlled the release up to ~91 days with the cumulative release of 96%. Significantly low ($p<0.05$) initial burst was observed as compared to insulin alone, zinc-insulin or chitosan-insulin containing formulations (figure 36B). The release constants (zero order) were 0.84, 0.93, 0.93, and 0.99 for formulations containing insulin alone, zinc-insulin, chitosan-insulin and chitosan-zinc-insulin complex, respectively.

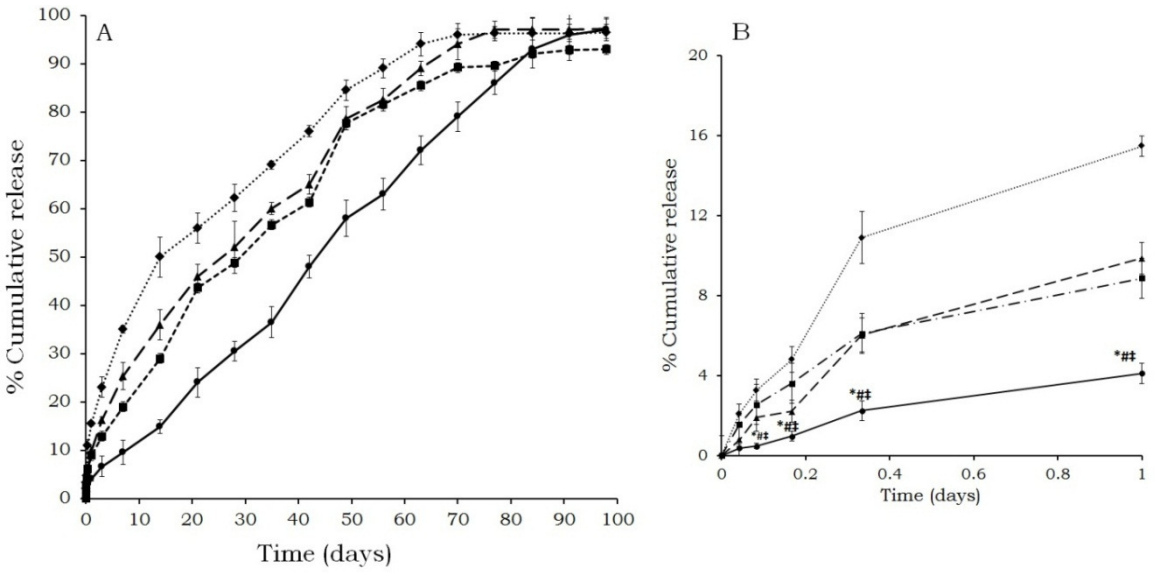

Figure 36. Effect of chitosan on in vitro release of insulin from 30% w/w copolymeric delivery system (A) at insulin loading 5 mg and initial burst release from the formulations (B) (♦) insulin alone, (■) chitosan-insulin, (▲) zinc-insulin, (●) chitosan-zinc-insulin complex; (n=4, mean ± SD, P <0.05, *: significant compared to insulin alone, #: significant compared to zinc-insulin, and ‡: significant compared to chitosan-insulin loaded delivery system)

3.9.1. Optimization of the delivery system for higher drug loading and in vitro release

From the results of the preliminary in vitro release experiments as well as stability studies the polymeric delivery systems were optimized. The delivery systems were formulated to deliver 30, 45, and 60 mg insulin in the form of chitosan-zinc-insulin complex. The amounts of insulin correspond to the basal level requirement for three months. The concentration of the thermosensitive polymer, amount of chitosan, zinc ions to insulin ratio were fixed to get the desired release profile. Initially in our preliminary studies it was noted that, at zinc: insulin hexamer ratio more than 4:1, some degradation products were observed might be due to the presence of higher amount of zinc in the delivery system. At the same time it was observed that at higher protein loading use of polymer concentration more than 30% w/w lead to highly viscous formulation which was difficult to inject from 25 G needle at room temperature. Hence zinc: insulin hexamer ratio was optimized to 4:1 and the concentration of the thermosensitive polymer was fixed at 30% w/w. During optimization studies, the amount of chitosan in the delivery system was varied keeping all other formulation parameters constant, to determine the effect of increasing chitosan concentration on initial burst release as well as the entire release profile of insulin. The in vitro release profile of insulin at higher loading (30, 45 and 60 mg) is displayed in figures 37-40. Figure 37 displayed the release profile of insulin in vitro from formulations containing 30 mg insulin alone, zinc-insulin, chitosan-insulin or chitosan-zinc-insulin in thermosensitive polymeric delivery system (formulations A-D). Addition of zinc to insulin (Formulation B) showed significant reduction ($P<0.05$) in the initial burst (7.64±0.91%), compared to the formulations containing insulin alone (10.28±1.2%) and chitosan-insulin (13.24±2.07%). The formulation containing chitosan-insulin showed high initial burst and the overall release period up to 45 days. Along with the initial burst, only 65% of the total protein

was released from the delivery system. Even though zinc helped to prolong the overall release period (~63 days) as compared to insulin alone or chitosan-insulin, a high secondary burst release was also observed after ~35 days. The correlation coefficients (r^2) for the insulin release profile from various formulations are presented in table 13. All delivery systems indicated best fit for Higuchi model, while chitosan-zinc-insulin containing delivery system showed best fit for zero order release model. This high zero order correlation is highly desirable to ensure a constant release from the delivery systems. The amount of insulin remained in the delivery systems (A, B and C) after three months of release was approximately 15-20%. On the other hand, continuous release of insulin was observed over 84 days from the delivery system containing chitosan-zinc-insulin complex (formulation D). A significant decrease ($p<0.05$) in initial burst (3.85±0.64) was observed compared to all other formulations. Additionally, the release of insulin was complete from formulation D compared to formulations A, B and C.

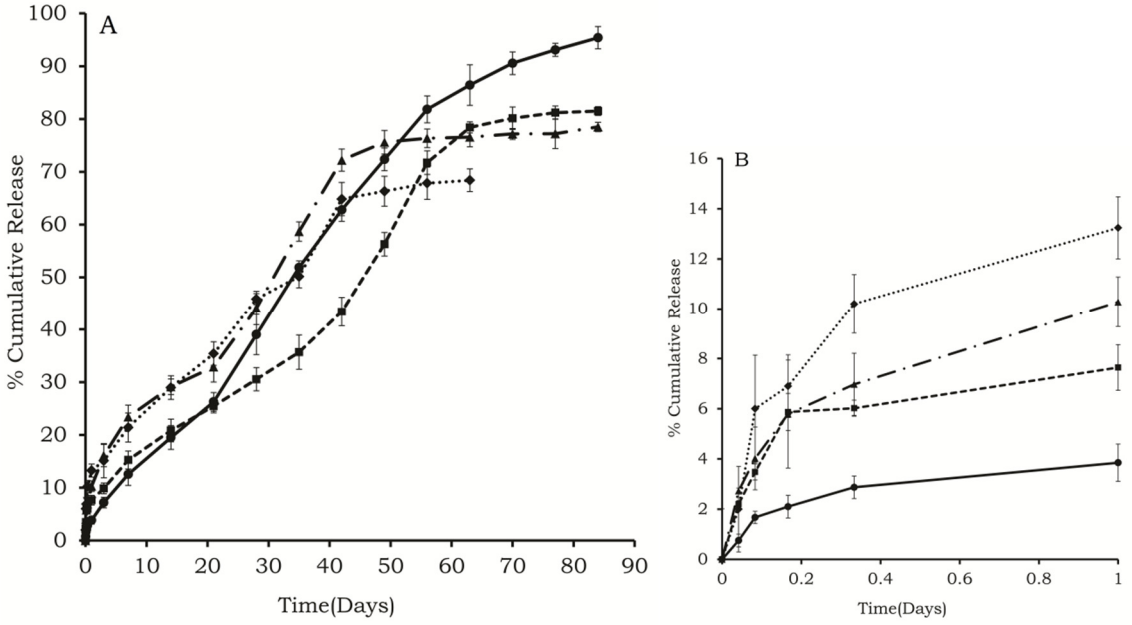

Figure 37. In vitro release of insulin from 30% w/w copolymeric delivery system (A) at insulin loading 30 mg, and initial burst release of insulin from formulations (B) ((♦) chitosan-zinc-insulin complex, (■) zinc-insulin, (▲) insulin alone, and (●) chitosan-insulin; (n=4, mean ± SD))

The influence of increasing amount of chitosan (0.4% w/v) on insulin release was also investigated. Increasing the amount of chitosan from 0.2% to 0.4% w/v in the delivery system (Formulation E) did not significantly affect the initial burst, as well as the release rate of insulin as shown in figure 38. When the chitosan amount in the delivery system was increased further, it was observed that it affects the injectability of the formulation. The insulin loading was increased further to 45 mg and the in vitro release of insulin was evaluated. With increase in insulin loading from 30 mg to 45 mg in polymeric formulation H (chitosan-zinc-insulin complex), increase in the initial burst was observed, and the release was controlled for ~91 days (figure 39).

Table 13. Release kinetics of insulin from formulations

Formulations	**Insulin loading**	**PLA-PEG-PLA Copolymer (w/w)**	**Zero order r^2**	**Higuchi r^2**	**First order r^2**
A (Insulin alone)	30 mg	30%	0.90	0.95	0.67
B (Zinc-insulin)	30 mg	30%	0.97	0.93	0.77
C (Chitosan-insulin)	30 mg	30%	0.89	0.97	0.64
D (Chitosan-zinc-insulin)	30 mg	30%	0.98	0.96	0.76
F (Insulin alone)	45 mg	30%	0.89	0.96	0.66
G (Zinc-insulin)	45 mg	30%	0.95	0.93	0.74
H (Chitosan-zinc-insulin)	45 mg	30%	0.98	0.94	0.78
I (Insulin alone)	60 mg	30%	0.87	0.89	0.80
J (Zinc-insulin)	60 mg	30%	0.90	0.807	0.58
K (Chitosan-zinc-insulin)	60 mg	30%	0.96	0.91	0.70

Even though the release was controlled in a better way compared to insulin alone (formulation F) and zinc-insulin (Formulation G), only 89% of the total drug was release at the end of three months. A small decrease in the secondary burst was observed compared to the formulations F and G. The in vitro release profile of insulin from the delivery system containing 60 mg insulin in the form of insulin alone, zinc-insulin or chitosan-zinc-insulin complex is depicted in figure 40. Formulation containing insulin alone (formulation I) showed high initial burst (11.45±1.9%) followed by a typical triphasic release pattern.

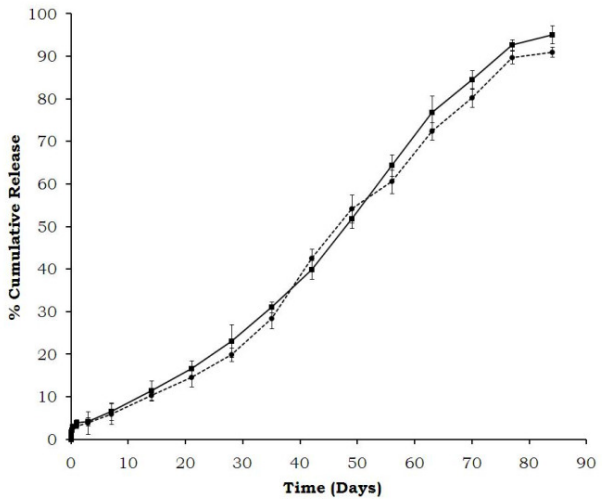

Figure 38. Effect of chitosan amount on in vitro release of zinc-insulin from triblock copolymer at insulin loading 30 mg
(chitosan amount (■) 0.2% w/v, and (●) 0.4% w/v of the delivery system, (n=4, mean ± SD))

Zinc-insulin containing delivery system (formulation J) showed reduction in initial burst release (6.83±0.59%), followed by a constant release rate that was observed up to ~56-63 days. Addition of zinc to insulin reduced the initial burst and prolonged the overall release period. As observed in our earlier studies, a high secondary burst after ~35 days was observed from zinc-insulin containing formulation and almost 55% of the total insulin loading was released in 20 days.

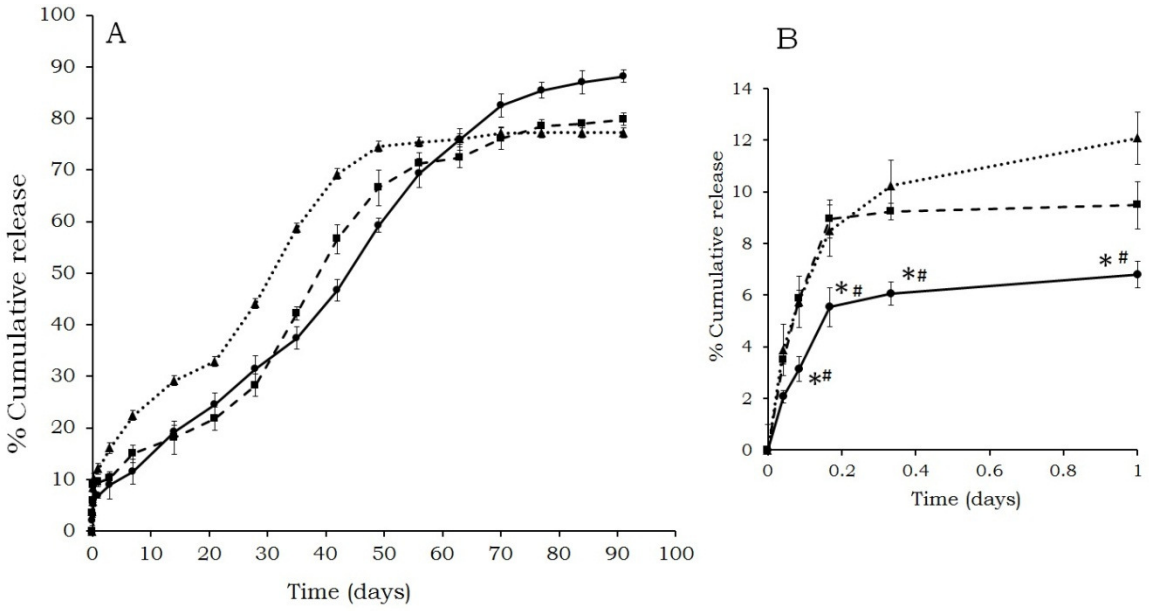

Figure 39. In vitro release of insulin from 30% (w/w) copolymer based delivery system at insulin loading 45 mg (A), and initial burst release of insulin from formulations (B) ((●) chitosan-zinc-insulin, (■) zinc-insulin, and (▲) insulin alone, (n=4, mean ± SD, *: significant compared to insulin alone, #: significant compared to zinc-insulin at P <0.05))

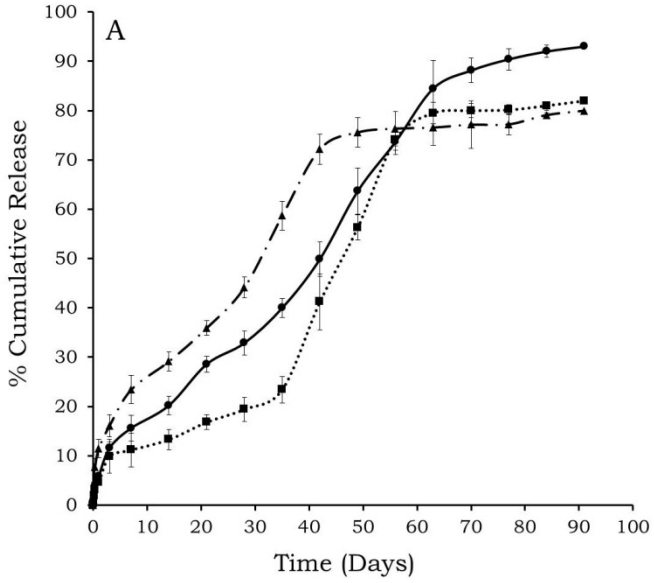

Figure 40. In vitro release of insulin from 30% (w/w) copolymer based delivery system at insulin loading 60 mg
((●) chitosan-zinc-insulin, (■) zinc-insulin, (▲) insulin alone (n = 4, mean ± SD))

Chitosan-zinc-insulin complex (formulation K) showed significant reduction ($P<0.05$) in the initial burst release of insulin (7.54±0.67%), as compared to the formulations containing insulin alone with the cumulative release of 91% of the total insulin loading in 98 days. Similar to our earlier studies, an incomplete release (~70%) was observed from insulin/zinc-insulin containing delivery systems.

3.10. Stability of Insulin Released In Vitro

The stability of released insulin was investigated using series of studies using CD, DSC, PAGE/ SDS-PAGE, HPLC and MALDI-TOF Mass Spectroscopy techniques.

3.10.1. Circular dichroism spectroscopy (CD)

Results depicted in figures 41 (A-D) showed the far UV-CD spectra of fresh and in vitro released insulin from formulations A-H. Native insulin showed well-defined negative bands in CD spectrum with two minima at ~208 and 222 nm, indicating the presence of major alpha helix structure (38%) with a small part of beta-sheets (~17%). Significant attenuation was observed in the percent of α helix (~18%) and β sheets (~4%) for formulation containing insulin alone after ~30 days of release in comparison to the formulations containing zinc-insulin and chitosan-insulin. Even though the released insulin CD spectra from formulation containing zinc closely resembles the native insulin spectrum up to 30 days, demonstrating the structural stabilizing effect of zinc, marked reduction in α helix (19%) and β sheets (8%) was observed in released samples after 45 days. Similarly, addition of chitosan to insulin (formulation C) did not improve its stability and increase in random ordered structures (>65%) was observed after ~30 days. Addition of chitosan to zinc-insulin (formulation D and H) showed additional stabilizing effect, indicated by preservation of secondary structure of released insulin up to 56 days. Reduction in α helix (17%) and β sheets (4%) with corresponding increase (~76%) in unordered structures was

observed in all released samples of insulin after ~60 days of release. The detailed secondary structure analysis of insulin released from formulations A-K is summarized in tables 14 and 15. At 60 mg insulin loading major loss of secondary structure was observed after 35 days of release in case of delivery systems containing insulin alone and zinc-insulin (formulations I and J, respectively). The signal intensity was further reduced after 56 days and the released insulin showed increase in random ordered structures (table 15). Chitosan-zinc-insulin complex helped preserve the secondary structure for ~63 days (formulation K).

The possible changes in the tertiary structure of released insulin were also investigated using near UV-CD spectrum (figures 42 A-D). Fresh insulin showed a negative signal at 278 nm. Increased intensity of near UV-CD signal at 278 nm was observed in released samples of insulin initially, indicating the presence of insulin dimers and hexamers in the released samples. No perturbation in the near UV-CD spectra of insulin confirmed that the tertiary structure of insulin was not affected during release from formulations containing chitosan-zinc-insulin up to 45 days in comparison to formulations containing zinc-insulin, chitosan-insulin and insulin alone. A slight reduction in the signal intensity was observed after 45 days, but it reduced substantially after 56 days. The results suggest that there was partial loss of tertiary structure of released insulin after 56 days.

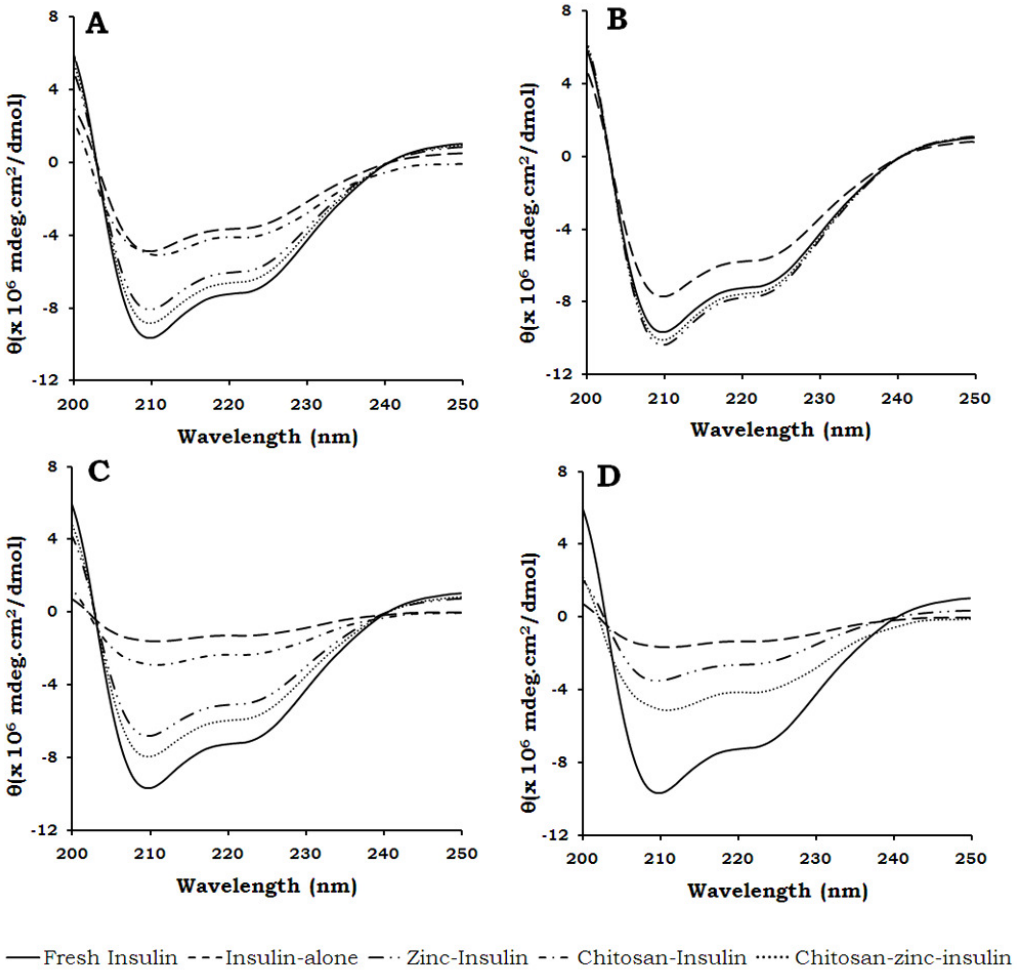

Figure 41. Far UV CD spectra of released insulin from the delivery system at 30 mg insulin loading at 15 (A), and 45 days (C), and released insulin from the delivery system containing 45 mg/ml of insulin at 30 (B), and 60 days (D)

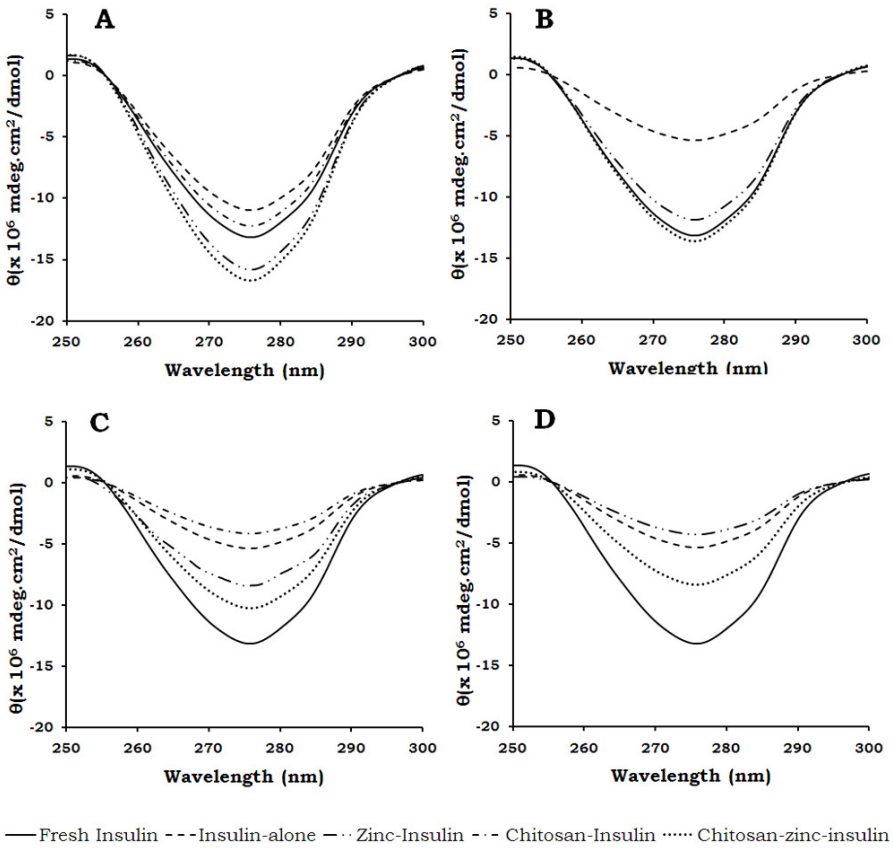

Figure 42. Near UV-CD spectra of released insulin from the delivery system containing 30 mg/ml of insulin, at 15 (A), and 45 days (C), and released insulin from the delivery system at 45 mg insulin loading, at 30 (B), and 60 days (D)

Table 14. Secondary structure analysis of insulin released from formulations (30 and 45 mg insulin loading)

Formulations	**Days**	**α Helix**	**β Sheets**	**β turns**	**Random Coils**
Fresh Insulin in PBS	---	38±1	17±2	23±2	22±4
	30	18±4	4±2	49±4	29±4
A (Insulin alone)	60	8±1	5±1	49±2	38±2
	90	7±3	6±2	46±3	41±3
	30	37±2	18±1	26±2	19±4
B (Zinc-insulin)	60	20±3	7±1	43±2	30±2
	90	12±3	7±4	45±3	36±5

(Continued)

Table 14. Secondary structure analysis of insulin released from formulations (30 and 45 mg insulin loading) (Continued)

Formulations	Days	α Helix	β Sheets	β turns	Random Coils
	30	20±2	12±5	45±1	23±2
C (Chitosan-insulin)	60	12±3	8±2	46±6	34±3
	90	6±2	6±2	44±5	44±2
	30	31±1	10±3	28±1	31±2
D (Chitosan-zinc-insulin)	60	19±2	4±1	41±3	36±1
	90	13±3	6±3	40±2	41±2
	30	17±1	5±3	44±1	34±2
F (Insulin alone)	60	10±3	5±1	51±3	34±4
	90	6±2	7±4	48±2	39±3
	30	28±1	12±1	28±1	32±2
G (Zinc-insulin)	60	17±3	9±3	44±3	30±1
	90	10±2	8±2	44±1	38±3
	30	29±4	10±2	29±1	32±4
H (Chitosan-zinc-insulin)	60	16±3	4±2	39±4	41±2
	90	13±3	7±3	46±5	34±3

(n=4, mean ± SD)

3.10.2. Differential scanning calorimetry (DSC)

DSC measurements were used for the assessment of conformational stability of various association states of insulin during release. Heat capacity scans originated from fresh insulin, and released samples of insulin, are presented here in figure 43. Fresh insulin showed two distinct transitions at 68.0±2.1°C (T_{m1}) and 82.4±1.41°C (T_{m2}). This biphasic denaturation was observed due to the presence of dimers and hexamers in the sample. Insulin released from the delivery system containing zinc-insulin (formulation B) showed the presence of insulin hexamers, indicated by a single peak observed at 83.3±1.2°C (T_{m2}) at day 7. Insulin released from (chitosan-insulin) formulation C showed presence of mixture of dimers and hexamers. Insulin

released initially from formulation D showed the presence of chitosan-zinc-insulin complex indicated by increased thermal transition observed at 90±0.8°C (T_{m2}) at day 7.

Table 15. Secondary structure analysis of released insulin (60 mg insulin loading)

Formulations	**Days**	**α Helix**	**β Sheets**	**β turns**	**Random Coils**
Fresh Insulin in PBS	---	36±3	17±1	25±4	22±3
	30	18±2	6±4	44±3	32±3
I (Insulin alone)	60	8±3	5±3	43±2	44±4
	90	7±3	6±2	45±2	42±3
	30	34±4	20±2	23±3	23±2
J (Zinc-insulin)	60	14±3	12±1	38±4	36±3
	90	10±4	13±5	44±3	33±3
	30	38±3	15±4	29±3	18±4
K (Chitosan-zinc-insulin)	60	28±3	16±2	26±6	30±3
	90	13±5	10±6	41±3	36±2

(n=4, mean ± SD)

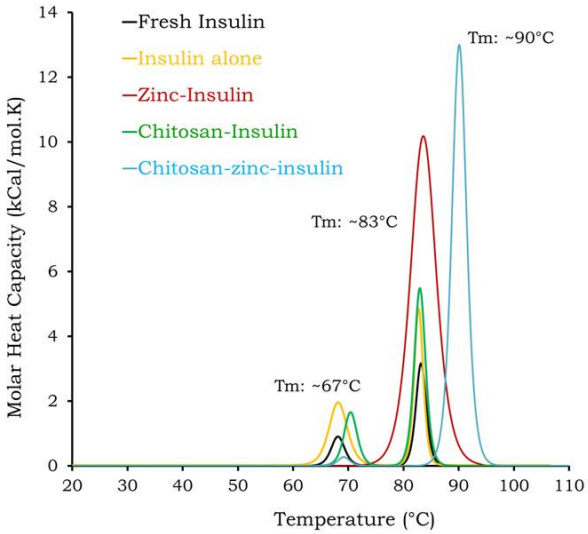

Figure 43. DSC fitted thermograms of released insulin after 7 days from polymeric delivery systems

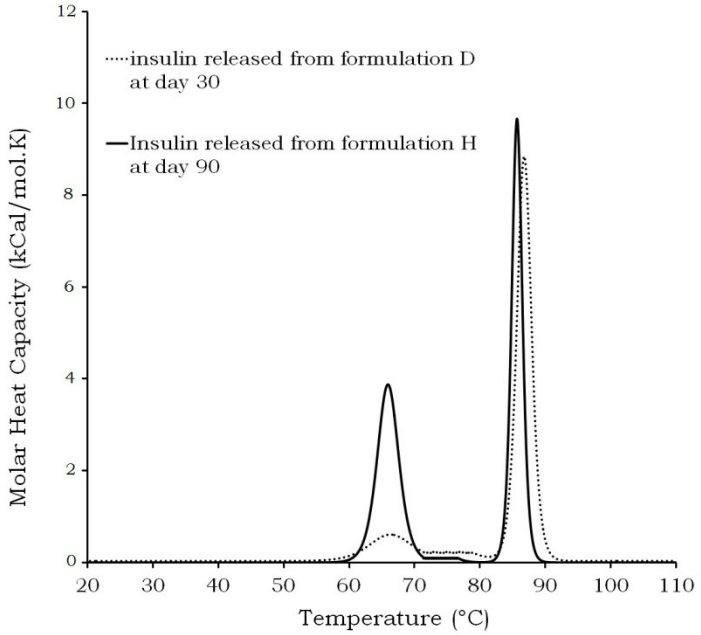

Figure 44. DSC fitted thermograms of released insulin after 30 and 60 days from polymeric delivery systems

The released insulin from formulations containing chitosan-zinc-insulin examined at 30 and 60 days showed the presence of peaks corresponding to unfolding of hexamers, and dimers indicating dissociation of chitosan-zinc-insulin complex over the period of time (figure 44). The thermal stability of insulin released at various time points from formulation K was determined by DSC and is presented in figure 45A. In accordance with our previous studies, it was noted that insulin was released only in the form of chitosan-zinc-insulin complex till day 15 indicated by higher T_m (~90°C). The released samples of insulin at 60 and 90 days showed the presence of monomers with very small amount of hexamers. Upon dilution, the initially released samples of insulin (day 7 and 15) were easily dissociated and showed the presence of monomers/dimers (Tm: ~68°C) and hexamers (Tm: ~84°C) (figure 45B).

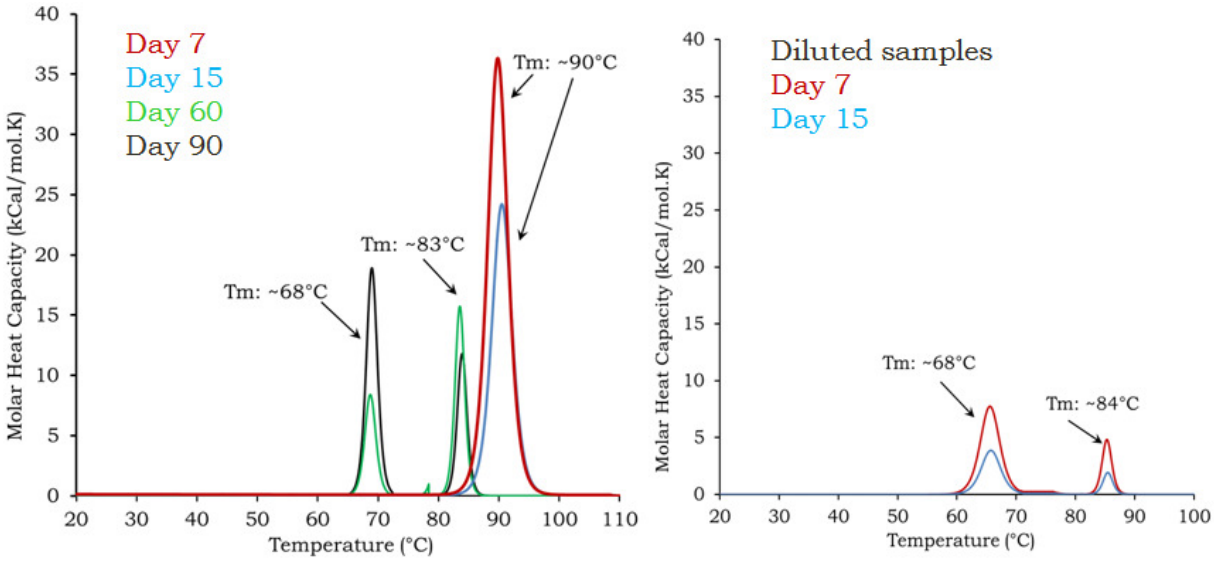

Figure 45. DSC thermograms of insulin released from formulation containing chitosan-zinc-insulin complex loaded thermosensitive polymer (formulation K, at 60 mg insulin loading) (A); and DSC thermograms of diluted samples of insulin released (B)

3.10.3. Polyacrylamide gel electrophoresis (Native and SDS PAGE)

The PAGE, and SDS-PAGE analysis results of insulin released from chitosan-zinc-insulin complex containing delivery systems is presented in figures 46-48. Fresh insulin analyzed using native PAGE showed a band at 6 kDa, while a band near 12 kDa was observed due to the presence of mixture of insulin monomers and dimers. Similar Molecular weight bands at 6, and 12 kDa were observed initially released samples (15 days) of insulin in native PAGE experiments implying the presence of dimers and monomers in the released insulin (figures 46A and 47). SDS-PAGE performed under non-reducing conditions showed the presence of single band corresponding to 6 kDa similar to fresh insulin (figures 46B and 48). Thus higher molecular weight products were dissociated in presence of SDS under non-reducing conditions.

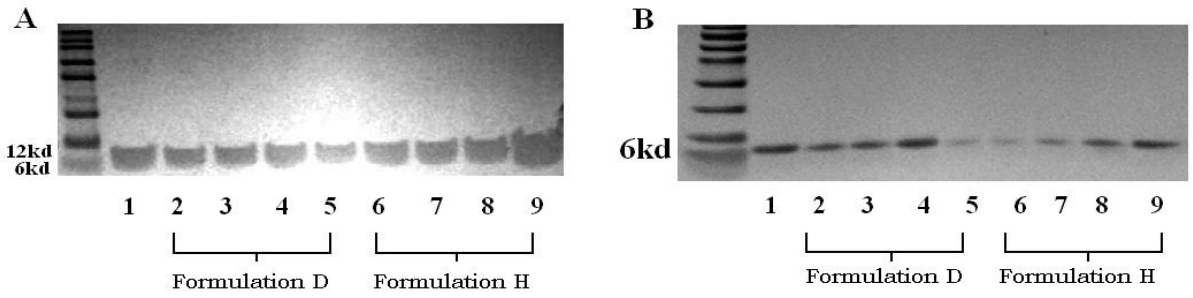

Figure 46. Native PAGE (A) and SDS-PAGE (B) of insulin released during in vitro release (lane 1: fresh insulin, lane 2-5: insulin released from the polymeric formulation D, and lane 6-9 insulin released from formulation H, at day 15, 30, 45 and 60, respectively)

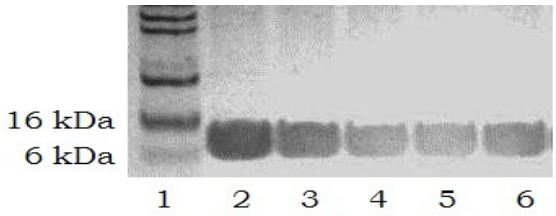

Figure 47. Native PAGE of insulin released from formulation K during in vitro release study (lane 1: molecular marker, lane 2: zinc-insulin, and lane 3-6: insulin released at day 1, 3, 7, and 15, respectively)

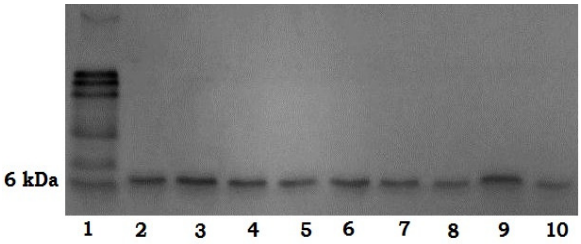

Figure 48. SDS-PAGE of insulin released from formulation K during in vitro release study (lane 1: molecular marker, lane 2: fresh insulin, lane 3: zinc-insulin, and lane 4-10: insulin released at day 1, 3, 7, 15, 30, 60 and 90, respectively)

3.10.4. High performance liquid chromatography (HPLC)

The HPLC analysis results of fresh and released samples of insulin from polymeric formulations D and H are presented in figure 49. Freshly prepared insulin showed a single peak at retention time around 9.8 min. The insulin released from all formulations showed a major absorption peak at 9.8 min, without any major sign of degradation till 30 days. Some degradation

products were observed in the released samples indicated by the presence of absorption peak at 4.8 min along with intact insulin after 45 days of incubation. The control insulin solution maintained at similar conditions showed a major peak of insulin at 9.8 min at day 7. A significant reduction in the peak height was observed after 15 days and no peak of intact insulin was detected after 30 days of incubation, indicating complete degradation of insulin.

The HPLC analysis was also performed to determine the presence of any degradation products of insulin released from formulation K (60 mg insulin loading in the form of chitosan-zinc-insulin complex). For fresh insulin the peak appeared at 9.8 min (retention time), and the released samples of insulin also showed similar peaks at 9.8 min without any degradation till 45 days. Though very small peaks appeared near 5.2, and 5.6 min indicating some insulin might have degraded during release, a distinct peak at retention time 9.8 min showed that the most of the protein was in native form during release (figure 50).

3.10.5. MALDI-TOF mass spectroscopy

MALDI-TOF mass spectrum of intact recombinant human insulin showed peaks at 5808 m/z corresponding to single (+1) protonated insulin molecule (figure 51a). The control insulin solution withdrawn at day 15 exhibited a major peak at of 5808.480 m/z ratio along with some degradation products (figure 51b). No peak analogous to intact insulin was observed in 30 days sample suggesting that all protein was degraded (figure 51c). A small signal corresponding to cyclic imide product at ~5789 m/z was observed in one and two month's released samples from formulations containing zinc-insulin (figures 51d and e). But the intensity of cyclic imide signal was increased in two month's released sample of insulin as compared to formulation containing chitosan-zinc-insulin complex. A peak at 2905.828 m/z was observed in two months released

sample from formulation containing chitosan-zinc-insulin complex which might be due to the double (+2) protonated insulin molecules (figure 51g).

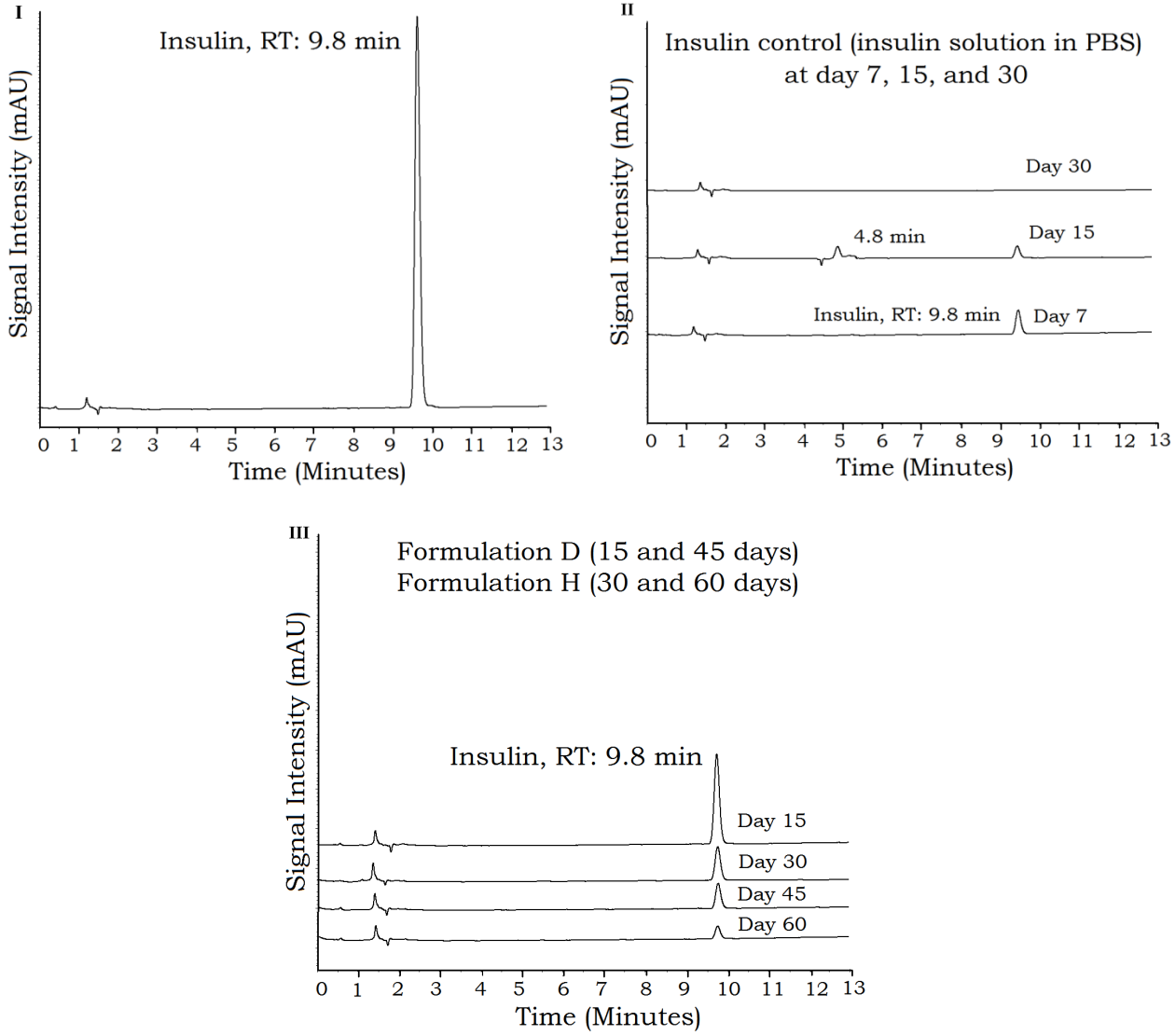

Figure 49. Chemical stability of insulin by HPLC: chromatogram of fresh insulin (I), insulin control (insulin solution in PBS incubated at 37°C) (II), and insulin released from the polymeric formulations at 30 and 45 mg insulin loading (III)

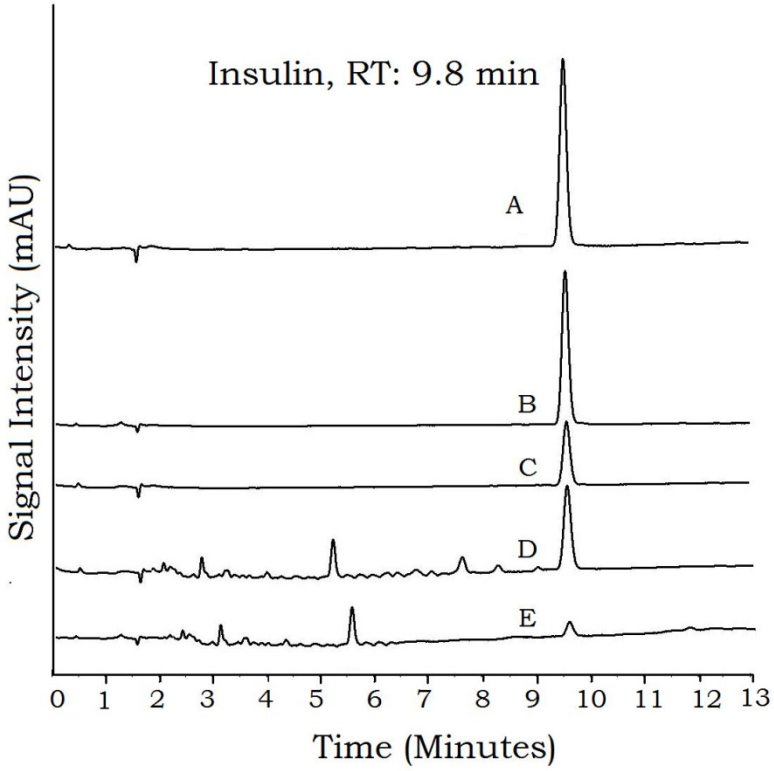

Figure 50. HPLC chromatograms of fresh insulin (A), and insulin released from delivery system containing chitosan-zinc-insulin complex at 15, 30, 60 and 90 days (B-E)

A peak at ~11685 m/z was also observed in the released sample of insulin from formulation A at day 30 (figure 51h). This could be due to the presence of a dimer of covalent [covalent insulin dimer (CID)] or non-covalent nature. Signal corresponding to dimer was found only at trace level in the released samples from formulation B moreover the data obtained confirmed that the monomeric form was predominant.

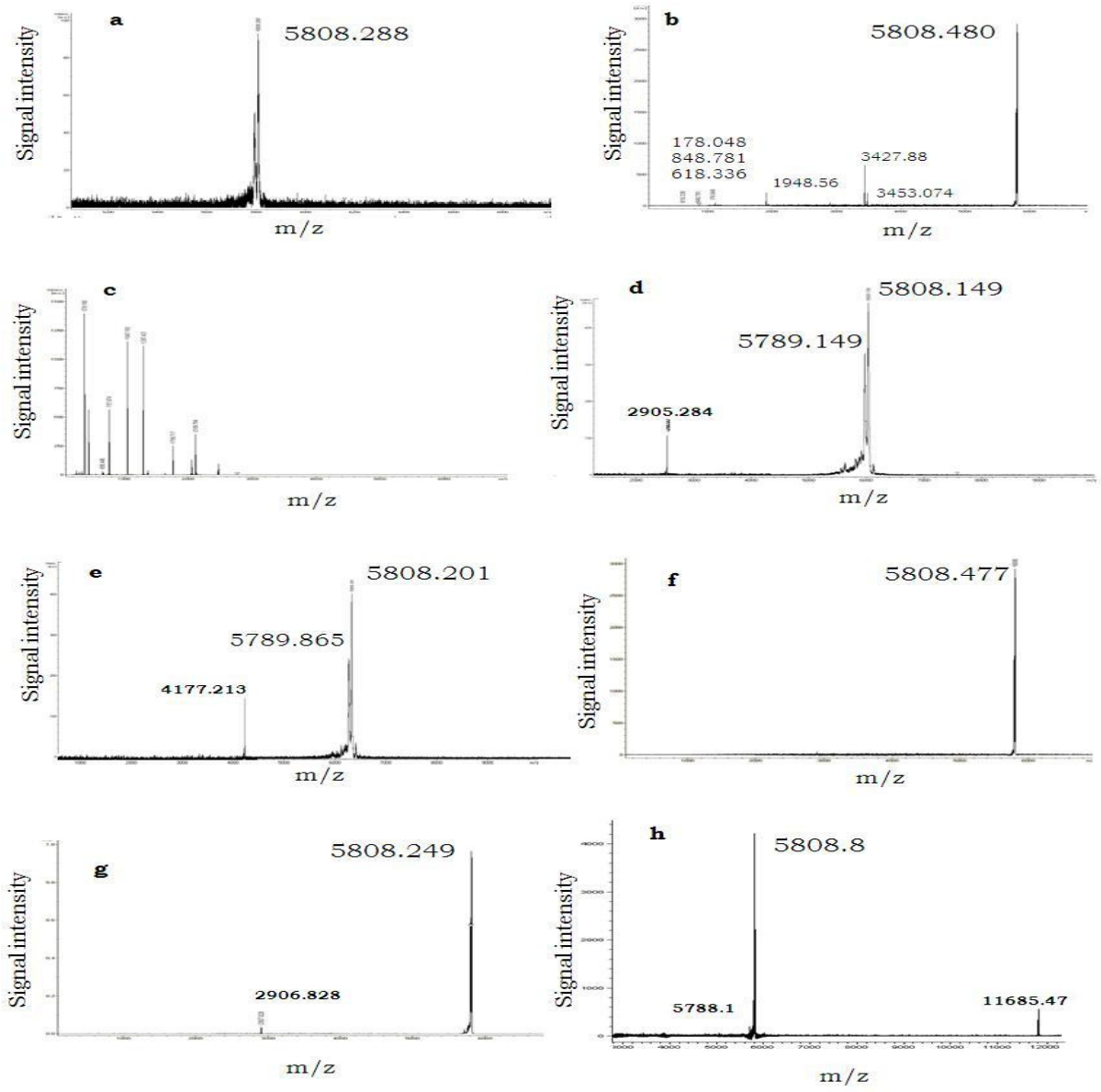

Figure 51. MALDI-TOF mass spectroscopy of fresh insulin (a), and insulin control at15 days (b), and 1 month (insulin solution maintained at 37°C) (c); insulin released from formulation containing zinc-insulin at 1 month (d) and 2 months (e); insulin released from formulation containing chitosan-zinc- insulin complex 1 month (f) and 2 months (g), and insulin released from polymeric formulation A at 1 month (30 and 45 mg insulin loading) (h)

3.11. Stability of Insulin in the Gel Depot During Release

Insulin remaining in the gel depot during release was extracted using 1:1 (v/v) mixture of acetonitrile and PBS with a mild shaking and was analyzed for its stability. Figures 52 and 53

show respectively, the MALDI-TOF and HPLC analysis of insulin samples extracted from polymeric delivery system during release.

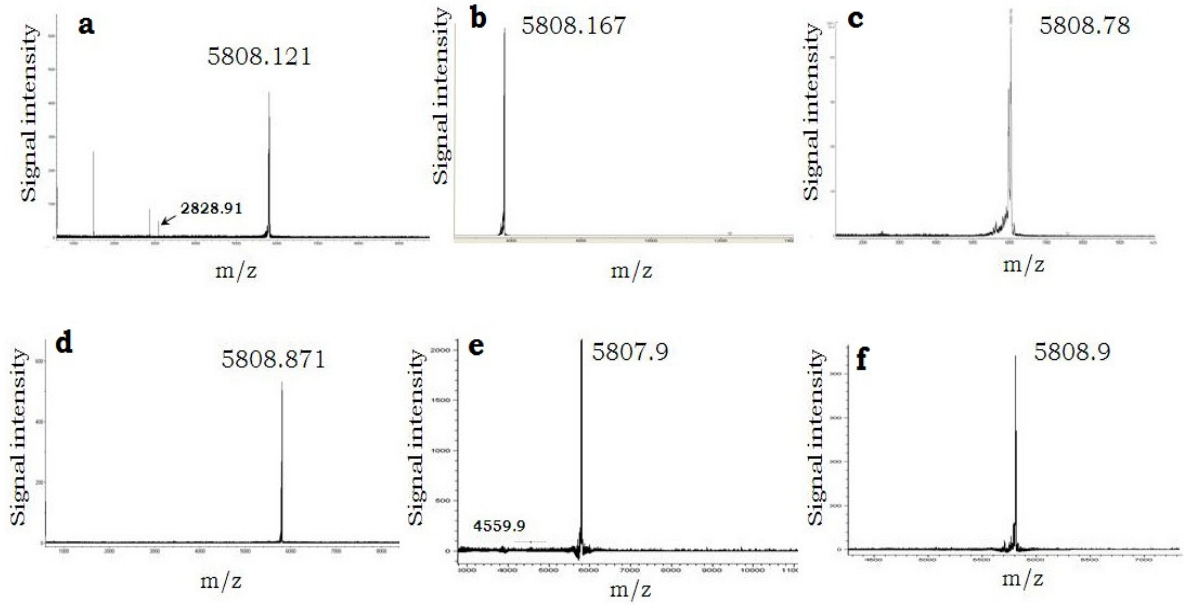

Figure 52. MALDI-TOF mass spectroscopy of insulin extracted from polymeric formulations during release, 1 month (a) and 2 months (b) from formulation containing insulin alone; 1 month (c) and 2 months (d) from formulation containing zinc-insulin; and 1month (e) and 2 months (f) from formulation containing chitosan-zinc-insulin (30 and 45 mg insulin loading)

Signals corresponding to some degradation products were observed in the extracted sample at 30 days from the formulation containing insulin alone during release (figure 52a). A signal corresponding to intact insulin at ~5808 m/z was observed from all samples, without the sign of degradation indicted the protecting effect of zinc as well as chitosan on insulin in the gel depot (figures 52b-f). HPLC results were in agreement with MALDI-TOF analysis (figure 53). Similarly the native PAGE experiments also showed a single band near 6 kDa for the insulin extracted from the gel depot (figure 54).

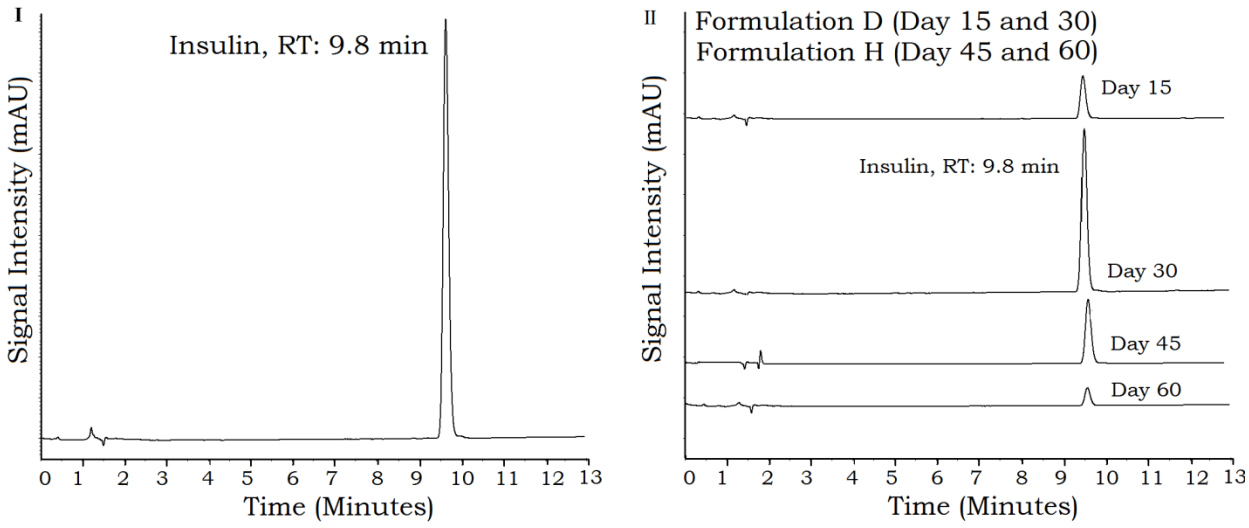

Figure 53. Chemical stability of insulin extracted from polymeric gel during release at 37°C determined by HPLC at 30 and 45 mg insulin loading

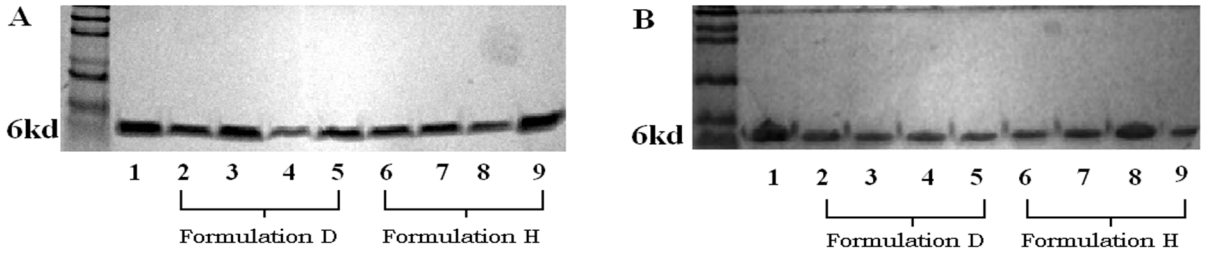

Figure 54. Native PAGE (A) and SDS-PAGE (B) of insulin extracted from depot during release (lane 1: fresh insulin, lane 2-5: insulin extracted from polymeric formulation D, and lane 6-9 insulin extracted from formulation H, at day 15, 30, 45 and 60)

3.12. Stability of Insulin in the Delivery System During Storage

The effect of zinc and chitosan on the stability of insulin inside the polymeric delivery systems during storage at 4°C and 37°C was determined using MALDI-TOF and HPLC, and the results are presented in figures 55 and 56. The stability of insulin in presence of zinc and chitosan was compared with fresh insulin. Figure 55 (a-d) shows the MALDI-TOF and HPLC (figures 56 IV-V) results of insulin extracted from the polymer hydrogel at predetermined time points. A major peak corresponding to intact insulin was observed in all extracted samples. A single peak at 9.8 min in HPLC also confirmed the presence of intact insulin in the stored

samples. A single band at 6 kDa was observed in native PAGE experiments, also confirmed the structural preservation of insulin during storage at 4 and 37°C (figure 57 C-D).

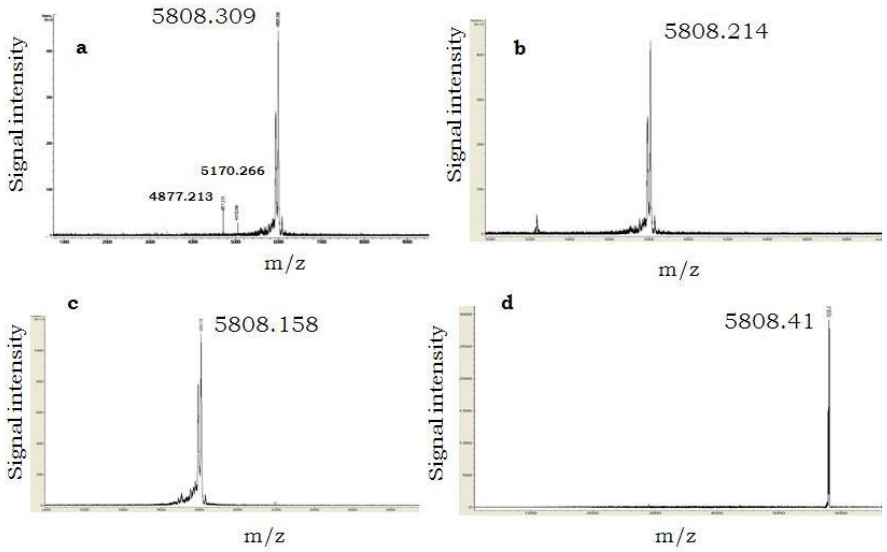

Figure 55. MALDI-TOF mass spectroscopy of insulin extracted from polymeric gel during storage, 1 month (a), and 2 months (b) at 37°C; and 1 month (c) and 2 months (d) stored at 4°C

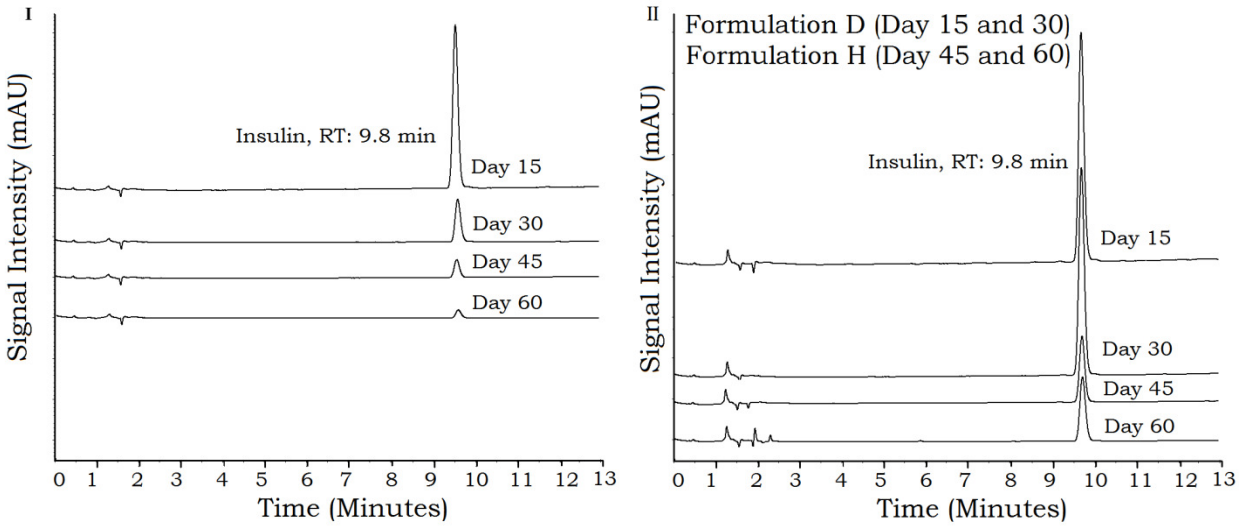

Figure 56. Chemical stability of insulin extracted from polymeric gel during storage determined by HPLC, insulin extracted from polymeric formulations stored at 4°C (I), and insulin extracted from polymeric formulations stored at 37°C (II)

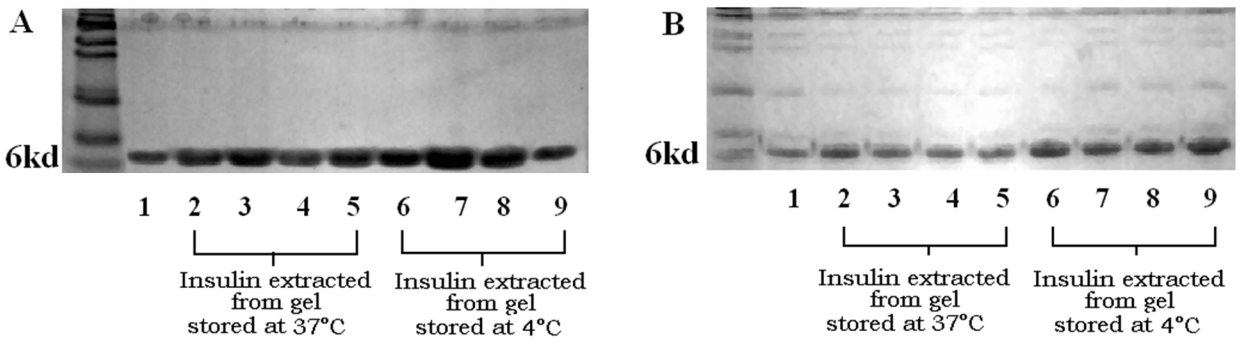

Figure 57. Native (A) and SDS-PAGE (B) of insulin extracted from polymeric gel during storage (lane 1: fresh insulin, lane 2-5: insulin extracted from polymeric gel depot stored at 37°C, and lane 6-9 insulin extracted from polymeric gel depot stored at 4°C at day 15, 30, 45 and 60)

3.13. In Vivo Absorption and Bioactivity of Insulin

The optimized formulations containing chitosan-zinc-insulin complex were selected for in vivo studies since they demonstrated a low initial burst release and controlled the release of insulin for longer duration during in vitro analysis. The formulations were injectable through 25 G needle, and formed gel depot quickly after incubation at body temperature. The pharmacokinetic profile of insulin released from the delivery systems and associated pharmacodynamic effects are presented in figures 58-59. Additionally, the serum insulin concentration and blood glucose levels of untreated (control), and STZ treated animals are also presented. The fasting blood glucose level of untreated animals remained in between 90-125 mg/dl throughout the study duration; while STZ treated rats showed fluctuating blood glucose levels between 300-550 mg/dl.

3.13.1. Comparison among the delivery systems at 30 IU/kg insulin loading

The release profile of insulin and blood glucose levels of the rats treated with different formulations at 30 IU/kg insulin loading is presented in figure 58 A and B, respectively. The animals treated with the delivery system containing insulin alone showed highest initial burst release (52.1±7.6 µU/ml) followed by a continuous release over the period of 42 days, and

subsequent rapid reduction in insulin levels. In case of formulation containing zinc-insulin, though the initial burst release was reduced significantly ($p<0.05$) as compared to the formulation containing insulin alone, after ~14 days, an appreciable decline in the insulin level was observed, and the levels dropped continuously in 21-42 days. The delivery system containing chitosan-zinc-insulin complex showed significantly lower ($P<0.05$) initial burst release of insulin (11.4±2.1 µU/ml) as compared to the formulations containing insulin alone and zinc-insulin loaded delivery systems. Also, significantly higher ($P<0.05$) serum insulin levels were maintained for ~63 days, and then declined gradually over the period of 91 days. AUC was used to determine the bioavailability of insulin released, and is presented in table 16.

Insulin bioavailability was enhanced in case of chitosan-zinc-insulin complex loaded delivery system, indicated by increase in AUC by 1.5 and 1.85 fold as compared to the formulations containing zinc-insulin and insulin alone, respectively. The physiological effects of released insulin denoted by reduction in blood glucose levels are depicted in figure 58B. The fasting blood glucose levels in rats administered with any of the delivery systems were significantly lower ($p<0.05$) than the diabetic rats in STZ treated group. In case of delivery systems containing insulin alone, and zinc-insulin it was observed that the blood glucose levels dropped suddenly in response to the large amount of insulin released and remained low until 21 days, and then returned to pretreatment levels (~400 mg/dl) quickly. While, chitosan-zinc-insulin complex helped to maintain the blood glucose levels in the range of 100-150 mg/dl until ~63 days. The blood glucose levels were significantly low as compared to the delivery systems containing insulin alone or zinc-insulin until 63 days suggesting that insulin was released slowly from the chitosan-zinc-insulin complex.

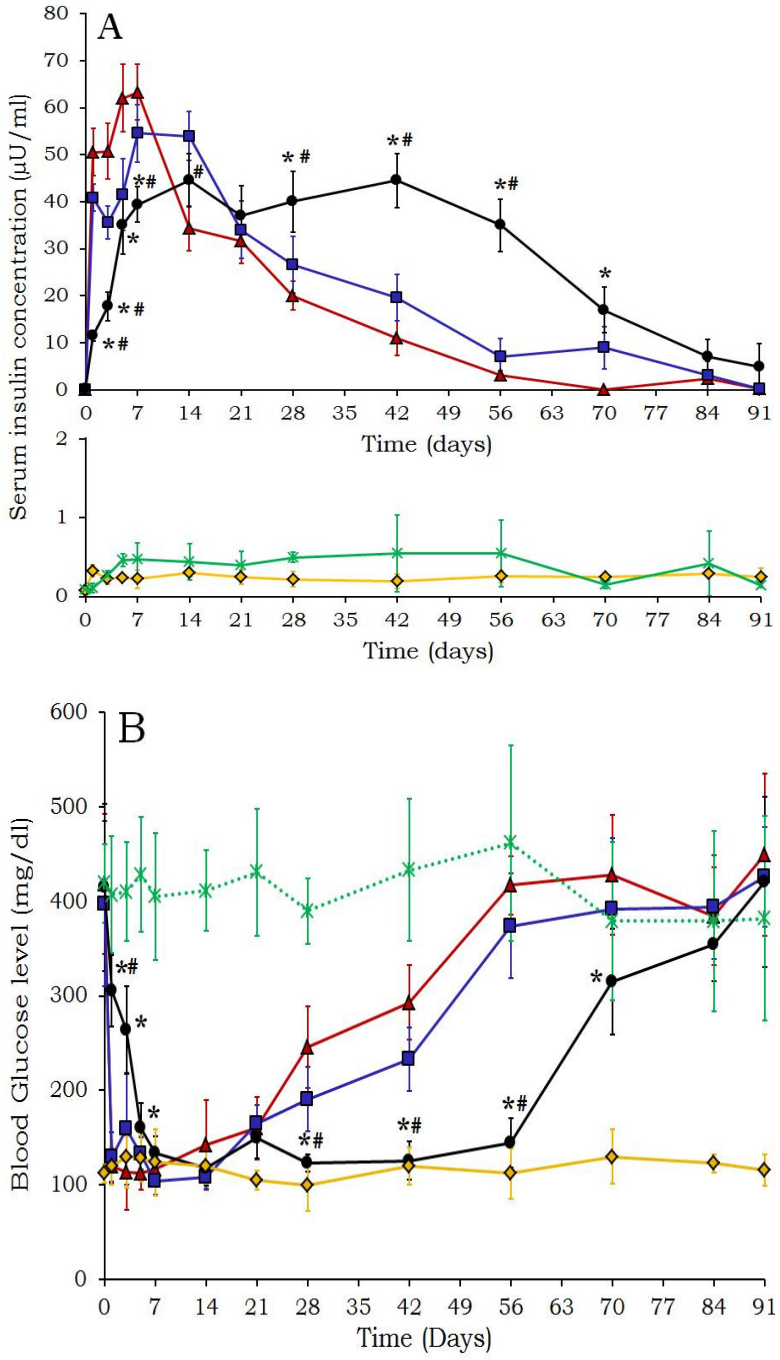

Figure 58. Serum human insulin (A), and blood glucose levels (B) of rats treated with (▲) insulin alone, (■) zinc-insulin, (●) chitosan-zinc-insulin complex loaded thermosensitive polymeric delivery systems, (×) streptozotocin control, and (♦) untreated control; (insulin loading; 30 IU/kg) (n=6, mean ± SD, *: significantly different than insulin alone, and #: significantly different than zinc-insulin at P<0.05)

3.13.2. Comparison among the delivery systems at 45 IU/kg insulin loading

The in vivo release profile of insulin released, and blood glucose levels of rats treated with the delivery system containing insulin alone, zinc-insulin, and chitosan-zinc-insulin complex at 45 IU/kg insulin loading are presented in figure 59 A and B, respectively. The serum insulin levels of animals treated with the delivery system containing chitosan-zinc-insulin complex were significantly different ($P<0.05$) as compared to that of insulin alone, and zinc-insulin. Serum insulin levels were maintained above 40 µU/ml over 70 days before gradually returning to baseline levels. Increase in insulin AUC by 1.3 and 2 fold was noticed as compared to zinc-insulin, and insulin alone containing formulations.

The pharmacodynamic response reflected the pharmacokinetic profile of released insulin in that reduction in blood glucose was observed until ~70 days, and as the insulin release was reduced, blood glucose levels increased and reached to the pretreatment levels. Animals treated with insulin alone or zinc-insulin containing delivery systems showed a sharp drop in insulin levels after ~10 and 16 days, respectively. In the case of formulations containing chitosan-zinc insulin complex, the fasting blood glucose levels remained significantly ($P<0.05$) low until ~70 days as compared to insulin alone, or zinc-insulin containing formulations. The blood glucose levels were comparable to that of control (untreated group) up to 63 days, and then increased gradually.

For comparing the insulin release and blood glucose levels, insulin solution (2 IU/Kg in PBS) was administered to the diabetic rats via SC route, and the blood glucose and serum insulin levels were measured at 0.5, 1, 2, 4, 6, 8, 12 and 24 h post-injection. Immediately after subcutaneous administration, serum insulin levels increased rapidly, and the data showed values of C_{max} and T_{max} of 55.75±6.4 µU/ml and 1 h, respectively (figure 60A). Corresponding sudden

decline in blood glucose levels was noticed, and reached to ~20% of the pre-administration levels within 1 h (figure 60B). Insulin levels reduced over the period of 12 h, and reached below the detection limit. Similarly, blood glucose reached to the pretreatment levels after 12 h.

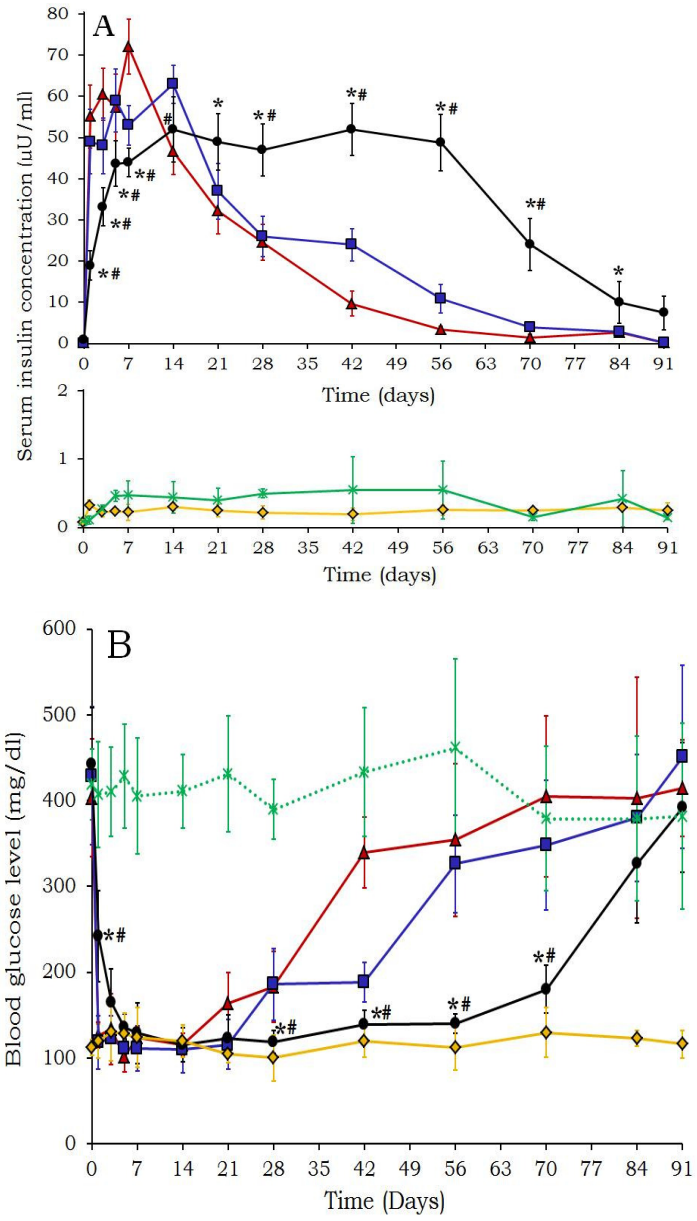

Figure 59. Serum human insulin (A) and blood glucose levels (B) of rats treated with (▲) insulin alone, (■) zinc-insulin, (●) chitosan-zinc-insulin complex loaded thermosensitive polymeric delivery systems, (×) streptozotocin control, and (♦) untreated control; (insulin loading; 45 IU/kg) (n=6, mean ± SD, *: significantly different than insulin alone, and #: significantly different than zinc-insulin at P<0.05)

Table 16. In vivo pharmacokinetic parameters of insulin in rats

Treatment groups	Insulin dose (IU/kg)	$AUC_{(0-t)}$ (µU.day/ml)	Fold increase in AUC compared to insulin alone	Fold increase in AUC compared to zinc-insulin
Insulin alone	30	1481.36±105.6	---	---
Zinc-insulin	30	1886.68±92.2	1.27	---
Chitosan-zinc-insulin	30	2733.08±103.8	1.85	1.5
Insulin alone	45	1686.79±93.8	---	---
Zinc-insulin	45	2073.58±110.1	1.23	---
Chitosan-zinc-insulin	45	3458.79±153.3	2.1	1.3

(Mean ± SD, n=6, t: 90 days for polymeric delivery systems; Solution group (Insulin dispersed in PBS, injected via SC route), C_{max}, T_{max}, and AUC_{0-t} for solution group: 55.75±6.4 µU/ml, 1 h, and 6.18±0.35 µU.day/ml, respectively)

3.13.3. Body weight determination

Initially after STZ injection a marked reduction in the body weight of rats was observed in all treatment groups. The STZ treatment group showed continuous loss of body weight at the end of three months (figures 61, and 62). The rats treated with insulin formulations showed a gradual weight gain, and was significantly ($P<0.05$) higher than STZ treated animals. Though there was no significant difference observed in the body weights of rats in either of the treatment groups, the chitosan-zinc-insulin complex treated animals showed progressive weight gain and were comparable to that of non-diabetic control.

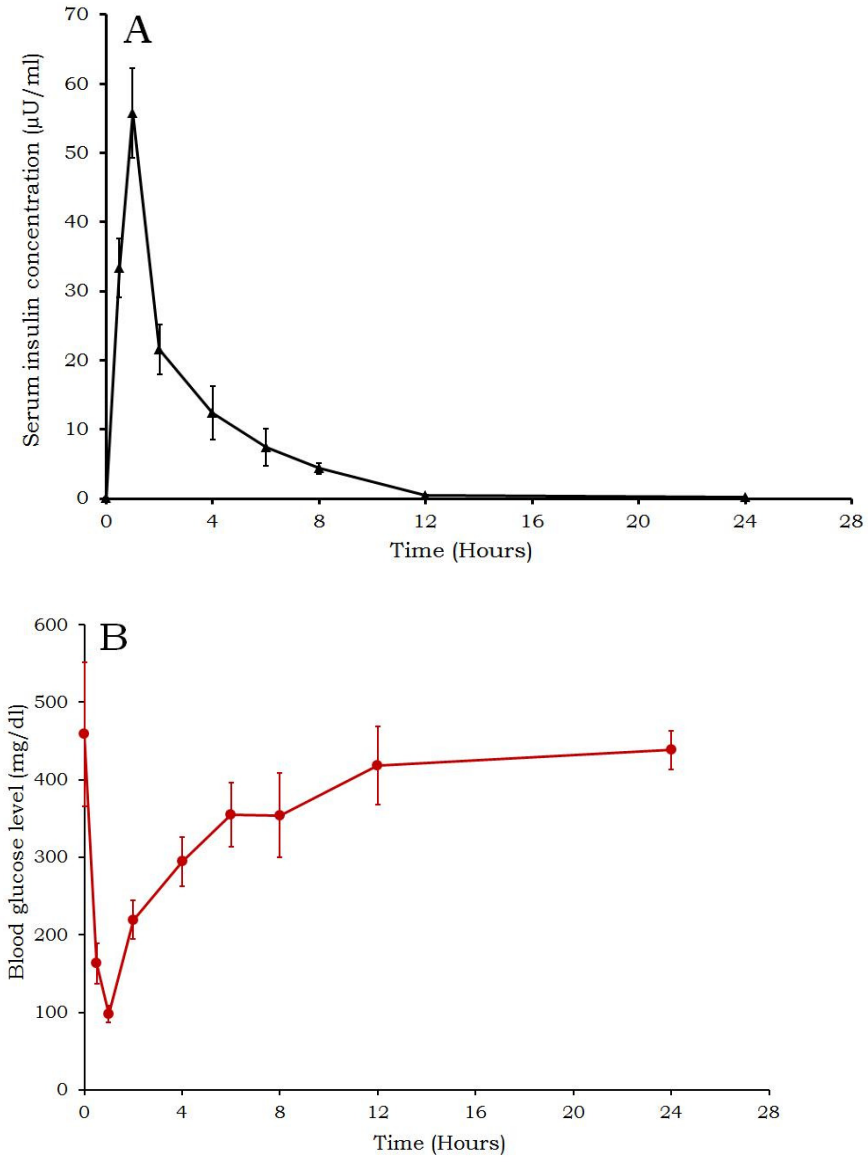

Figure 60. Serum insulin concentration (A), and blood glucose levels (B) of rats treated with insulin solution (2 IU/kg, in PBS pH 7.4 via subcutaneous route, (n=6, mean ± SD))

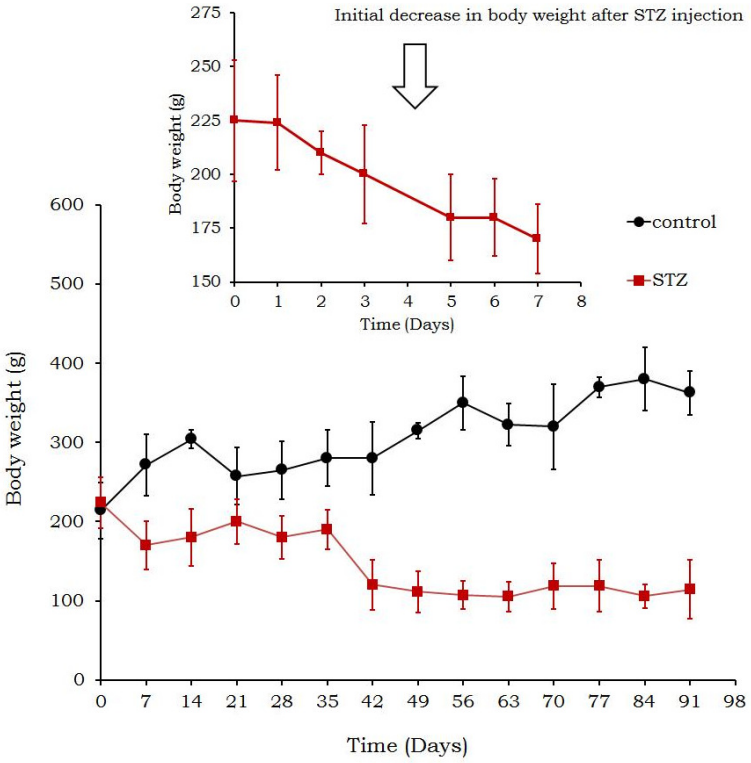

Figure 61. Body weight profile of rats in (●) control (untreated) group, and treated with (■) streptozotocin (n=6, mean ± SD), (Inset shows the reduction in body weight after STZ treatment)

3.13.4. Detection of anti-insulin (rH) antibodies

The rat serum samples collected at 1, 2 and 3 month time points were screened for the presence of antibodies against insulin released from the delivery systems, and it was observed that no antibodies against human insulin (rH) were developed (figure 63). For comparison purposes, rat IgG were used as control. No antibodies were observed against released insulin initially or after 90 days of treatment and the antibody response was comparable to that of control (untreated) group. It indicated that the released insulin was non-immunogenic in nature.

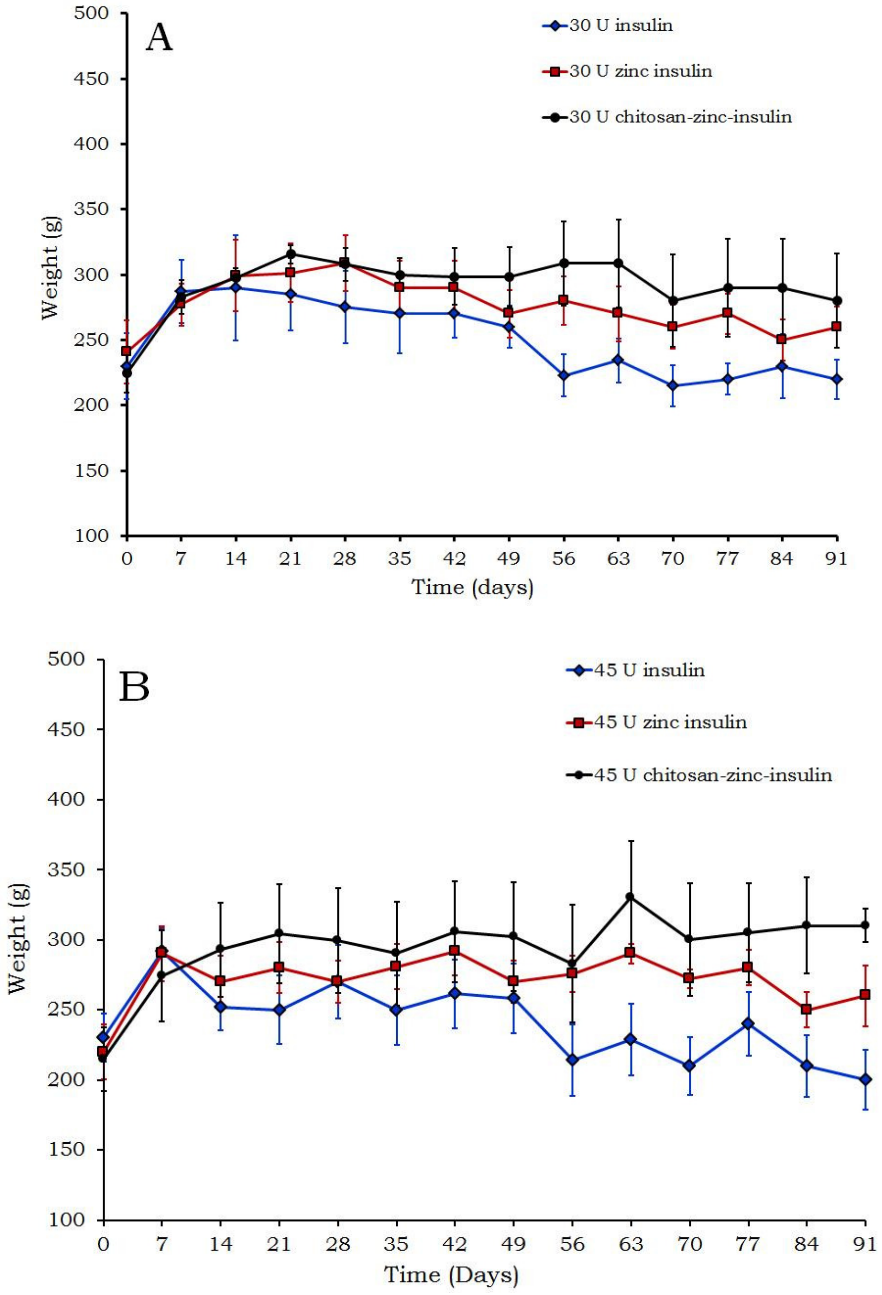

Figure 62. Body weight profile of rats treated with (♦) insulin alone, (■) zinc-insulin, and (●) chitosan-zinc-insulin incorporated thermosensitive polymeric delivery systems (Insulin dose: A) 30 IU/kg, and B) 45 IU/kg, n=6, mean ± SD)

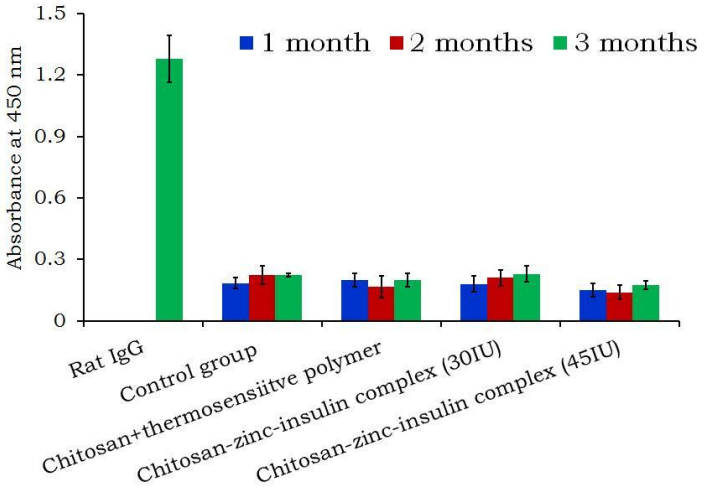

Figure 63. Detection of anti-insulin (rH) antibodies in rat serum treated with formulations at different insulin dosing

3.14. Biocompatibility of the Delivery Systems

The in vitro and in vivo biocompatibility studies of the delivery systems performed using an MTT assay, and skin histological analysis is discussed in following sections.

3.14.1. In vitro biocompatibility of the delivery systems

Figure 64 shows the cell viability quantitatively measured by an MTT assay for thermosensitive polymeric delivery system with and without chitosan incubated at 37 and 70°C, respectively for 10 days. It was observed that the HEK293 cells grew better in the extracts prepared from chitosan containing thermosensitive delivery systems than unmodified (thermosensitive polymer only), and PBS, or DMSO treated cells (Figure 65). Initially, at 24 h the cell viability was ~60-80% for the concentrated polymeric extracts (1:1 dilution with growth medium), while the extracts diluted to 1:16 ratio showed close to 100% cell growth. At 48 and 72 h, no significant difference ($p>0.05$) in the cell viability was observed as compared to control (growth medium only), and instead the polymeric delivery system containing chitosan showed higher cell viability as compared to the cells treated with polymeric extracts without chitosan.

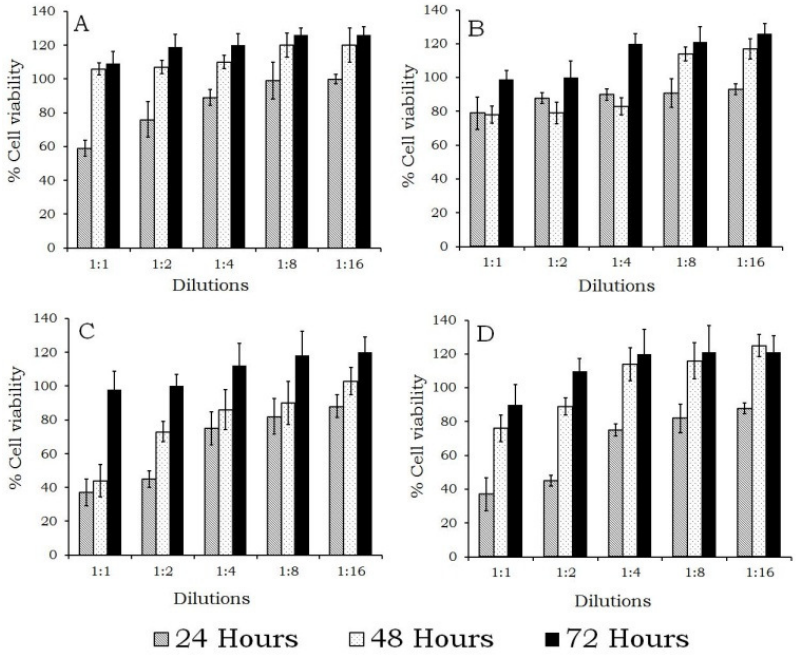

Figure 64. In vitro biocompatibility of the delivery systems containing chitosan + thermosensitive polymer extracts prepared by incubating the delivery systems for 10 days, 37°C (A), and 70°C (B), and thermosensitive polymer only at 37°C (C), and 70°C (D)

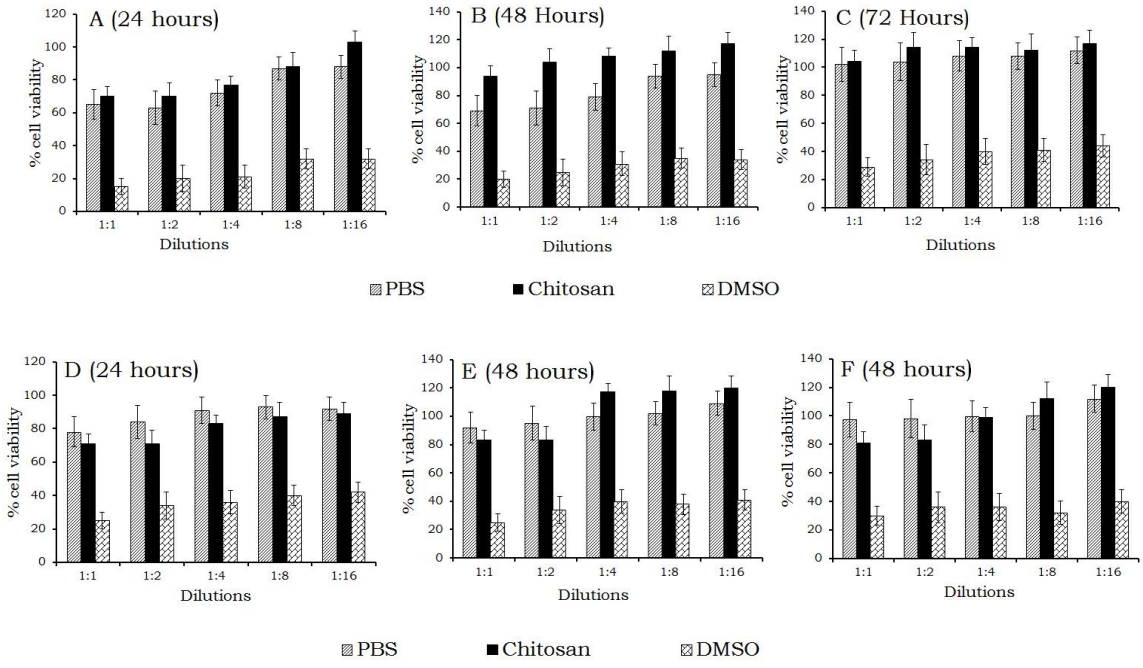

Figure 65. In vitro biocompatibility of chitosan, DMSO, and PBS extracts prepared by incubating for 10 days at 37°C (A-C), and 70°C (D-F), determined by MTT cell viability assay (n=6, mean ± SD)

3.14.2. In vivo biocompatibility of the delivery systems

Figures 66 and 67 represent the in vivo biocompatibility analysis of the polymeric delivery systems with and without chitosan. The rats were injected with the polymeric delivery systems containing chitosan, and the inflammatory response to the foreign material was observed, and compared to that of control (untreated), and is presented in figure 66. Histology of untreated skin (control group) is presented in figure 66A. The representative light microscopy images of skin following administration of chitosan containing thermosensitive polymeric delivery system at 1, 7, 30 and 90 days is shown in figure 66B-E.

The severity of the response to the foreign material was observed by the presence of leukocytes and fibroblasts near the site of injection. The nuclei of the neutrophils or other inflammatory cells are stained purple after H & E staining, and thus can be easily identified from the surrounding connective tissue. Figures 66 B and C represent the clear incidence of acute inflammatory response to the polymeric delivery system containing chitosan, at day 1 and 7, respectively. Large neutrophil infiltration at the site of injection was observed initially. Chronic inflammatory response to the delivery system at day 30 is depicted in figure 66D. However, this response subsided considerably 30 days post-injection, indicated by the presence of few inflammatory cells, and the skin tissue surrounding the delivery system closely resembled to that of control at 90 days (figure 66E).

Similar type of inflammatory behavior was observed in case of rats treated with only thermosensitive polymeric delivery system without chitosan as presented in figure 67 (A-D). Thus, it was noticed that the subcutaneous administration of polymeric delivery systems with/without chitosan showed an inflammatory response due to injection and continual presence

of polymeric gel in the body. But, at the end of the study no signs of chronic inflammation, or necrosis were observed.

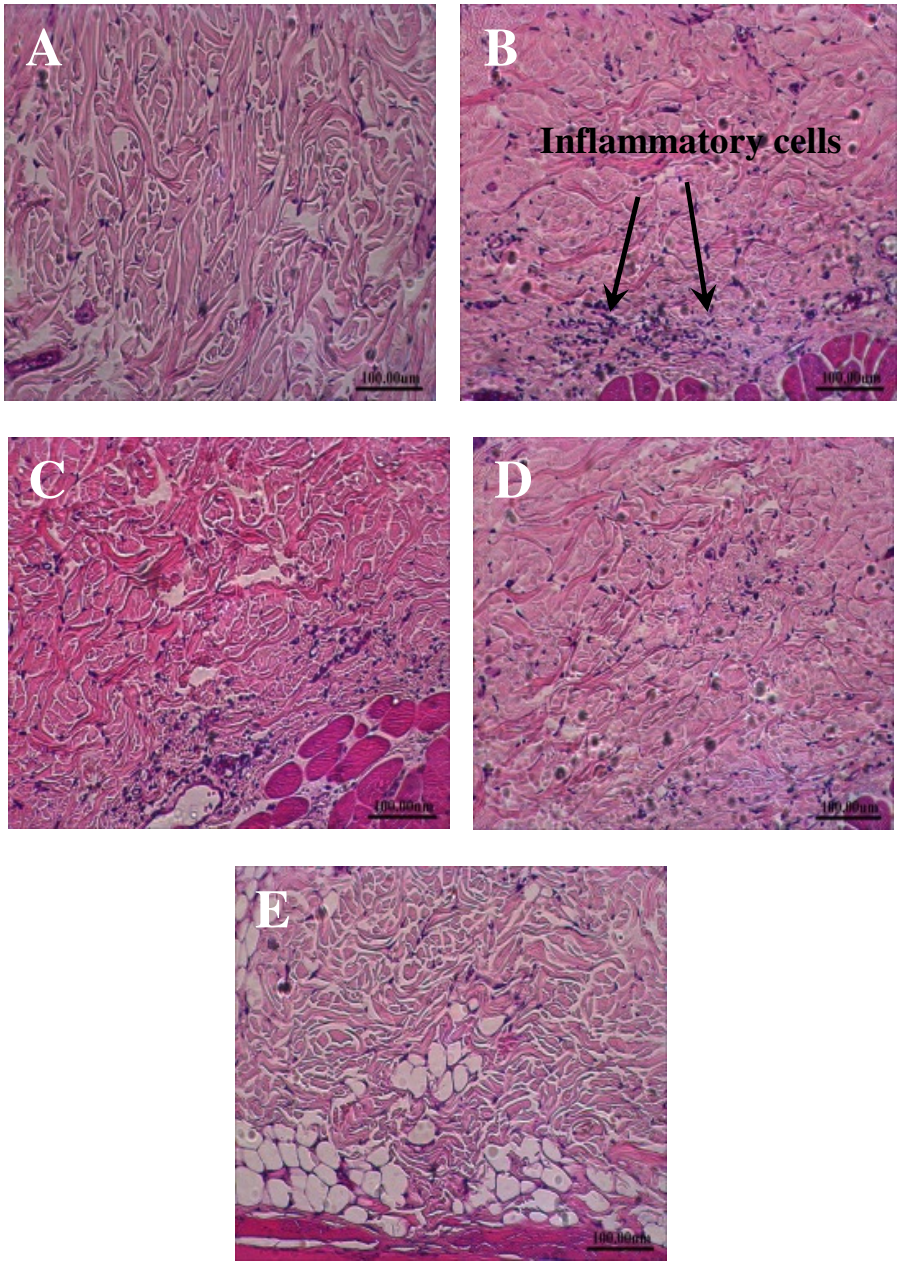

Figure 66. Light micrographs of rat skin histology after H and E staining: control (A); and subcutaneous skin tissue sampled after injecting the delivery systems containing chitosan + thermosensitive polymer at day 1 (B), day 7 (C), day 30 (D) and day 90 (E)

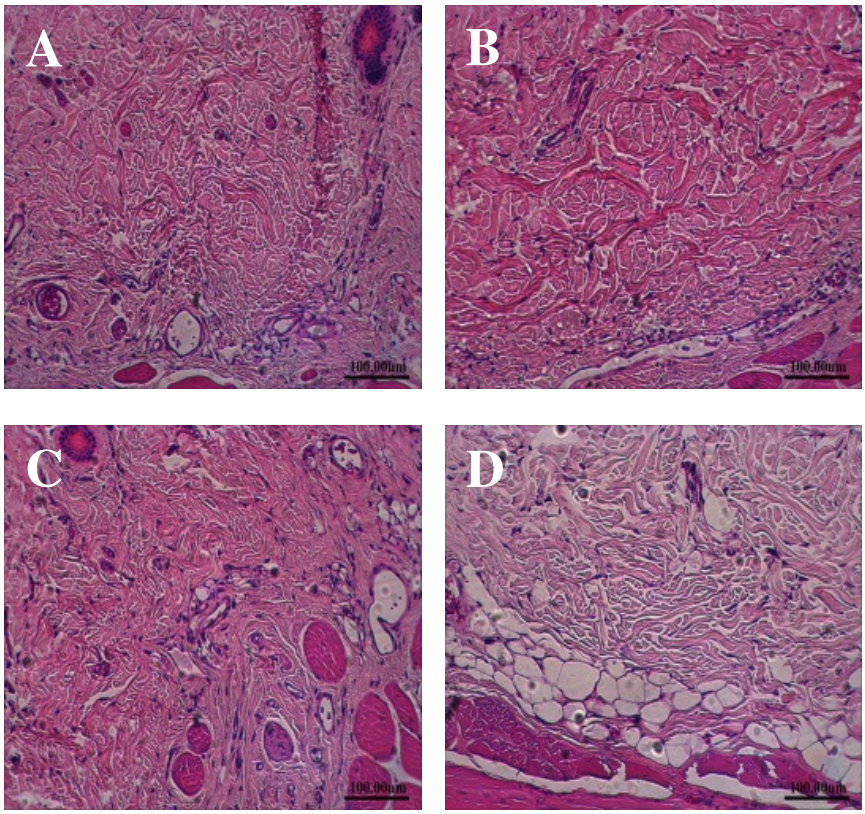

Figure 67. Light micrographs of rat skin histology after H and E staining: the subcutaneous skin tissue sampled after injecting the delivery system containing thermosensitive polymer only: day 1 (A), day 7 (B), day 30 (C), and day 90 (D)

To determine the degree of collagen deposition at the tissue-delivery system interface, the skin samples were also stained with Gomori's trichome stain which specifically stains collagen (figures 68A-C). The collagen density determined by ImageJ 1.45 software showed that the collagen deposition increased until 30 days (figure 68B), but was comparable to the control at the end of the study (90 days) (figure 68C). The skin histology of animals treated with thermosensitive polymer (without chitosan), is presented in supplementary information (figures 69 A-B). The results indicate that the addition of chitosan did not change the biocompatible nature of the thermosensitive polymeric delivery system.

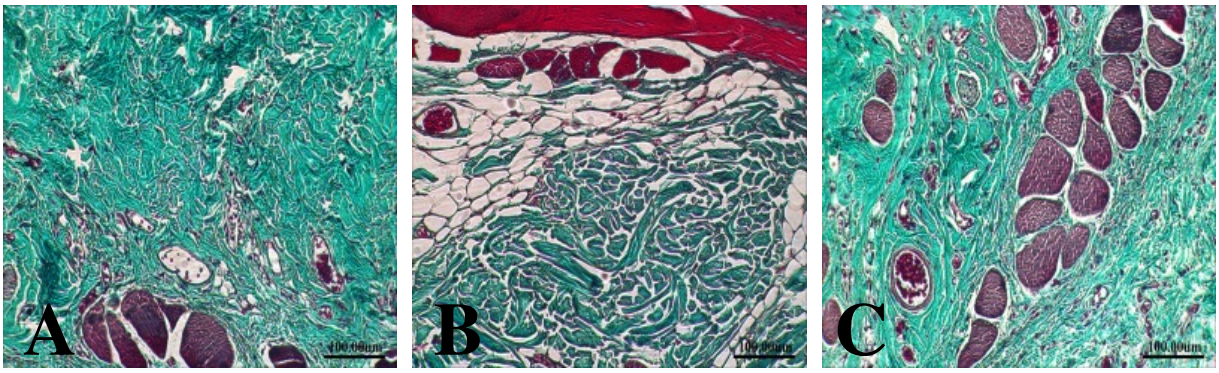

Figure 68. Light micrographs of rat skin histology after staining with Gomori's trichrome stain: control (A); and skin subcutaneous tissue sampled after injecting the delivery systems containing chitosan + thermosensitive polymer at day 30 (B), and day 90 (C)

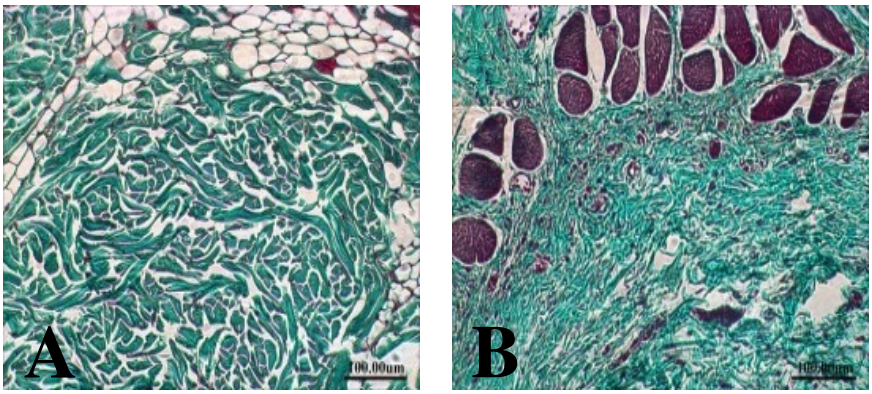

Figure 69. Light micrographs of rat skin histology after staining with Gomori's trichrome stain: skin subcutaneous tissue sampled after injecting the delivery system containing thermosensitive polymer: day 30 (A), and day 90 (B)

4. DISCUSSION

4.1. Synthesis, Characterization of Triblock Copolymer and Factors Affecting Polymer Degradation

The development of controlled delivery systems primarily focuses on the release of therapeutics at a constant rate in order to achieve and maintain the desired therapeutic level for prolonged period. The drug release from polymeric delivery system occurs via diffusion of incorporated molecule or degradation of polymer matrix or by combination of both (216). Typically the initial phase is diffusion-controlled while later stage is both diffusion and polymer degradation controlled (217). High water solubility and small size of incorporated drug, as well as highly porous microstructure, low degree of crosslinking and increased swelling of polymer are some factors which increase the diffusion of drug out from the polymer matrix. While the proportion of hydrophobic/hydrophilic components of polymer influence its degradation rate. Due to the high water content/retention, in situ gel forming delivery systems are considered ideal for entrapment of variety of macromolecules and extensively studied in biomedical field. The important characteristic of polymer hydrogels is their ability to absorb water, and it constitutes at least 10% of the total weight of a hydrogel (218). The water retention and swelling properties provide a suitable pathway for diffusion of incorporated molecules (219). It has been observed that the swelling of polymer hydrogel depends on the hydrophobic/hydrophilic content of the polymer. Higher degree of swelling was observed in case of PLA-PEO-PLA polymer gels with higher PEG content or lower LA/EG ratio (220). Water absorption and retention capacity of the degradable polymer, however, reduces eventually due to the loss of the polymer chains over the period of time. Similar findings have been reported in case of a thermosensitive polymer containing poly (N-(2-hydroxypropyl) methylacrylamide lactate (pHPMAm-lac), and PEG

blocks (30). The delivery systems containing copolymer (1500-1500-1500) and (1600-1500-1600) exhibited a zero-order release kinetics for the incorporated model protein which is highly desired for controlled delivery systems (84). In our studies, the degradation profile of PLA-PEG-PLA triblock copolymer was investigated in detail and the effect of various molecules on degradation behavior and in vitro release pattern was also evaluated. Two thermosensitive triblock copolymers with 1500-1500-1500 (copolymer A), and 1600-1500-1600 (copolymer B) chain lengths were synthesized by the ring opening polymerization of D, L lactide, catalyzed by stannous octoate, using polyethylene glycol (PEG 1500 Da) as an initiator.

The proton and ^{13}C NMR spectroscopy results confirmed the structure of the synthesized copolymers. Integrating the proton NMR signals helped in molecular weight determination. The chromatogram from GPC analysis showed unimodal distribution, and the polydispersity index indicated the narrow molecular weight distribution, showing the sufficient purity of the synthesized copolymers. The aqueous copolymeric solutions of PLA-PEG-PLA showed concentration dependent sol-gel transition in response to changes in temperature. The copolymer consists of both hydrophobic and hydrophilic residues and the gelation takes place due to the aggregation of micelles in response to temperature. Increasing polymer concentration causes increase in aggregation of micelles, leading to gelation at lower temperatures due to packing of aggregated micelles. Increasing hydrophobicity of the copolymer reduces its LCST and increases UCST (84), and therefore aqueous copolymer solutions containing higher number of PLA units, showed gelation at lower temperature and concentration. It indicated that polymer concentration in the delivery system is an important factor which alters its physical state. The aqueous solutions of both copolymers at a concentration of 30% and 40% w/w existed in sol state with sufficiently low viscosity at room temperature, and passed through 25 G needle easily.

The cryo-SEM images of the polymeric delivery system maintained at room temperature and body temperature showed a noticeable difference in their morphologies. The delivery system maintained at room temperature did not show any particular three dimensional surface characteristics, but the freshly cut surface of the delivery system maintained at body temperature showed presence of two distinct domains. The polymer-rich area (white area) was observed showing the presence of polymer network, and dark area was seen in which no structure was observed (water filled pores). The results suggested that the delivery system showed a distinct temperature dependent phase separation.

The weight loss measurements during hydrolytic degradation of copolymers A and B showed that the copolymer with higher PLA chain length took more time to degrade than copolymer with smaller chains. It was also noted that increasing copolymer concentration in the delivery system (40%w/w) reduced the rate of degradation and was significantly ($P<0.05$) different from the delivery system containing 30% w/w copolymer. But, both the delivery systems showed similar degradation rate after ~50 days onwards. The results suggest that higher polymer concentration resulted in tighter connection between polymer chains which reduced the pore size of hydrogel matrix. This might have led to the formation of less water accessible pores during initial period of degradation, which could have decreased the water exposure, and chain mobility, and thereby degradation of copolymer B. The reduce speed of degradation could help in extending the overall release period of the incorporated molecules. As the polymer degraded, bigger pores were formed in the gel network resulting in absorption of more water.

PLA-PEG-PLA copolymer contains two different sites where hydrolysis can takes place, namely, ester bonds within PEG segments, and another is in LA segments. During degradation of the ester bonds, PLA and PEG undergo hydrolysis randomly along the chain as well as by chain

unzipping process (cleavage of end unit of the chain). However, which end group of the PLA segment (carboxylic or hydroxyl end) degrades faster than internal bonds is still not well understood (221). The studies in case of similar polyester, PLGA, indicated that the degradation occurs by similar processes including i) random scission of chain, ii) chain unzipping process, and iii) complete solubilization of degradation products (222-224). The copolymer A and B containing delivery systems did not show any significant change in LA/EG ratio over the period of 45 days, and hence it was difficult to determine the specific degradation/hydrolysis sites. The results also indicated that increasing polymer concentration did not significantly affect the LA/EG ratio. A rapid loss of EG fraction, with a gradual and slow hydrolysis of LA segments was observed as the time proceeded. Random scission and hydrolysis of internal bonds in both PLA and PEG chains might have occurred leading to increased mobility and loss of PEG segments from the pores of the hydrogel. Thus, due to the loss of hydrophilic content, the polymer gel became more opaque in appearance. This preferential loss of PEG segments along with loss of molecular weight might have resulted in loss of overall strength of the gel over time (225). Our results were in agreement with the previous studies reporting that the preferential diffusion of a significant amount of hydrophilic PEG rich blocks from the thermosensitive PLA-PEG-PLA copolymer based gel results in the formation of an opaque gel (226).

GPC helped in determining the change in molecular weight of copolymer during hydrolytic degradation. The initial chromatogram for copolymer A showed unimodal distribution with a bell-shaped peak. This single peak was attributed to the similar molecular weight (MW) of the copolymer. But, as the degradation proceeded, a slight increase in RT, and a bimodal peak in GPC chromatogram suggested that the polymer might have degraded into smaller chains. This

point onwards, the bimodal distribution increased with reduction in MWs illustrated by increased RT.

4.2. Effect of Drug Type on Polymer Degradation and In Vitro Release

The factors affecting in vitro release of two model proteins including lysozyme and insulin from thermosensitive PLA-PEG-PLA polymer based delivery systems were investigated by Al-Tahami K (84). Increasing polymer concentration, molecular weight, and chain length of PLA residues reduced the release rate of proteins from the delivery systems. The polymeric delivery systems containing shorter PLA chains even at increasing polymer concentrations did not show any significant difference in the release profile of lysozyme. The result suggested that though increasing copolymer concentration often results in reduction of release rate, higher amount of short PLA chains did not improved the hydrophobicity of copolymer and hence did not alter the release profile (84). Similar type of behavior is reported in case of ketoprofen release from polymeric hydrogels (217). It suggests that the drug release from the delivery system also depends on some additional factors, such as size of hydrogel, pore size, polymer degradation, amount and nature of incorporated molecules, and interaction between incorporated molecule and hydrogel matrix.

In our studies, the in vitro drug release behavior of three model drug molecules namely, insulin, BSA and risperidone from the PLA-PEG-PLA (copolymer A) was studied in detail. Since these three molecules differ in their solubility and hydrophobicity, their distribution in the copolymeric delivery system differs. PLA-PEG-PLA forms micelles in aqueous environment with hydrophilic PEG facing the aqueous phase forming ‘shell’ and hydrophobic PLA forms the ‘core’ region. Due to the core-shell structure the partitioning of drug molecules depends on their hydrophobicity and results into different release profiles. Hydrophobic drug usually partitions

into micellar core and results in sustained release (217). Therefore, along with the polymer structure and concentration, the release profile also depends on the physical and chemical properties of the incorporated molecule.

The size of protein is another key factor affecting its release from the porous hydrogel. Larger protein is supposed to be released slowly than smaller protein, because it takes more time for larger molecule to diffuse out through the narrow interconnected channels of the hydrogel matrix (227). BSA is an ellipsoid protein with ~66400 Da molecular weight, while insulin is a small protein (~6000 Da), and hence, BSA should be released slower than insulin; however, it was observed that the release of BSA was much faster than insulin (128,228). Water solubility is another feature which influences the release pattern and duration of various molecules. Molecules with high water solubility show immediate release from the hydrogel probably due to faster dissolution and diffusion from the delivery system. BSA has high water solubility (aqueous solubility: ~40 mg/ml) (228), while risperidone is a small hydrophobic molecule (molecular formula: $C_{23}H_{27}FN_4O_2$) with very low water solubility about 2.8 µg/ml (229). Insulin also has limited solubility at neutral pH (~0.1 mg/ml), and addition of zinc further reduces its solubility (2). Our studies indicated that BSA showed highest initial burst release and released over shorter duration, followed by insulin and risperidone. But, once polymer degradation became predominant, larger pores were formed in the hydrogel resulting in widening the channels leading to increased release irrespective of the size of the molecule. Still, the release rate for risperidone was much lower which was exclusively contributed to its high hydrophobicity. Sandor et al., (230) reported that the delivery systems containing larger proteins form larger pores on the surface which allows initial dissolution of protein aggregates present on the surface. The polymeric delivery system consisting of BSA (large hydrophilic protein, ~66400

Da) might have formed larger channels near the surface during initial release, which led to rapid penetration of water molecules inside the gel. Interconnecting channels formation and/solvation of protein in the previously formed channels within the polymer matrix along with the water penetration enhances polymer degradation (230). All these combined effects might have resulted in the faster release of BSA. Since the delivery systems containing a smaller protein (Insulin~ 5808 Da), and a hydrophobic molecule (Risperidone, 410 Da) formed smaller channels in the gel matrix, they got entrapped in the polymer matrix resulting in low initial burst release and prolonged release duration. Though the delivery system containing small protein forms higher percentage of small pores, this type of structure entraps protein within the delivery system due to the collapsing of channels (230). Some additional factors, such as affinity of protein for polymer due to ionic and hydrophobic interactions, charge on protein at physiological pH, and polymer degradation/erosion can also play an important role in protein release from the polymeric delivery systems (231).

The in vitro release studies demonstrated that the release of large hydrophilic protein from the delivery system led to increased water uptake resulting in faster degradation of polymer matrix. BSA containing delivery systems showed significantly ($P<0.05$) higher LA/EG ratio after 30 days of degradation than that of initial, indicating preferential loss of hydrophilic PEG segments. The residual polymer appearance was visually compared and it was observed that the blank polymeric delivery system appeared more solid, while the drug loaded delivery systems appeared more porous. The rate of degradation of delivery system was also faster in case of BSA formulations than that of insulin and risperidone. The type of drug incorporated in the delivery system can alter the mechanism of polymer degradation (232). The effect of six different drugs on the release profile and degradation of polylactic-co-glycolic acid (PLGA) polymer pellets was

investigated, and it is reported that rate of polymer degradation and the drug release pattern were significantly different for those molecules, and the type of drug incorporated influences the mechanism of polymer degradation (232). Incorporation of a cationic copolymer, chitosan in the delivery system also affected the degradation rate of the delivery system. The results suggested that due to the excellent buffering ability of chitosan, it resisted the change in the pH of the release medium for longer duration and might have resulted in reduction in acid-catalyzed degradation of copolymer chains.

The GPC results also indicated that BSA containing delivery system showed rapid reduction in in molecular weight of the copolymer, and at the end of 60 days most of the polymer was hydrolyzed into smaller segments indicated by corresponding increase in RT. At the end of 90 days period no peak corresponding to original polymer was detected. SEM studies showed that the BSA containing delivery system appeared more porous, indicating that the polymer degradation took place faster in presence of large hydrophilic protein. A striking difference in the porous morphologies of the delivery systems was seen during release of risperidone, BSA or insulin. The results also suggested that the hydrophobic nature and solubility of the incorporated molecule considerably affected the porous structure of the hydrogel. BSA loaded delivery systems showed presence of large pores on the surface which suggested that BSA might have escaped easily from the gel creating bigger, open, water accessible pores as compared to risperidone and insulin.

4.3. In Vitro Release of Insulin from Thermosensitive Polymeric Delivery Systems

To achieve zero-order release kinetics from the delivery system capable of delivering a therapeutic agent regardless of its concentration over extended period is a challenging task. Usually a characteristic phenomenon of ‘burst release’ observed often shortens the lifetime of

delivery system. Also it is difficult to maintain the constant release rate as the drug in the delivery system depletes. Especially in case of insulin which has a narrow therapeutic window, high initial burst release is not favorable since it leads to high drug concentrations near or above toxic levels in vivo. The scope of our work was to determine the effect of various formulation factors on release profile of insulin from thermosensitive delivery system and, ultimately, optimize the delivery system which could deliver insulin at basal level over extended period with no or minimal initial burst. Since this was the most promising copolymer in terms of release period and rate as reported by Al-Tahami (84) it was further used to study the release profiles of various molecules. The thermosensitive PLA-PEG-PLA copolymer was used as the delivery system and was optimized to deliver insulin at basal level for three months in its conformationally and chemically stable and biologically active form. It has been demonstrated that increasing copolymer concentration in the delivery system from 30 to 40% w/w led to reduced initial burst and extended the release of insulin. The insulin loading also governed the overall release profile and affected the initial burst release (84). We observed in our initial studies that though higher copolymer concentration controlled the release for longer period, it did not significantly affect the initial burst release at higher insulin loading. The results indicated the importance of protein loading on the release profile. It was obvious to observe higher initial burst release with increasing insulin loading in the delivery system which is mainly attributed to the presence of higher amount of unassociated insulin on the surface of the delivery system. With increasing polymer concentration the secondary burst release of insulin was reduced showing that smaller pores/channels could have formed in the delivery system at higher polymer concentration. These smaller channels possibly occluded the pathway of entrapped insulin molecules and reduced their escape from the polymer matrix. There are number of reasons which

could affect the secondary burst release of insulin. All formulations showed secondary burst release which may be due to the degradation of polymer matrix, leading to increased size of the pores/channels formed or because of increased solubility of insulin inside the polymer matrix due to development of acidic conditions. In case of formulation containing insulin alone the faster release of insulin during initial phase could form larger pores and channels in the polymer matrix that are more release medium accessible. Therefore it would increase the diffusion of insulin from the delivery system release duration than expected (233).

Almost all formulations showed slow and incomplete release of insulin at the end stage and a significant amount of insulin remained in the delivery system. As described earlier formation of acidic degradation products of PLA may be one of the reasons for incomplete release (234, 235). Other reason could be due to the irreversible aggregation, precipitation, and/or degradation of insulin in the formulation or during release that made it unavailable for release. Incomplete release may also be attributed to the protein adsorption onto the surface of degrading delivery system, or due to the ionic interactions between the protein and charged end groups in the polymer, which can lead to many problems related with protein instability (236). Sluzky et al., (237) have highlighted the importance of mechanical stress on insulin aggregation, and showed that agitation and hydrophobic surfaces lead to insulin aggregation in the formulation. Insulin fibril formation could be one of the reasons of its aggregation and precipitation. The main driving force of for fibril formation is the exposure of hydrophobic surfaces, and formation of β-sheets which stabilize the fibril structure. For the initiation of fibril formation and aggregation, the dissociation of insulin hexamers/dimers into monomers is necessary. When a large portion of insulin is in the form of hexamers or in oligomeric state, the effective surface available for unfolding of monomers and hydrophobic interaction is very low.

Zinc is a well-known divalent cation used to stabilize the insulin hexameric assembly, and can be used to reduce dissociation of insulin oligomers which in turn avoid the exposure of hydrophobic surfaces leading to inhibition of fibril formation/aggregation (238). In our body zinc ions also control the biosynthesis and storage of insulin in the crystal form in pancreatic beta cells, and help preventing its degradation within the storage vesicle.(239) Zinc has been used to control the insulin release from various formulations including polyanhydride, PLGA microspheres and ethylene-vinyl acetate copolymer matrix (2,3,240,241). Addition of zinc to insulin helped to reduce the initial burst release and controlled the release of insulin from the PLA-PEG-PLA copolymer based delivery system (84). Being small (Mw: 5808 Da) and high water solubility, monomeric insulin can easily diffuse through the pores/channels of the polymer matrix leading to high initial burst. Formation of zinc-insulin hexamer reduces its water solubility, increases its size and hence reduces its diffusion from the porous polymer matrix. Zinc imparts stability to insulin but as the amount of insulin depletes in the delivery system, zinc dissociates and diffuses out, leading to the dissociation of hexamers and dimers into monomers. Thus, in attempt to improve the release profile of insulin at higher loading and to improve its stability, zinc was added to the formulations (5:1 zinc ions: insulin hexamer). Our preliminary studies showed that addition of zinc (5:1 zinc: insulin hexamer) helped to control the release of insulin for longer duration from the thermosensitive polymeric delivery system as compared to insulin alone, and helped to decrease the initial burst release. But it did not significantly reduce the initial burst release as the insulin loading was increased. Additionally, the delivery system did not release the incorporated protein completely and about 20-25% of the total insulin loading remained in the delivery system at the end of release period. The incomplete release could be due to the highly compact nature of hexamers which might have precipitated and did not release out.

It is very important for a suitable controlled delivery system to be able to release protein in its conformationally and chemically stable and biologically active form, since protein can be easily destabilized during formulation processes. Structural deformation is one of the reasons for the loss of protein's activity and incomplete release. For proper biological response, the tertiary, secondary, as well as primary structure of the protein has to be maintained. Therefore, it is important to examine the stability of proteins released from the polymeric delivery systems. Hence the effect of zinc addition on stability of insulin at higher insulin loading was also evaluated. Our preliminary studies showed that the pH of the release medium dropped after 30 days of in vitro release, and the internal pH within the hydrogel might be more acidic than the releasing medium. Insulin is a very fragile molecule and undergoes degradation or aggregation due to moisture and the acidic environment created by the degradation products of polymer during release. Various analytical techniques were utilized to evaluate the stability of the released insulin from the delivery systems containing zinc-insulin. CD studies provided valuable information about the secondary and tertiary structure of insulin released from the delivery systems. CD spectra of released insulin in far UV region showed the presence of two minima due to the major contribution of α helix, and indicated that the secondary structure of insulin was preserved. But after ~42 days, an increase in random coils and reduction in α-helix and β-sheets was observed indicating the loss of secondary structure of insulin released. This reduction can be explained on the basis of an additional time gap between the actual insulin release from the delivery system and the sampling period. Marked increase in tyrosyl signal was observed in all released samples of insulin initially in near UV-CD region, and this spectrum provided some helpful information about the aggregation state of insulin (tyrosyl signal intensity). The hexameric form of insulin shows highest negative intensity, while monomer intensity is least

negative in near UV region (242). Tyrosyl contributes about 50-85% of the near UV-CD signal and increased tyrosyl signal intensity indicates the presence of insulin hexamer/dimers. Along with tyrosine residues, disulfide bridges also contribute to the near UV-CD signal, but the exact contribution and the proportions are difficult to determine experimentally (242). Tyrosyl signal intensity reduced eventually and two months released samples showed marked decrease in the signal intensity as compared to fresh insulin indicating loss of its tertiary structure.

Insulin is a small protein with molecular weight of 6 kDa, and has a tendency to self-associate to form oligomers. The presence of higher ordered structures in native PAGE indicated that the released insulin was in the form of mixture containing monomers, dimers and hexamers. SDS-PAGE under non-reducing conditions was performed to dissociate non-covalent aggregates of insulin. Under non-reducing conditions a single band corresponding to native insulin was observed in SDS-PAGE experiments. These results helped to conclude that the higher ordered aggregates detected in native PAGE analysis were non-covalent and there was no aggregation of insulin during formulation and release. Similarly no additional bands below 6 kDa during native and SDS-PAGE indicated that insulin did not undergo degradation during formulation. As mentioned earlier, there are number of factors which could affect the chemical stability of insulin during release from the polymeric depots.

Insulin is susceptible to several chemical modifications which could alter its primary structure and its biological activity. When the peptide/protein is encapsulated inside the poly (lactic-co-glycolic acid) (PLGA) copolymer matrix the most common reactions that can occur are, deamidation, acylation and peptide bond cleavage. The acylation products can be observed due to the reactions between polymer and peptide under neutral pH and low moisture content (243). The results of MALDI-TOF MS analysis showed that the primary structural integrity of

insulin was conserved in the released samples without any major degradation products till one month release period. A very small peak corresponding to a split product was observed which might be due to the double (+2) protonated insulin molecule. Some degradation products were detected in the released samples after two months which were difficult to identify. They could have formed due to the prolonged time gap between the actual release and sampling, or due to the acidic microenvironment due to polymer degradation. Another reason could be due to degradation of insulin in the delivery system. But a peak corresponding to intact insulin at ~5808 Da indicated that the primary structure of insulin was conserved. The stability studies suggested that some degradation/aggregation products of inulin were formed during in vitro release even in presence of zinc indicating that zinc alone is not sufficient to stabilize insulin in the polymeric delivery system.

To reduce the initial burst release from the delivery system, insulin should be made unavailable for immediate diffusion after placement of the delivery system in the release medium. Most importantly, the rate of insulin diffusion through the polymer matrix should be controlled. In order to reduce the initial diffusion of insulin monomers from the polymeric delivery system, chitosan-zinc-insulin complexes were prepared. The electrostatic interaction between chitosan and insulin is weak in nature, but can help to reduce the diffusion of protein from the polymeric hydrogel matrix by increasing its size. Since chitosan is also known to stabilize proteins, the complex will also help to stabilize insulin in the delivery system during release. It was observed that the complexes were formed at optimized pH conditions. The essential factors such as stability of insulin in presence of chitosan, complex formation and its dissociation were evaluated. It was noted that the chitosan-zinc-insulin complex formation took place in the pH range of 6.5-6.8. The entrapment efficiency of complex was found to be ~70-

76%. Gel retardation assay confirmed that chitosan and insulin form stable complexes since most of the protein was retained in the gel well during native PAGE analysis. The results also showed that the complex formation between zinc-insulin and chitosan was influenced by the amount of chitosan present in the system. The complex formed was weak in nature and dissociated very easily in the presence of an anionic surfactant SDS, and released insulin preserved its structural integrity. Fluorescence, Circular Dichroism spectroscopy and Differential Scanning Calorimetry helped to determine the structural integrity of insulin in presence of chitosan during complex formation. The fluorescence property of the proteins can give some information regarding the molecular environment of the protein. The aromatic residues like tryptophan and tyrosine dominate the fluorescence property of a protein, and any change in this gives the information about their environment (244). Since insulin does not contain any tryptophan residues, the fluorescence signal is solely affected by the presence of tyrosine and phenylalanine residues on the surface which contribute towards oligomer formation. The interaction between chitosan and hemoglobin was studied by fluorescence spectroscopy. There was no shift in the intrinsic fluorescence property of hemoglobin after addition of chitosan. These results indicate the partially reversible nature of the interaction (244). Our studies also demonstrated that the fluorescence property of insulin (tyrosine/phenylalanine fluorescence) did not alter after addition of increasing chitosan amounts. It also supports our observation that the interaction between chitosan and insulin is very weak and does not change the tertiary structure of insulin. We observed a small change in the secondary structure of insulin which could be due to hydrophobic interactions or hydrogen bonding between chitosan and insulin at increasing chitosan amount. The results of CD analysis also confirmed that chitosan did not alter the secondary structure of insulin in the concentration range used in this study. DSC helped to determine the stability of

insulin in dilute solution by analyzing the changes in its midpoint of transition (T_m). The change in ΔH and T_m of a compound eventually reflects its ability to absorb heat in response to gradual increase in temperature. It has been reported that addition of divalent cations help to stabilize insulin by neutralizing the charges at the center of insulin hexamer and which increases its T_m (2,3,84). The effect of different ligands like phenol, m-cresol, resorcinol, at various zinc concentrations on the stability of insulin has also been evaluated by DSC, and it was observed that these compounds helped to stabilize zinc-insulin hexamers (245). Our results showed that addition of chitosan has further stabilized the zinc-insulin hexameric assembly as indicated by increased thermal stability (i.e., T_m and ΔH values) in comparison to the zinc-insulin. The increase in T_m compared to chitosan-free zinc-insulin was ~4.5°C. Increased hydrophobic interactions between hexamers and chitosan could be one of the reasons for increased stabilization of hexameric assembly. It was also noticed that increasing zinc: insulin hexamer ratio beyond 4:1 did not show any additional stabilizing effect determined by DSC. To determine the amount of insulin loading in the complex, the chitosan-zinc-insulin complexes were centrifuged and the supernatant was tested for free insulin. The insulin loading was found to be ~75% of the total insulin used. After quantification the insulin loading in the delivery system was adjusted.

Chitosan-zinc-insulin complexes were mixed with the thermosensitive polymer solution (30% w/w) and thermoreversible nature of the delivery system was checked. The incorporation of chitosan-zinc-insulin complex in the delivery system did not change its thermosensitive nature. After increasing insulin loading in the delivery system, a slight increase in the gelling time was observed, but all formulations were injectable at room temperature, and showed rapid conversion from sol to gel near body temperature. Initially the effect of chitosan addition on in

vitro release of insulin and zinc insulin was observed at low protein loading. Significant reduction in the initial burst release was observed after incorporating chitosan-zinc-insulin complex in the polymeric delivery system as compared to insulin alone or zinc-insulin. The coefficient of determination values showed best fit for zero order release with chitosan-zinc-insulin complex. The results showed that by increasing the size of the insulin decreased its diffusion from the polymer matrix, and the release rate was more dependent on the dissociation of chitosan-zinc-insulin complex as well as the polymer degradation. Depending on these results the formulation parameters were optimized. It seems logical that adding surplus zinc ions to insulin increases stability of its hexameric structure and could help inhibiting fibril formation. But, studies have also shown that, the insulin formulations containing zinc ions > 4/hexamer are prone to hydrolytic cleavage at A8-A9 position (131). Though no specific split products corresponding to hydrolysis at A8-A9 were observed in MALDI-TOF mass analysis, some low molecular weight products were detected. These products might have formed due to hydrolysis or deamidation of insulin due to excess zinc ions present. Hence for our further studies zinc: insulin hexamer ratio of 4:1 was used. The concentration of the thermosensitive polymer selected was 30% w/w for our further experiments since the delivery system was easily injectable at this concentration even at higher insulin loading. The chitosan amount was varied and the effect of increasing chitosan amount on initial burst release as well as the release profile of zinc-insulin was determined. At the same time it was observed that formulations were injectable. The release profile of insulin from chitosan-zinc-insulin complex loaded thermosensitive delivery system at higher loading was studied. The stability of released insulin was determined by above mentioned analytical techniques. Formulation containing zinc-insulin showed significant reduction in the initial burst release as compared to the formulations without zinc and prolonged the release of

insulin up to 63 days. Even though zinc addition controlled the release initially in a better way as compared to the formulation without zinc, a high secondary burst was also observed. It was noted that addition of chitosan to insulin did not help to improve the initial burst as well as overall release duration. A high initial burst followed by a short-term release was observed, and only 65% of the total protein was released from the delivery system. Large amount of insulin remained inside the delivery system after two months of release from the formulations containing insulin alone, zinc-insulin and chitosan-insulin. Though we quantified the amount of insulin remaining in the delivery system, we did not find a simple mass balance between the amount of unreleased and released insulin. The sum of the released insulin amount and the insulin remaining in the delivery systems after completion of the release period was not equal to the amount of insulin incorporated in the delivery system. This difference (~8-13% of the total insulin amount incorporated in the delivery system) could be attributed to the degradation/precipitation or aggregation of insulin in the release medium after successful release. Delivery system containing chitosan-zinc-insulin complex showed significant reduction in the initial burst as well as showed almost complete release of insulin (~95%) within three months as described in results. This might be due to the ionic interactions present between chitosan and insulin which might have stabilized the insulin inside the delivery system, and during release. These ionic interactions, along with slow dissociation of insulin hexamers into dimers/monomers, may have contributed to the prolonged and complete release. Thus, use of zinc or chitosan alone was not sufficient to reduce the initial burst and to control the insulin release. Similarly, it was observed that at higher protein loading (formulation H: 45 mg insulin loading) chitosan-zinc-insulin complex containing delivery system performed better as compared to the formulations containing insulin alone or zinc-insulin. Increasing protein loading from 30 to

45 mg in the delivery system showed slight increase in initial burst release, but the overall release period was unaffected. A slight increase in initial burst release was seen due to increased insulin loading leading to the formation of more pores in the polymer matrix and thereby shortening the overall release period (26). Increasing chitosan amount in the delivery system led to a small reduction in the initial burst, but there was no significant difference in the release pattern observed. The formulations containing chitosan-zinc-insulin complex showed higher correlation (r^2) for zero order release kinetics. The results indicate that the chitosan-zinc-insulin complex plays an important role in reducing the initial burst release of insulin as compared to the formulations containing insulin alone and zinc-insulin. But interestingly in our recent studies it was noticed that after increasing insulin loading to 60 mg in the delivery system, zinc-insulin containing formulation showed minimal initial burst release as compare to the formulations containing insulin alone as well as chitosan-zinc-insulin complex.

Additionally, it was noted that the release of insulin was very slow until ~1 month followed by a sharp secondary burst release probably caused due to degradation of the delivery system resulting in release of precipitated/aggregated insulin. This secondary burst released most of the insulin in approximately 20 days, and then a plateau appeared. The results indicated that though zinc decreased initial burst by reducing solubility of insulin, it did not control the release which reduced the usefulness of the delivery system. In case of delivery system containing insulin alone, similar release pattern was observed but the majority of the insulin (~50%) was released in 30-35 days with overall release duration up to 60 days. As discussed earlier, acidic microenvironment within the delivery system during polymer degradation is one of the major factors of insulin instability. This acidic environment can be reduced by incorporating a basic excipient in the delivery system (246). Chitosan carries abundant amino groups on its surface

and gets ionized in acidic pH leading to swelling of the polymer network (247). This may reduce the exposure of protein to the damaging environment and results in increased stability. The effect of acidic microenvironment on the stability of insulin was also assessed. Insulin alone, zinc-insulin and chitosan-zinc-insulin complexes, were incubated with the lactic acid which is the major end product during polymer degradation, and the thermostability of insulin was investigated using DSC. The DSC results showed that presence of lactic acid reduces the thermostability of insulin alone and zinc-insulin but did not significantly alter insulin structure in the form of chitosan-zinc-insulin complex. These results demonstrate the additional stabilizing effect of chitosan on insulin structure. Chitosan also possesses good buffering ability which might have resisted the major pH change in the microenvironment of the delivery system. Addition of chitosan to zinc-insulin shifted the best fit model from higuchi to zero order, which is an ideal model for the long-term controlled release.

4.4. Stability of Released Insulin

Stability of insulin released from the delivery systems during in vitro studies was studied using CD, DSC, PAGE/SDS-PAGE, HPLC and MALDI-TOF mass spectroscopy. As mentioned earlier, presence of moisture, agitation, and acidic pH influence insulin stability. The CD spectroscopy results showed attenuation in the CD signal intensities indicating loss of α helix and increase in random ordered structures. Insulin gets exposed to the harsh conditions like agitation, acidic polymer degradation products as well as aqueous environment once it is released from the delivery systems. This can lead to its degradation in the release media. Since aromatic residues play important role in insulin dimer, tetramer and hexamer formation their removal from insulin surface leads to loss or reduction in near UV-CD signal (248). All released samples of insulin showed reduction in the intensity of near as well as far UV spectra indicating reduction in

α helix and β sheets as well as tertiary structure of insulin during release. However, the presence of two minima in far UV region and minima at 278 nm due to tyrosyl residues in near UV-CD region indicated that the secondary and tertiary structure of insulin was relatively conserved during release. It has been established that zinc addition helped to preserve the secondary structure of insulin, and prevented its aggregation when exposed to harsh manufacturing conditions during microsphere preparation (2).

Our DSC results also confirmed that the addition of chitosan to zinc-insulin complex stabilized the zinc-insulin hexamer and enhanced its stability during release. The DSC results also showed that chitosan-zinc-insulin complex released insulin in its native form upon dilution. In addition to secondary and tertiary structural changes, insulin aggregates can be formed due to exposure to various formulation conditions as well as during release. PAGE helped to determine the presence of aggregates while SDS-PAGE under non-reducing conditions helped to determine the nature of aggregates. PAGE results indicated the presence of dimers in the released samples but a single band corresponding to native insulin (6 kDa) in SDS-PAGE allowed us to conclude that the aggregates detected were non-covalent. The results also suggested that the primary structure of insulin was conserved throughout the release period as evidenced by the presence of monomers.

Insulin is known to undergo many chemical modifications that limit its biological activity. It has been reported that the terminal amino acid residue of A chain (Asn 21), is prone to deamidation at acidic pH. Rate of deamidation at A21 decreases with increasing pH, and near neutral pH this reaction is slower and takes place exclusively at asparagine residue present in B chain (Asn B3) (128). The interactions between polymer and incorporated protein, as well as the acidic climate inside the matrix are known to accelerate the acid-catalyzed reactions of the

peptide bonds, which is one of the reasons of insulin instability and incomplete release (249,250). Hence it is critical for the delivery system to protect incorporated insulin in its intact form during release. HPLC and MALDI-TOF mass spectroscopy techniques helped to determine the presence and nature of chemical modifications that might have occurred in insulin during release. Our MALDI-TOF MS results showed that with increasing the time of incubation, insulin solution (control) showed large amount of degradation products and signal corresponding to intact insulin disappeared after 30 days of incubation. The results suggest that insulin gradually lost its structural stability in PBS at 37°C. Formulations containing insulin alone and zinc-insulin showed presence of deamidation and cyclic imide product formation after one month of release. Since cyclic imide is stable at acidic pH, increase in its signal intensity observed in two months released samples suggested the presence of acidic microenvironment due to degradation/hydrolysis of polymer (243). The delivery system containing insulin alone showed the presence of insulin dimer with a peak corresponding to 11685.47 m/z indicated that there is formation of covalent insulin dimers in the released sample. Polymeric formulation containing chitosan-zinc-insulin complex showed a major peak corresponding to intact insulin with a negligible peak at 5789 m/z. the results indicate that addition of chitosan to zinc-insulin (4 zinc ions/insulin hexamer) has helped to preserve its primary structure during entire release period. Addition of chitosan has also helped to reduce the acidic environment inside the polymeric hydrogel indicated by the presence of a very small peak corresponding to cyclic imide in two months released sample. The extent of degradation in the released insulin samples was also assessed using RP-HPLC. Chemically intact insulin showed a single peak at 9.8 min. In contrast to intact insulin, incubated insulin control showed an additional peak at 4.8 min indicating degradation of protein at day 15. The prolonged incubation time increased the appearance of

degradation peaks with concurrent reduction of peak at 9.3 min for intact insulin, and the peak disappeared after 30 days of incubation showed complete degradation of insulin. The HPLC chromatograms showed that primary structure of insulin did not change during release. HPLC chromatograms of insulin released from the delivery system showed presence of some degradation products, but still the major peak corresponding to native insulin provided the evidence that chemical integrity of insulin was retained.

4.5. Stability of Insulin in the Delivery System During Release and Storage

Although insulin was structurally stable during release, the information was insufficient to demonstrate the stability of insulin remaining in the delivery system during release. The microenvironment present in the delivery system plays an important role in maintaining the stability of protein. Tang and Singh, (4) reported that the presence of acidic environment caused due to hydrolysis of polymer backbone, and protein degradation products can affect the stability of protein inside the delivery system. As discussed earlier, protein can undergo deamidation, acylation, or peptide bond cleavage in the polymeric delivery systems. Increased cyclic imide product formation in case zinc-insulin containing delivery systems (formulation B) indicated increased hydrolysis and deamidation reactions occurred. The delivery system containing insulin is stored at 4°C, and also remains at body temperature for extended duration after administration. Therefore insulin should be stable for intended storage duration as well as in the gel depot during entire release period at body temperature. Therefore structural stability of insulin was evaluated at storage and body temperatures after extracting it from polymer matrix. The HPLC and MALDI-TOF MS analysis confirmed that the insulin extracted from gels showed major signal similar to intact insulin, indicating that no significant degradation occurred inside the gel depot during release as well as storage. Similarly, native PAGE results also showed that the insulin

extracted from the gels during release and storage at 37 and 4°C was chemically intact. Our results confirmed that addition of chitosan helped stabilizing insulin in the delivery system by shielding it from the acidic environment developed inside the delivery system due to polymer degradation over the period of time.

The acidic byproducts formed during degradation of the triblock copolymer lead to decrease in pH of microenvironment in the gel matrix, which is the major cause of insulin instability. This acidic microclimate can be reduced by incorporating a basic excipient in the delivery system (246). Chitosan possesses abundant amino groups on its surface, and hence, acts as proton sponge (247,251). It also possesses good buffering ability which could resist the major pH change in the microenvironment of during degradation of polymer gel matrix. Our preliminary results indicated that the addition of chitosan to zinc-insulin could have reduced the exposure of protein to the damaging environment resulting from PLA degradation, leading to increased stability. Our studies also demonstrated that the presence of lactic acid residues reduced the thermostability of insulin alone and zinc-insulin, but did not significantly affect insulin in the form of chitosan-zinc-insulin complex determined by DSC. These results further confirmed the stabilizing effect of chitosan on insulin structure.

4.6. In Vivo Absorption and Bioactivity of Insulin

Our in vitro release studies, and stability studies indicated that the increased size (zinc-insulin hexamer), and slow dissociation of zinc-insulin after complex formation with chitosan helped to reduce insulin diffusion from the thermosensitive polymer gel matrix, and prolonged the insulin release in vitro. This slow diffusion of insulin resulted in reduced initial burst release, and further the complex helped to stabilize insulin during release and storage, while providing controlled release over extended duration in vitro. Therefore, optimized delivery systems

containing chitosan-zinc-insulin complex were further evaluated for their ability to deliver insulin in vivo using streptozotocin (STZ) induced diabetic rat model. A single dose STZ induced diabetic rat model is widely accepted experimental model to study the effect of various controlled release insulin formulations. A single dose STZ (55 mg/kg) causes selective toxicity to pancreatic beta cells, and produces type 1 diabetes in the experimental animals (252). STZ action is manifested via alkylation of DNA, which in turn causes drastic reduction in insulin level affecting overall glucose metabolism in the body, and thereby producing hyperglycemia. The blood glucose levels of rats after STZ treatment increased rapidly, and were hyperglycemic after 5-7 days. As expected, SC injection of insulin solution demonstrated the shortest duration of action and the blood glucose levels reverted to the pretreatment levels within 12 h post treatment. The factors which alter the insulin absorption after subcutaneous administration are its molecular weight, and association state at the administration site (253). The results showed that after SC administration of insulin solution, insulin being in its monomeric form was absorbed quickly leading to a spike in insulin levels. The polymeric delivery system containing insulin alone also demonstrated a rapid increase in serum insulin concentration, indicating an initial burst release due to the quick escape of unassociated surface-localized insulin monomers after injection. These surface localized insulin monomers being smaller in size might have escaped easily by diffusion, resulting in a spike in insulin levels. Additionally, the delivery system showed a short-term release of insulin which could be due to the aggregation or degradation of insulin in the delivery system. These results were also supported by the reduction in pharmacodynamic response of insulin. Addition of zinc to insulin reduced the initial burst due to the increased size and reduced solubility of insulin. It also helped in relatively sustaining the release of insulin for longer duration as compared to insulin alone. Zinc is known to exhibit

fibrillation inhibitory effect on insulin, and stabilizes hexameric assembly (35). Although zinc-insulin hexamer formation helped to reduce the initial burst release of insulin and prolonged the release duration, there was no appreciable improvement in the bioavailability as compared to the formulations containing insulin alone. The delivery systems containing chitosan-zinc-insulin complex showed marked reduction in the initial burst release, indicated by a gradual and slow rise in serum insulin levels. This might be due to the enlarged size (zinc-insulin hexamer), and the complex formation with chitosan by electrostatic interactions which might have helped in reducing insulin diffusion from the polymer gel matrix.

The initial burst release of insulin is the major cause of hypoglycemia and is a critical aspect which needs to be addressed during the development of controlled delivery systems. The balance between glucose production and its utilization gets altered due to the large variation in plasma insulin levels after its administration (254). Reduction in peak/trough ratio of insulin (i.e. lowering the variability) is highly desirable to lower/prevent the occurrence of hypoglycemia-associated complications (155). Formulations containing chitosan-zinc-insulin showed a gradual increase in serum insulin with very low peak-free levels after administration, and additionally the release was continuous for ~70 days. These formulations also showed increase in AUC by 1.2-2 fold as compared to zinc-insulin and insulin alone containing formulations, respectively. This could be due to the slow dissociation of large chitosan-zinc-insulin complexes, into insulin oligomers and finally to zinc-free insulin monomers. The chitosan-zinc-insulin complex loaded thermosensitive polymeric delivery system released small amount of insulin over prolonged period of time leading to higher absorption rates. It has been well documented that the absorption rate of insulin via subcutaneous route is a complex phenomenon, and is inversely related to its concentration (255). Thus, the slow dissociation of insulin from the chitosan-zinc-insulin

complex might have reduced its degradation by the proteases present at the injection site, and thereby improved its absorption (35). Since chitosan is known to stabilize proteins (168,172-174), the complex formation might have offered additional stabilizing effect which protected insulin after administration. These results also confirmed our earlier findings showing that chitosan-zinc-insulin containing thermosensitive polymeric delivery system maintained at body temperature preserved the structural integrity of incorporated insulin for prolonged period (256).

The pharmacodynamic effect of insulin released from different delivery systems was evaluated by the regulation of blood glucose levels. The high initial burst release of insulin observed after administration of formulations containing inulin alone caused rapid reduction in blood glucose levels below the normal levels, and suggested that the delivery system containing insulin alone would not be a good choice, since it may lead to a hypoglycemic shock. Zinc-insulin containing formulations did not show a sharp drop in blood glucose, indicating reduction in initial burst release due to formation of zinc-insulin hexamers (increased size, and reduced solubility), but lowered the blood glucose levels for slightly longer duration as compared to insulin alone. The results suggest that the incorporated insulin might have precipitated/degraded in the delivery system, and failed to elicit the biological response. Chitosan-zinc-insulin containing formulations (insulin loading: 30 and 45 IU/kg) showed gradual and sustained reduction in blood glucose over the period of 7 days, without any sign of hypoglycemia. This is considered as the most important and desirable property of insulin containing controlled delivery systems. The delivery systems containing chitosan-zinc-insulin complexes helped maintaining the blood glucose levels below 200 mg/dl, for prolonged duration as compared to insulin alone or zinc-insulin containing delivery systems. Additionally, the blood glucose levels were comparable to that of control (untreated rats) for considerably longer duration and then increased gradually.

The results also showed that there was no significant difference ($P>0.05$) in blood glucose levels in two consecutive time points until 56-63 days, which can be interpreted as the pharmacodynamic manifestation of the continuous release of insulin at a steady rate. This data also demonstrates that the biological activity of insulin released from chitosan-zinc-insulin complex was preserved during fabrication and maintained during the entire release duration. All the delivery systems released insulin for relatively shorter period in vivo as compared to in vitro release. It has been well documented and also observed in our earlier studies that the in vivo release duration of insulin was shorter as compared to that of observed during in vitro release, which could be as a result of faster degradation of the delivery system in vivo than in vitro (35,257). But, as far as the biological activity of released insulin is concerned, chitosan-zinc-insulin complex containing delivery systems showed better glycemic control over longer duration as compared to the delivery system containing insulin alone or zinc-insulin.

Some of the macro and micro vascular complications due to diabetes include stroke, neuropathy, amputations, retinopathy, and renal failure, leading to increased disability, reduced life expectancy, and huge health costs (258). The animals in the streptozotocin treatment group developed not only diabetes as indicated by increased fasting blood glucose values, but also showed signs of cataract which is one of the earlier complications of diabetes mellitus. Similarly, the animals treated with the delivery systems containing insulin alone also showed signs of cataract by the end of study indicating that the delivery system did not release insulin sufficient enough to alleviate the diabetic complications. No signs of retinopathy were observed in rats treated with zinc-insulin or chitosan-zinc-insulin containing formulations indicated that the released insulin helped in preventing the onset of diabetes related microvascular complications. It has been reported that STZ induced diabetes causes reduction in body weight due to the

loss/degradation of structural proteins, which mainly contribute to the body weight (259). Thus, after STZ treatment, a significant and drastic weight loss was observed in all groups. A gradual improvement in body weight was noticed after administering the rats with insulin formulations, while the rats in STZ treatment group showed continuous weight loss. This increase in body weight may be due to the prolonged release and in turn effect of insulin from the delivery system.

Proteins undergo physical degradation like unfolding, misfolding, aggregation, or chemical degradation such as oxidation, deamidation, isomerization, that can result in an immune response (260). Protein aggregation in the commercially available preparations has reported to be a key factor underlying the unwanted immune responses of therapeutic proteins. Insulin aggregates are known to invoke antibody formation (261), and hence insulin aggregation inside the delivery system could alter its release, stability, activity, safety and overall duration of action after administration. Fineberg et al. (262), have reported that the formulation is one of the crucial factors that alter the immunogenic potential of insulin. Soluble forms of insulin are known to be less allergenic than intermediate or long-acting insulin preparations. The acidic preparations of insulin are reported to be more immunogenic than neutral formulations. Our ELISA results indicated that no immune response against human insulin observed in all treatment groups, which signified that the released insulin was non-immunogenic in nature.

4.7. Biocompatibility of the Delivery Systems

Biocompatibility is an array of complex characteristics and indicates the level of interaction between the implanted delivery system and the host tissue. It is difficult to determine the biocompatibility of a material by a single method, and always require complex set of in vitro and in vivo methods. In our earlier studies we have already demonstrated the biodegradable and

biocompatible nature of the thermosensitive polymeric delivery system (PLA-PEG-PLA, Mw: 4500 Da) in vitro (35). Chitosan, another polymer used in this study is a linear polysaccharide composed of β-(1-4)-linked D-glucosamine and N-acetyl-D-glucosamine units distributed randomly. Chitosan is eliminated from the body by renal clearance, and the degree of acetylation as well as its molecular weight affects the degradation rate. High molecular weight chitosan undergoes degradation by chitinases in the body leading to the formation of smaller chains (263,264). It is reported as a biocompatible and biodegradable positively charged polymer with minimum immunogenic potential and also possesses low cytotoxic potential (166). Zinc also gets eliminated from body via renal clearance (265). It is important to consider the potential cytotoxicity of the thermosensitive polymer (PLA-PEG-PLA) with or without chitosan, and its residual degradation products. An indirect cytotoxicity method was used, where the cells were exposed to the polymer extracts prepared at 37 and 70°C which simulated the long-term effects of the injected depot forming delivery system (65,266). Prior to the treatment, the extracts were neutralized to disregard the effect of pH, and to emphasize on the effect of polymer degradation products on cell viability. Thus, the results showed the effect of concentration of polymer and its degradation products only on the cell viability. Growth medium without polymer addition served as negative control and used to determine the percent cell viability. Our in vitro cytotoxicity study results indicated that the addition of chitosan did not change the biocompatible nature of the delivery system containing thermosensitive polymer. The polymer extracts of thermosensitive copolymer containing chitosan prepared at 70°C showed higher cell viability in comparison to extract prepared at 37°C. Chitosan has been found to exhibit good biocompatibility and extremely low cell toxicity (166). Chitosan accelerates cell proliferation, and also possesses wound healing property (267). Since greater amount of chitosan would be

extracted in its low molecular weight soluble form at 70°C, which has led to lesser cell toxicity than the extract prepared at 37°C. In an effort to determine the biocompatible nature of the delivery system in vivo, the subcutaneous tissue surrounding the depot was excised and observed for inflammatory reactions. Tissue healing process is usually initiated through cascade of inflammatory stages including acute inflammation, chronic inflammation, and granular tissue formation at the injection site (61,268). During in vivo biocompatibility evaluation, it was noticed that the subcutaneous administration of polymeric systems with/without chitosan showed an inflammatory response due to injection and continual presence of polymeric gel in the body. But, at the end of the study no signs of chronic inflammation, or necrosis were observed. Thus, as expected the inflammatory response to the developed delivery systems was short-lived, and the delivery systems were biocompatible.

The extent of fibrosis, organization of collagen fibers and collagen density around the depot are also important in determining the biocompatible nature of the depot forming systems. Gomori's trichrome stain was used to determine the nature and presence of collagen deposition at the subcutaneous tissue-delivery system interface. Though frequent removal and replacement of the release medium during in vitro release reduces the acidic environment with subsequent reduction in protein degradation, it is difficult to predict whether it reflects in vivo conditions (269). It has been reported that the fibrous capsule formation around the delivery system possibly retards the effective elimination of the polymer degradation products out of the site (269). This leads to increased acidic microenvironment near injection site, and in turn reduces the stability of encapsulated protein. It has been reported that usually the collagen fibers are arranged randomly without a specific organization with a sparse density, but in response to injury due to implanted material, collagen become well-defined and increased collagen deposition is usually observed

near the site of implantation (270). In our experiments, it was noted that the collagen deposition at the site of injection was a short-term response. Increased collagen deposition was observed initially, but the its density reduced eventually and the skin tissue observed at the end of the study period showed absence of residual scar tissue indicated the biocompatible nature of the delivery system. Since no scar tissue/fibrous capsule were observed near the gel depot, it allowed us to conclude that polymer degradation products are removed continuously after degradation from the injection site.

5. SUMMARY, CONCLUSION AND FUTURE DIRECTIONS

Smart polymers have revolutionized the field of polymeric drug delivery to achieve sustained and/or targeted delivery of numerous therapeutic agents. These polymers are becoming progressively relevant in the field of protein and peptide delivery, as researchers are learning the ways to take advantage of their interesting properties and control them. Thermosensitive polymers, a class of smart polymers which exhibit temperature-dependent reversible sol/gel transitions, have been studied and used extensively in past decade for drug delivery due to their unique and fascinating properties (14).

In our studies, PLA-PEG-PLA thermosensitive copolymers were synthesized and were used to deliver various drug molecules in vitro and in vivo. This research consisted of two parts; the first part deals with the degradation behavior of copolymers in response to changes in formulation parameters. PLA-PEG-PLA triblock copolymers with chain lengths 1500-1500-1500, and 1600-1500-1600 were synthesized and characterized for their structure, molecular weight, and polydispersity index, and phase transition behavior. The proton and ^{13}C NMR spectra confirmed the structure of the synthesized copolymers, while integrating the proton NMR signals helped in molecular weight determination. The GPC analysis indicated the narrow molecular weight distribution, showing the sufficient purity of the synthesized copolymers. The polymeric delivery systems showed temperature dependent sol-gel transition, and can exist in solution form outside the body (room temperature). The injectability is an essential property for the proposed controlled delivery systems. The delivery systems were freely injectable and formed semisolid depots at body temperature within seconds upon injection.

The hydrolytic degradation behavior of copolymer, and release profile of incorporated agents were investigated in detail. The PLA-PEG-PLA triblock polymer preferentially degraded

by the hydrolysis, and the concentration as well as PLA chain length affected its degradation. Increasing the copolymer concentration, and PLA chain length significantly ($P<0.05$) reduced hydrolytic degradation of polymer. NMR analysis also showed an increase in LA/EG ratio as the degradation proceeded.

The release profile of three different molecules BSA, insulin and risperidone from the thermosensitive delivery systems was evaluated. BSA showed higher initial burst release (13.54±0.89%), followed by insulin (7.32±3.1%), and risperidone (2.13±0.047%). BSA was released rapidly and the release period lasted for ~42 days, including a fast release phase for 7 days, followed by a slow release; while insulin and risperidone were released in a controlled manner for ~70-80 days. The GPC analysis of polymer residuals showed increased degradation rate in the presence of BSA as compared to polymer alone, insulin or risperidone. The size of pores formed in the delivery system as determined by SEM was dependent on the type of drug incorporated. BSA containing hydrogel showed significantly ($p<0.05$) larger pores than insulin or risperidone loaded hydrogels at day 30, but pore size increased and was comparable irrespective of drug type at day 60. The results suggested that not only polymer structure and concentration, but the drug properties are also important while designing the delivery systems. BSA being a large hydrophilic protein showed higher initial burst release, followed by insulin and risperidone. BSA could have formed larger channels near the surface during initial release phase, which led to rapid penetration of water molecules inside the gel matrix. This channel formation, and/solvation of protein in the previously formed channels and water penetration enhanced the polymer degradation. All these combined effects could have resulted in the faster release of BSA. Therefore, it is essential to consider the hydrophobicity, solubility, and size of the incorporated drugs while formulating a delivery system. SEM studies also showed a striking

difference in the porous morphologies of the delivery systems containing risperidone, BSA or insulin. BSA containing delivery system showed was more porous and therefore BSA might have escaped easily from the gel creating even bigger, open, water accessible pores as compared to risperidone and insulin.

It was also noted that the presence of a cationic polymer, chitosan also modulated the polymer degradation behavior. The thermosensitive polymer based delivery system in presence and absence of a cationic polymer showed a marked difference in pH of the release medium. In case of thermosensitive polymer, the pH of the release medium dropped rapidly after and reached to ~4.5 at the end of the study. While, the delivery system containing chitosan resisted the change in pH for longer duration and then pH reduced gradually. However, the pH of the release medium still remained higher as compared to the delivery system without chitosan. Due to the excellent buffering ability of chitosan it has resisted the change in the pH of the release medium for longer duration leading to reduction in acid-catalyzed degradation of copolymer chains.

The second part of this research involved development of an injectable, biodegradable polymeric controlled delivery system to deliver insulin at basal level for prolonged period after a single injection. Proteins represent a vast majority of the biologics, which face issues like short half-life, delicate structure and the physical/chemical instabilities. These problems, combined with their delivery issues, necessitate the need of frequent injections to obtain the desired therapeutic effect. Insulin is one of such proteins requiring frequent injections for treatment of the patients with diabetes. The chronic insulin administration leads to numerous complications and the pain from multiple daily injections adversely affects the quality of life of patients. Controlled delivery of insulin can be helpful to address the difficulties associated with the

traditional administration methods. The choice of delivery system reflects the clinical outcome of the insulin delivered, and involves simultaneous consideration of number of interdependent factors. Some of important factors include stability, release rate, release duration, and biological activity of incorporated insulin, as well as biocompatibility and biodegradability of the delivery system.

Since PLA-PEG-PLA triblock copolymer with 1500-1500-1500 chain length was the most promising copolymer in terms of release rate and duration, it was used in our experiments.

Polymer concentration, insulin loading, chitosan and zinc addition were shown to affect the insulin release in vitro. Addition of zinc to insulin helped to reduce its solubility, increased its size so that its diffusion thorough the polymeric delivery system is reduced. Formulations containing zinc-insulin significantly ($P<0.05$) reduced the burst release and prolonged the release as compared to insulin alone. With increasing insulin loading in the delivery system from 60 to 100 mg increased the initial burst release but did not alter duration of release. Insulin released from zinc-insulin and insulin alone containing delivery systems showed partial loss of secondary structure over the release duration. MALDI-TOF MS analysis showed presence of degradation products during release. The presence of additional free zinc ions (>4) in insulin preparations increased its hydrolytic degradation. Hence, there should be an optimum balance between zinc and insulin amount, and zinc alone is not sufficient to stabilize insulin in the delivery system. Also, increasing zinc:insulin hexamer ratio beyond 4:1 did not show any additional stabilizing effect during our preliminary studies, and hence was used in our further experiments.

A new approach of incorporating insulin in the form of chitosan-zinc-insulin complex was utilized to reduce the initial burst release of insulin from the polymeric delivery systems. A controlled delivery system for insulin based on the chitosan-zinc-insulin complex incorporated in

PLA-PEG-PLA thermosensitive polymer was successfully developed. The chitosan-zinc-insulin complex is weak in nature and easily dissociates in presence of an anionic surfactant. Addition of chitosan did not alter the structural integrity of insulin determined by UV, fluorescence and CD spectroscopy, and has helped stabilizing the zinc-insulin hexameric assembly. The delivery systems prepared after incorporation of chitosan-zinc-insulin complexes in aqueous copolymer solutions (30%w/w) were easily injectable, and were able to form gel at body temperature. Formulations containing chitosan-zinc-insulin (30 to 60 mg) released insulin continuously over 84 to 90 days with a significant ($P<0.05$) reduction in the initial burst release and minimal secondary burst while the formulations containing insulin, zinc-insulin, and chitosan-insulin exhibited high initial burst (7 to 14%) accompanied by a large secondary burst and incomplete release.

CD and DSC studies indicated that the released insulin was stable. MALDI-TOF MS analysis showed that the chemical integrity of insulin released and extracted from gel was conserved after two months of release. Native and SDS-PAGE showed that the insulin aggregates observed were non-covalent nature. HPLC analysis showed that after two months, released and extracted insulin was comparable to native insulin. Thus, our results indicated that chitosan-zinc-insulin complex formation improved the stability of the insulin inside the delivery system and protected it from aggregation during the entire release and storage period determined by PAGE, HPLC, and MALDI-TOF MS.

The ability of the delivery system to provide basal level of insulin for three months after a single subcutaneous injection was investigated in vivo using streptozotocin-induced diabetic rat model. In vivo studies indicated chitosan-zinc-insulin complex containing delivery systems controlled the release of insulin over 70 days, necessary to maintain the basal insulin levels. The

complex formation significantly ($P<0.05$) reduced the initial burst release of insulin from the polymeric delivery system in comparison to zinc-insulin or insulin alone. The released insulin was in its monomeric and biologically active form which was absorbed in the body as evident by reduced blood glucose levels. The blood glucose levels were comparable to that of control (untreated group), and were significantly ($P<0.05$) lower than untreated diabetic rats. No significant difference ($P>0.05$) in blood glucose levels in two consecutive time points until 56-63 days was observed, which is an indicator of pharmacodynamic manifestation of continuous release of insulin at steady rate. The delivery systems also showed increase in bioavailability of insulin as compared to zinc-insulin and insulin alone. The formulations containing insulin did not provoke any immunogenic response, and helped reduce the diabetic complications.

The biocompatibility of the delivery system containing thermosensitive polymer incorporated chitosan was tested in vitro and in vivo. The in vitro cytotoxicity study results showed that the addition of chitosan did not change the biocompatible nature of the thermosensitive polymeric delivery system. The results were confirmed by histological examination of skin tissue samples removed at specific time points from injection sites of rats determined by light microscopy. Though a typical inflammatory reaction was observed at the injection site initially, the skin tissue showed no signs of chronic inflammation, fibrous capsule formation, or necrosis, and was highly comparable to control skin samples after 90 days. The results suggest that the polymeric delivery system containing chitosan was biodegradable and biocompatible in vivo. This signifies that the chitosan-zinc-insulin complex incorporated in the thermosensitive polymeric delivery system can be used as an alternative to the conventional daily multiple dose basal insulin therapy.

Gomori's trichrome stain was used to determine the nature and presence of collagen deposition at the subcutaneous tissue-delivery system interface. It was observed that increased collagen deposition at the site of injection was a short-term response, and the collagen density reduced eventually at the end of the study and showed no presence of any residual scar tissue indicating the biocompatible nature of the delivery system. The results also helped to conclude that the polymer degradation products are removed continuously after degradation at the injection site.

In conclusion, our in vivo studies indicated chitosan-zinc-insulin complex containing delivery systems controlled the release of insulin for prolonged period, necessary to maintain the basal insulin levels. The formulations containing insulin did not provoke any immunogenic response, and helped to reduce the diabetic complications. The polymeric delivery system containing chitosan was biodegradable and biocompatible in vivo. This signifies that the chitosan-zinc-insulin complex incorporated in the thermosensitive polymeric delivery system can be used as an alternative to the conventional daily multiple dose basal insulin therapy.

5.1. Future Directions

The choice of polymer reflects the clinical outcome of the therapeutics, and hence simultaneous consideration of number of interdependent factors is important while developing a delivery system. This study was confined to the PLA-PEG-PLA copolymer based in situ gel forming delivery system with limited PLA and PEG content. There are number of biodegradable polymers which can be used with different hydrophobic/hydrophilic content, and can be optimized for the delivery of various small as well as large molecules. The polymers include PCL-PEG-PCL (59), poly(beta-amino ester) (PAE) pentablock copolymer PAE-PCL-PEG-PCL-PAE (59), mPEG-PLGA-mPEG (4), thermosensitive hydrogel/collagen/chondroitin sulphate

(CS) (271), cationic Poly(organophosphazenes) (272), cyclotriphosphazenes (273), and hyaluronic acid/Pluronic F127 (274) to name a few.

Polyelectrolyte complex formation between charged polymers and peptides and proteins has been the focus of applied research, and there are various research directions which could be pursued based on our work. In most of the cases during polyelectrolyte complex formation, the structural integrity of incorporated molecule is preserved, and hence numbers of studies have been carried out in order to make use of this unique physicochemical property for drug delivery purposes. The factors influencing polyelectrolyte complex formation include overall charge on the molecules, concentration, as well as temperature, pH, ionic strength of the medium, and presence of salts. Though we have used some of the methods for characterizing the complex formation, it should be investigated in detail using other instrumental techniques such as light scattering, Infrared Spectroscopy (IR), and Isothermal Scanning Calorimetry (ITC). The weight ratio of polymer: protein is an important factor determining the complex formation, and hence needs to be optimized further.

Various chemical alterations in the thermosensitive polymer backbone itself which could potentially interact with different charged molecules could be another approach in modifying the release pattern from the delivery system. Additionally, the effect of natural/synthetic polymers or stabilizing agents (sugars, polyols), which are able to form complexes with various therapeutic agents could help modifying the release rate and duration of incorporated molecules. A combination of delivery systems can be an another approach where encapsulated proteins/peptides in the form of microspheres or nanoparticles can be incorporated into the in situ gel forming delivery system so as to control the release rate. Various therapeutic proteins or

peptides such as erythropoietin, growth hormone, calcitonin, bone morphogenetic protein-2 (rhBMP-2) can be ideal candidates for such a type of delivery system.

6. REFERENCES

1. Protein Drugs: Global Markets and Manufacturing Technologies - BIO021C [Internet]. 2008 [cited 2012 Jan 27].
2. Manoharan C, Singh J. Insulin loaded PLGA microspheres: effect of zinc salts on encapsulation, release, and stability. J Pharm Sci. 2009;98(2):529-42.
3. Manoharan C, Singh J. Evaluation of polyanhydride microspheres for basal insulin delivery: Effect of copolymer composition and zinc salt on encapsulation, in vitro release, stability, in vivo absorption and bioactivity in diabetic rats. J Pharm Sci. 2009;98(11):4237-50.
4. Tang Y, Singh J. Thermosensitive drug delivery system of salmon calcitonin: in vitro release, in vivo absorption, bioactivity and therapeutic efficacies. Pharm Res. 2010;27(2):272-84.
5. García J, Dorta MJ, Munguía O, Llabrés M, Fariña JB. Biodegradable laminar implants for sustained release of recombinant human growth hormone. Biomaterials. 2002;23(24):4759-64.
6. des Rieux A, Ucakar B, Mupendwa BPK, Colau D, Feron O, Carmeliet P, et al. 3D systems delivering VEGF to promote angiogenesis for tissue engineering. J Control Release. 2011;150(3):272-8.
7. Al-Tahami K, Singh J. Smart polymer based delivery systems for peptides and proteins. Recent Pat Drug Deliv Formul. 2007;1(1):65-71.
8. Kumar A, Srivastava A, Galaev IY, Mattiasson B. Smart polymers: Physical forms and bioengineering applications. Prog Polym Sci. 2007;32(10):1205-37.
9. Mahajan A, Aggarwal G. Smart polymers: Innovations in novel drug delivery. International Journal of Drug Development & Research. 2011;3(3):16-30.

10. Bawa P, Pillay V, Choonara YE, du Toit LC. Stimuli-responsive polymers and their applications in drug delivery. Biomed Mater. 2009;4(2):022001.
11. Hoffman AS, Stayton PS, Bulmus V, Chen G, Chen J, Cheung C, et al. Really smart bioconjugates of smart polymers and receptor proteins. J Biomed Mater Res. 2000;52(4):577-86.
12. Jeong B, Gutowska A. Lessons from nature: stimuli-responsive polymers and their biomedical applications. Trends Biotechnol. 2002;20(7):305-11.
13. Oak M, Mandke R, Singh J. Smart polymers for peptide and protein parenteral sustained delivery. Drug Discovery Today: Technologies, 2012;9(2):e131–e140.
14. Singh S, Webster DC, Singh J. Thermosensitive polymers: synthesis, characterization, and delivery of proteins. Int J Pharm. 2007;341(1-2):68-77.
15. Jeong B, Kim SW, Bae YH. Thermosensitive sol-gel reversible hydrogels. Adv Drug Deliv Rev. 2002;54(1):37-51.
16. Qiu Y, Park K. Environment-sensitive hydrogels for drug delivery. Adv Drug Deliv Rev. 2001;53(3):321-39.
17. Aguilar MR, Elvira C, Gallardo A, Vázquez B, Román JS. Smart Polymers and Their Applications as Biomaterials. In: Ashammakhi N, Reis R, Chiellini E, editors. Topics in Tissue Engineering. 2007. p. 1-27.
18. Ruel-Gariépy E, Leroux J-C. In situ-forming hydrogels--review of temperature-sensitive systems. Eur J Pharm Biopharm. 2004;58(2):409-26.
19. Schmaljohann D. Thermo- and pH-responsive polymers in drug delivery. Adv Drug Deliv Rev. 2006;58(15):1655-70.

20. Ward MA, Georgiou TK. Thermoresponsive polymers for biomedical applications. Polymers. 2011;3(3):1215-42.
21. Choi S, Baudys M, Kim SW. Control of blood glucose by novel GLP-1 delivery using biodegradable triblock copolymer of PLGA-PEG-PLGA in type 2 diabetic rats. Pharm Res. 2004;21(5):827-31.
22. He C, Kim SW, Lee DS. In situ gelling stimuli-sensitive block copolymer hydrogels for drug delivery. J Control Release. 2008;127(3):189-207.
23. Jeong B, Han Bae Y, Wan Kim S. Biodegradable thermosensitive micelles of PEG-PLGA-PEG triblock copolymers. Colloids Surf B Biointerfaces. 1999;16(1-4):185-93.
24. Cui Z, Lee BH, Vernon BL. New hydrolysis-dependent thermosensitive polymer for an injectable degradable system. Biomacromolecules. 2007;8(4):1280-6.
25. Du J, Peng Y, Zhang T, Ding X, Zheng Z. Study on pH-sensitive and thermosensitive polymer networks containing polyacetal segments. J Appl Polym Sci. 2002;83(14):3002-6.
26. Chen S, Pieper R, Webster DC, Singh J. Triblock copolymers: synthesis, characterization, and delivery of a model protein. Int J Pharm. 2005;288(2):207-18.
27. Soga O, van Nostrum CF, Fens M, Rijcken CJF, Schiffelers RM, Storm G, et al. Thermosensitive and biodegradable polymeric micelles for paclitaxel delivery. J Control Release. 2005;103(2):341-53.
28. Alexandridis P, Holzwarth JF, Hatton TA. Micellization of Poly(ethylene oxide)-Poly(propylene oxide)-Poly(ethylene oxide) triblock copolymers in aqueous solutions: thermodynamics of copolymer association. Macromolecules. 1994;27(9):2414-25.

29. Basu Ray G, Chakraborty I, Moulik SP. Pyrene absorption can be a convenient method for probing critical micellar concentration (cmc) and indexing micellar polarity. J Colloid Interface Sci. 2006;294(1):248-54.
30. Vermonden T, Jena SS, Barriet D, Censi R, van der Gucht J, Hennink WE, et al. Macromolecular diffusion in self-assembling biodegradable thermosensitive hydrogels. Macromolecules. 2010;43(2):782-9.
31. Tang Y, Singh J. Biodegradable and biocompatible thermosensitive polymer based injectable implant for controlled release of protein. Int J Pharm. 2009;365(1-2):34-43.
32. Vermonden T, Besseling NAM, van Steenbergen MJ, Hennink WE. Rheological studies of thermosensitive triblock copolymer hydrogels. Langmuir. 2006;22(24):10180-4.
33. Lee BH, Lee YM, Sohn YS, Song S-C. Synthesis and characterization of thermosensitive Poly(organophosphazenes) with methoxy-poly(ethylene glycol) and akylamines as side groups. Bull Korean Chem Soc. 2002;23(4):549-54.
34. Hu DS-G, Liu H-J. Structural analysis and degradation behavior in polyethylene glycol/poly(L-lactide) copolymers. J Appl Polym Sci. 1994;51(3):473-82.
35. Al-Tahami K, Oak M, Mandke R, Singh J. Basal level insulin delivery: in vitro release, stability, biocompatibility, and in vivo absorption from thermosensitive triblock copolymers. J Pharm Sci. 2011;100(11):4790-803.
36. Fogueri LR, Singh S. Smart polymers for controlled delivery of proteins and peptides: a review of patents. Recent Pat Drug Deliv Formul. 2009;3(1):40-8.
37. Chen S, Singh J. Controlled delivery of testosterone from smart polymer solution based systems: in vitro evaluation. Int J Pharm. 2005;295(1-2):183-90.

38. Tang Y, Singh J. Controlled delivery of aspirin: effect of aspirin on polymer degradation and in vitro release from PLGA based phase sensitive systems. Int J Pharm. 2008;357(1-2):119-25.
39. Lambert WJ, Peck KD. Development of an in situ forming biodegradable poly-lactide-coglycolide system for the controlled release of proteins. J Control Release. 1995;33(1):189-95.
40. Wang L, Venkatraman S, Kleiner L. Drug release from injectable depots: two different in vitro mechanisms. J Control Release. 2004;99(2):207-16.
41. Singh S, Singh J. Controlled release of a model protein lysozyme from phase sensitive smart polymer systems. Int J Pharm. 2004;271(1-2):189-96.
42. Kranz H, Yilmaz E, Brazeau GA, Bodmeier R. In Vitro and In Vivo Drug Release from a Novel In Situ Forming Drug Delivery System. Pharm Res. 2007;25(6):1347-54.
43. Chen X, Wu W, Guo Z, Xin J, Li J. Controlled insulin release from glucose-sensitive self-assembled multilayer films based on 21-arm star polymer. Biomaterials. 2011;32(6):1759-66.
44. Kost J, Langer R. Responsive polymeric delivery systems. Adv Drug Deliv Rev. 2001;46(1-3):125-48.
45. Roy D, Cambre JN, Sumerlin BS. Future perspectives and recent advances in stimuli-responsive materials. Prog Polym Sci. 2010;35(1-2):278-301.
46. Suzuki A, Tanaka T. Phase transition in polymer gels induced by visible light. Nature. 1990;346(6282):345-7.
47. Lavon I, Kost J. Mass transport enhancement by ultrasound in non-degradable polymeric controlled release systems. J Control Release. 1998;54(1):1-7.

48. Sershen S, West J. Implantable, polymeric systems for modulated drug delivery. Adv Drug Deliv Rev. 2002;54(9):1225-35.
49. Hsieh DS, Langer R, Folkman J. Magnetic modulation of release of macromolecules from polymers. Proc Natl Acad Sci U S A. 1981;78(3):1863-7.
50. Saslawski O, Weingarten C, Benoit JP, Couvreur P. Magnetically responsive microspheres for the pulsed delivery of insulin. Life Sci. 1988;42(16):1521-8.
51. Finotelli PV, Da Silva D, Sola-Penna M, Rossi AM, Farina M, Andrade LR, et al. Microcapsules of alginate/chitosan containing magnetic nanoparticles for controlled release of insulin. Colloids Surf B Biointerfaces. 2010;81(1):206-11.
52. Kwon IC, Bae YH, Kim SW. Electrically erodible polymer gel for controlled release of drugs. Nature. 1991;354(6351):291-3.
53. Kagatani S, Shinoda T, Konno Y, Fukui M, Ohmura T, Osada Y. Electroresponsive pulsatile depot delivery of insulin from poly(dimethylaminopropylacrylamide) gel in rats. J Pharm Sci. 1997;86(11):1273-7.
54. Murdan S. Electro-responsive drug delivery from hydrogels. J Control Release. 2003;92(1-2):1-17.
55. Jensen M, Birch Hansen P, Murdan S, Frokjaer S, Florence AT. Loading into and electro-stimulated release of peptides and proteins from chondroitin 4-sulphate hydrogels. Eur J Pharm Sci. 2002;15(2):139-48.
56. Lee KY, Peters MC, Anderson KW, Mooney DJ. Controlled growth factor release from synthetic extracellular matrices. Nature. 2000;408(6815):998-1000.
57. Miyata T, Asami N, Uragami T. A reversibly antigen-responsive hydrogel. Nature. 1999;399(6738):766-9.

58. Ju X-J, Xie R, Yang L, Chu L-Y. Biodegradable “intelligent” materials in response to chemical stimuli for biomedical applications. Expert Opin Ther Pat. 2009;19(5):683-96.
59. Huynh DP, Nguyen MK, Pi BS, Kim MS, Chae SY, Lee KC, et al. Functionalized injectable hydrogels for controlled insulin delivery. Biomaterials. 2008;29(16):2527-34.
60. Nguyen MK, Lee DS. Injectable Biodegradable Hydrogels. Macromol Biosci. 2010;10(6):563-79.
61. Onuki Y, Bhardwaj U, Papadimitrakopoulos F, Burgess DJ. A review of the biocompatibility of implantable devices: current challenges to overcome foreign body response. J Diabetes Sci Technol. 2008;2(6):1003-15.
62. Biological evaluation of medical devices. Geneva, Switzerland; 2007. Report No.: Part 1.
63. Chen S, Singh J. Controlled release of growth hormone from thermosensitive triblock copolymer systems: In vitro and in vivo evaluation. Int J Pharm. 2008;352(1-2):58-65.
64. Al-Tahami K, Oak M, Singh J. Controlled delivery of basal insulin from phase-sensitive polymeric systems after subcutaneous administration: in vitro release, stability, biocompatibility, in vivo absorption, and bioactivity of insulin. J Pharm Sci. 2011;100(6):2161-71.
65. Ignatius AA, Claes LE. In vitro biocompatibility of bioresorbable polymers: poly(L, DL-lactide) and poly(L-lactide-co-glycolide). Biomaterials. 1996;17(8):831-9.
66. Shive M, Anderson J. Biodegradation and biocompatibility of PLA and PLGA microspheres. Adv Drug Deliv Rev. 1997;28(1):5-24.
67. Natu MV, Gaspar MN, Ribeiro CAF, Correia IJ, Silva D, de Sousa HC, et al. A poly(ε-caprolactone) device for sustained release of an anti-glaucoma drug. Biomed Mater. 2011;6(2):025003.

68. Cun D, Jensen DK, Maltesen MJ, Bunker M, Whiteside P, Scurr D, et al. High loading efficiency and sustained release of siRNA encapsulated in PLGA nanoparticles: quality by design optimization and characterization. Eur J Pharm Biopharm. 2011;77(1):26-35.
69. Dhanaraju MD, Gopinath D, Ahmed MR, Jayakumar R, Vamsadhara C. Characterization of polymeric poly(epsilon-caprolactone) injectable implant delivery system for the controlled delivery of contraceptive steroids. J Biomed Mater Res A. 2006;76(1):63-72.
70. Weidenauer U, Bodmer D, Kissel T. Microencapsulation of hydrophilic drug substances using biodegradable polyesters. Part II: Implants allowing controlled drug release--a feasibility study using bisphosphonates. J Microencapsul. 2004;21(2):137-49.
71. Tarvainen T, Karjalainen T, Malin M, Pohjolainen S, Tuominen J, Seppälä J, et al. Degradation of and drug release from a novel 2,2-bis(2-oxazoline) linked poly(lactic acid) polymer. J Control Release. 2002;81(3):251-61.
72. Yasukawa T, Kimura H, Kunou N, Miyamoto H, Honda Y, Ogura Y, et al. Biodegradable scleral implant for intravitreal controlled release of ganciclovir. Graefes Arch Clin Exp Ophthalmol. 2000;238(2):186-90.
73. Athanasiou KA, Singhal AR, Agrawal CM, Boyan BD. In vitro degradation and release characteristics of biodegradable implants containing trypsin inhibitor. Clin Orthop Relat Res. 1995;(315):272-81.
74. Cleland JL, Barrón L, Berman PW, Daugherty A, Gregory T, Lim A, et al. Development of a single-shot subunit vaccine for HIV-1. 2. Defining optimal autoboost characteristics to maximize the humoral immune response. J Pharm Sci. 1996;85(12):1346-9.
75. Huang X, Brazel CS. On the importance and mechanisms of burst release in matrix-controlled drug delivery systems. J Control Release. 2001;73(2-3):121-36.

76. Sheikh Hassan A, Sapin A, Lamprecht A, Emond E, El Ghazouani F, Maincent P. Composite microparticles with in vivo reduction of the burst release effect. Eur J Pharm Biopharm. 2009;73(3):337-44.

77. Amol J. Thote, John T. Chappell J, Rajesh Kumar, Ram B. Gupta. Reduction in the Initial-Burst Release by Surface Crosslinking of PLGA Microparticles Containing Hydrophilic or Hydrophobic Drugs. 2008

78. Li JK, Wang N, Wu XS. Poly(vinyl alcohol) nanoparticles prepared by freezing-thawing process for protein/peptide drug delivery. J Control Release. 1998;56(1-3):117-26.

79. Atkins TW, Tighe BJ, McCallion RL. Incorporation and release of fluorescein isothiocyanate-linked dextrans from a bead-formed macroporous hydrophilic matrix with potential for sustained release. Biomaterials. 1993;14(1):16-20.

80. Chen P-C, Park YJ, Chang L-C, Kohane DS, Bartlett RH, Langer R, et al. Injectable microparticle-gel system for prolonged and localized lidocaine release. I. In vitro characterization. J Biomed Mater Res A. 2004;70(3):412-9.

81. Shukla A, Fleming KE, Chuang HF, Chau TM, Loose CR, Stephanopoulos GN, et al. Controlling the release of peptide antimicrobial agents from surfaces. Biomaterials. 2010;31(8):2348-57.

82. Rosa GD, Iommelli R, La Rotonda MI, Miro A, Quaglia F. Influence of the co-encapsulation of different non-ionic surfactants on the properties of PLGA insulin-loaded microspheres. J Control Release. 2000;69(2):283-95.

83. Lee PI. Effect of non-uniform initial drug concentration distribution on the kinetics of drug release from glassy hydrogel matrices. Polymer. 1984;25(7):973-8.

84. Al-Tahami K. In situ gel forming smart polymers for the controlled release of proteins. [Fargo, North Dakota]: North Dakota State University; 2007.

85. Degim IT, Celebi N. Controlled delivery of peptides and proteins. Curr Pharm Des. 2007;13(1):99-117.

86. Voet D, Voet JG. Biochemistry. 3rd ed. Hoboken, NJ, USA: John Wiley & Sons, Inc.; 2003.

87. Malavolta L, Cabral FR. Peptides: Important tools for the treatment of central nervous system disorders. Neuropeptides [Internet]. 2011 [cited 2011 Jul 15];In Press, Corrected Proof. Available from: http://www.sciencedirect.com/science/article/pii/S0143417911000217

88. Lu Y, Yang J, Sega E. Issues Related to Targeted Delivery of Proteins and Peptides. AAPS J. 2006;8(3):E466-E478.

89. Putney SD, Burke PA. Improving protein therapeutics with sustained-release formulations. Nat. Biotechnol. 1998;16(2):153-7.

90. Fu K, Klibanov AM, Langer R. Protein stability in controlled-release systems. Nat Biotech. 2000;18(1):24-5.

91. Stefani M, Dobson CM. Protein aggregation and aggregate toxicity: new insights into protein folding, misfolding diseases and biological evolution. J Mol Med. 2003;81(11):678-99.

92. Costantino HR, Schwendeman SP, Griebenow K, Klibanov AM, Langer R. The secondary structure and aggregation of lyophilized tetanus toxoid. J Pharm Sci. 1996;85(12):1290-3.

93. Jain NK, Roy I. Role of trehalose in moisture-induced aggregation of bovine serum albumin. Eur J Pharm Biopharm. 2008;69(3):824-34.

94. Flores-Fernández GM, Solá RJ, Griebenow K. The relation between moisture-induced aggregation and structural changes in lyophilized insulin. J Pharm Pharmacol. 2009;61(11):1555-61.

95. Stirpe A, Pantusa M, Rizzuti B, Sportelli L, Bartucci R, Guzzi R. Early stage aggregation of human serum albumin in the presence of metal ions. Int J Biol Macromol. 2011;49(3):337-42.

96. Tutar Y, Arslan D, Tutar L. Heat, pH induced aggregation and surface hydrophobicity of S. cerevesiae Ssa1 protein. Protein J. 2010;29(7):501-8.

97. Katakam M, Bell LN, Banga AK. Effect of surfactants on the physical stability of recombinant human growth hormone. J Pharm Sci. 1995;84(6):713-6.

98. Eu B, Cairns A, Ding G, Cao X, Wen Z-Q. Direct visualization of protein adsorption to primary containers by gold nanoparticles. J Pharm Sci. 2011;100(5):1663-70.

99. Geng Y, Yuan W, Wu F, Chen J, He M, Jin T. Formulating erythropoietin-loaded sustained-release PLGA microspheres without protein aggregation. J Control Release. 2008;130(3):259-65.

100. Kerwin BA, Heller MC, Levin SH, Randolph TW. Effects of Tween 80 and sucrose on acute short-term stability and long-term storage at -20 degrees C of a recombinant hemoglobin. J Pharm Sci. 1998;87(9):1062-8.

101. Sarciaux JM, Mansour S, Hageman MJ, Nail SL. Effects of buffer composition and processing conditions on aggregation of bovine IgG during freeze-drying. J Pharm Sci. 1999;88(12):1354-61.

102. Hamada H, Arakawa T, Shiraki K. Effect of additives on protein aggregation. Curr Pharm Biotechnol. 2009;10(4):400-7.

103. Rodríguez-Martínez JA, Rivera-Rivera I, Griebenow K. Prevention of benzyl alcohol-induced aggregation of chymotrypsinogen by PEGylation. J Pharm Pharmacol. 2011;63(6):800-5.

104. Yang C, Lu D, Liu Z. How PEGylation enhances the stability and potency of insulin: a molecular dynamics simulation. Biochemistry. 2011;50(13):2585-93.

105. Marin A, Decollibus DP, Andrianov AK. Protein stabilization in aqueous solutions of polyphosphazene polyelectrolyte and non-ionic surfactants. Biomacromolecules. 2010;11(9):2268-73.

106. Zhu G, Schwendeman SP. Stabilization of proteins encapsulated in cylindrical poly(lactide-co-glycolide) implants: mechanism of stabilization by basic additives. Pharm Res. 2000;17(3):351-7.

107. Kang J, Schwendeman SP. Comparison of the effects of Mg(OH)2 and sucrose on the stability of bovine serum albumin encapsulated in injectable poly(D,L-lactide-co-glycolide) implants. Biomaterials. 2002;23(1):239-45.

108. Park PS-H, Sapra KT, Koliński M, Filipek S, Palczewski K, Muller DJ. Stabilizing effect of Zn2+ in native bovine rhodopsin. J Biol Chem. 2007;282(15):11377-85.

109. Veronese FM, Mero A. The impact of PEGylation on biological therapies. BioDrugs. 2008;22(5):315-29.

110. Francis GE, Fisher D, Delgado C, Malik F, Gardiner A, Neale D. PEGylation of cytokines and other therapeutic proteins and peptides: the importance of biological optimisation of coupling techniques. Int J Hematol. 1998;68(1):1-18.

111. Wang W. Protein aggregation and its inhibition in biopharmaceutics. Int J Pharm. 2005;289(1-2):1-30.

112. Greenfield NJ. Using circular dichroism spectra to estimate protein secondary structure. Nat Protoc. 2006;1(6):2876-90.

113. Kelly SM, Price NC. The use of circular dichroism in the investigation of protein structure and function. Curr Protein Pept Sci. 2000;1(4):349-84.

114. Holzwarth G, Doty P. The Ultraviolet Circular Dichroism of Polypeptides. J Am Chem Soc. 1965;87(2):218-28.

115. Circular Dichroism [Internet]. 2011 [cited 2011 Jul 21]. Available from: http://www.ap-lab.com/circular_dichroism.htm

116. Pain R. Determining the CD Spectrum of a Protein. Current protocols in Food Analytical Chemistry. 2003;B3.5.1-B3.5.25.

117. Characterizing protein stability by DSC, Life Sciences Application Note. Calorimetry Sciences Corporation; 2006.

118. Bruylants G, Wouters J, Michaux C. Differential scanning calorimetry in life science: thermodynamics, stability, molecular recognition and application in drug design. Curr Med Chem. 2005;12(17):2011-20.

119. HPLC of Peptides and Proteins Basic Theory and Methodology. METHODS IN MOLECULAR BIOLOGY. Totowa, NJ: Humana Press Inc.; p. 9-22.

120. Electrophoric Separation of Proteins.

121. Bustamante JJ, Garcia M, Gonzalez L, Garcia J, Flores R, Aguilar RM, et al. Separation of proteins with a molecular mass difference of 2 kDa utilizing preparative double-inverted gradient polyacrylamide gel electrophoresis under nonreducing conditions: application to the isolation of 24 kDa human growth hormone. Electrophoresis. 2005;26(23):4389-95.

122. Fitzgerald MC, Parr GR, Smith LM. Basic matrices for the matrix-assisted laser desorption/ionization mass spectrometry of proteins and oligonucleotides. Anal Chem. 1993;65(22):3204-11.

123. Zaluzec EJ, Gage DA, Watson JT. Matrix-Assisted Laser Desorption Ionization Mass Spectrometry: Applications in Peptide and Protein Characterization. Protein Expres Purif. 1995;6(2):109-23.

124. Nelson RW. The use of bioreactive probes in protein characterization. Mass Spectrom Rev. 1997;16(6):353-76.

125. Bilati U, Pasquarello C, Corthals GL, Hochstrasser DF, Allémann E, Doelker E. Matrix-assisted laser desorption/ionization time-of-flight mass spectrometry for quantitation and molecular stability assessment of insulin entrapped within PLGA nanoparticles. J Pharm Sci. 2005;94(3):688-94.

126. National Diabetes Statistics, 2007: http://diabetes.niddk.nih.gov/dm/pubs/statistics/

127. World Health Organization Consultation. Definition, Diagnosis and Classification of Diabetes Mellitus and its Complications [Internet]. World Health Organization. 1999.

128. Brange J. Stability of insulin: studies on the physical and chemical stability of insulin in pharmaceutical formulation. Dordrecht, The Netherlands: Kluwer Academic Publishers; 1994.

129. Sheldon B, Russell-Jones D, Wright J. Insulin analogues: an example of applied medical science. Diabetes Obes Metab. 2009;11(1):5-19.

130. Dyer AM, Hinchcliffe M, Watts P, Castile J, Jabbal-Gill I, Nankervis R, et al. Nasal delivery of insulin using novel chitosan based formulations: a comparative study in two

animal models between simple chitosan formulations and chitosan nanoparticles. Pharm Res. 2002;19(7):998-1008.

131. Brange J, Langkjaer L. Chemical stability of insulin. 3. Influence of excipients, formulation, and pH. Acta Pharm Nord. 1992;4(3):149-58.

132. Hassiepen U, Federwisch M, Mülders T, Wollmer A. The lifetime of insulin hexamers. Biophys J. 1999;77(3):1638-54.

133. Brader ML. Zinc Coordination, Asymmetry, and Allostery of the Human Insulin Hexamer. J Am Chem Soc. 1997;119(32):7603-4.

134. Emdin SO, Dodson GG, Cutfield JM, Cutfield SM. Role of zinc in insulin biosynthesis. Diabetologia. 1980;19(3):174-82.

135. Adhikari S, Adams-Huet B, Wang Y-CA, Marks JF, White PC. Institution of basal-bolus therapy at diagnosis for children with type 1 diabetes mellitus. Pediatrics. 2009;123(4):e673-678.

136. Guthrie R. Is There a Need for a Better Basal Insulin? Clin Daibetes. 2001;19(2):66 -70.

137. Kruszynska YT, Home PD, Hanning I, Alberti KG. Basal and 24-h C-peptide and insulin secretion rate in normal man. Diabetologia. 1987;30(1):16-21.

138. Galloway JA, Chance RE. Improving insulin therapy: achievements and challenges. Horm. Metab. Res. 1994;26(12):591-8.

139. Moses RG, Bartley P, Lunt H, O'Brien RC, Donnelly T, Gall M -A, et al. Safety and efficacy of inhaled insulin (AERx® iDMS1) compared with subcutaneous insulin therapy in patients with Type 1 diabetes: 1-year data from a randomized, parallel group trial. Diabet Med. 2009;26(3):260-7.

140. Jani R, Triplitt C, Reasner C, Defronzo RA. First approved inhaled insulin therapy for diabetes mellitus. Expert Opin Drug Deliv. 2007;4(1):63-76.

141. Leary AC, Dowling M, Cussen K, O'Brien J, Stote RM. Pharmacokinetics and Pharmacodynamics of Intranasal Insulin Spray (Nasulin^{TM}) Administered to Healthy Male Volunteers: J Diabetes Sci Technol. 2008;2(6):1054-60.

142. Modi P, Mihic M, Lewin A. The evolving role of oral insulin in the treatment of diabetes using a novel RapidMist System. Diabetes Metab Res Rev. 2002;18 Suppl 1:S38-42.

143. Radermecker RP, Renard E, Scheen AJ. Circulating insulin antibodies: influence of continuous subcutaneous or intraperitoneal insulin infusion, and impact on glucose control. Diabetes Metab Res Rev. 2009;25(6):491-501.

144. Robertson KJ, Schoenle E, Gucev Z, Mordhorst L, Gall M -A, Ludvigsson J. Insulin detemir compared with NPH insulin in children and adolescents with Type 1 diabetes. Diabet Med. 2007;24(1):27-34.

145. Philips J-C, Scheen A. Insulin detemir in the treatment of type 1 and type 2 diabetes. Vasc Health Risk Manag. 2006;2(3):277-83.

146. Heller S, Koenen C, Bode B. Comparison of insulin detemir and insulin glargine in a basal—bolus regimen, with insulin aspart as the mealtime insulin, in patients with type 1 diabetes: A 52-week, multinational, randomized, open-label, parallel-group, Treat-to-Target noninferiority trial. Clin Ther. 2009;31(10):2086-97.

147. Meneghini LF, Rosenberg KH, Koenen C, Merilainen MJ, Lüddeke H-J. Insulin detemir improves glycaemic control with less hypoglycaemia and no weight gain in patients with type 2 diabetes who were insulin naive or treated with NPH or insulin glargine: clinical

practice experience from a German subgroup of the Predictive study. Diabetes Obes Metab. 2007;9(3):418-27.

148. Hirsch IB. Insulin analogues. N Engl J Med. 2005;352(2):174-83.

149. Choi S, Kim SW. Controlled release of insulin from injectable biodegradable triblock copolymer depot in ZDF rats. Pharm Res. 2003;20(12):2008-10.

150. Huynh DP, Im GJ, Chae SY, Lee KC, Lee DS. Controlled release of insulin from pH/temperature-sensitive injectable pentablock copolymer hydrogel. J Control Release. 2009;137(1):20-4.

151. Kempe S, Metz H, Bastrop M, Hvilsom A, Contri RV, Mäder K. Characterization of thermosensitive chitosan-based hydrogels by rheology and electron paramagnetic resonance spectroscopy. Eur J Pharm Biopharm. 2008;68(1):26-33.

152. Yamaguchi Y, Takenaga M, Kitagawa A, Ogawa Y, Mizushima Y, Igarashi R. Insulin-loaded biodegradable PLGA microcapsules: initial burst release controlled by hydrophilic additives. J Control Release. 2002;81(3):235-49.

153. Hinds KD, Campbell KM, Holland KM, Lewis DH, Piché CA, Schmidt PG. PEGylated insulin in PLGA microparticles. In vivo and in vitro analysis. J Control Release. 2005;104(3):447-60.

154. De Rosa G, Larobina D, Immacolata La Rotonda M, Musto P, Quaglia F, Ungaro F. How cyclodextrin incorporation affects the properties of protein-loaded PLGA-based microspheres: the case of insulin/hydroxypropyl-[beta]-cyclodextrin system. J Control Release. 2005;102(1):71-83.

155. Takenaga M, Yamaguchi Y, Kitagawa A, Ogawa Y, Mizushima Y, Igarashi R. A novel insulin formulation can keep providing steady levels of insulin for much longer periods in-vivo. J Pharm Pharmacol. 2002;54(9):1189-94.

156. Kim YH, Sioutas C, Shing KS. Influence of stabilizers on the physicochemical characteristics of inhaled insulin powders produced by supercritical antisolvent process. Pharm Res. 2009;26(1):61-71.

157. Kumar PS, Saini TR, Chandrasekar D, Yellepeddi VK, Ramakrishna S, Diwan PV. Novel approach for delivery of insulin loaded poly(lactide-co-glycolide) nanoparticles using a combination of stabilizers. Drug Deliv. 2007;14(8):517-23.

158. Lougheed WD, Albisser AM, Martindale HM, Chow JC, Clement JR. Physical stability of insulin formulations. Diabetes. 1983;32(5):424-32.

159. Zhang Y, Deng Y, Wang X, Xu J, Li Z. Conformational and bioactivity analysis of insulin: freeze-drying TBA/water co-solvent system in the presence of surfactant and sugar. Int J Pharm. 2009;371(1-2):71-81.

160. Layman H, Li X, Nagar E, Vial X, Pham SM, Andreopoulos FM. Enhanced Angiogenic Efficacy through Controlled and Sustained Delivery of FGF-2 and G-CSF from Fibrin Hydrogels Containing Ionic-Albumin Microspheres. J Biomater Sci Polym Ed 2010.

161. El-Sherbiny IM, Smyth HDC. Biodegradable nano-micro carrier systems for sustained pulmonary drug delivery: (I) self-assembled nanoparticles encapsulated in respirable/swellable semi-IPN microspheres. Int J Pharm. 2010;395(1-2):132-41.

162. Lee J, Lee KY. Injectable microsphere/hydrogel combination systems for localized protein delivery. Macromol Biosci. 2009;9(7):671-6.

163. Lee J, Tan CY, Lee S-K, Kim Y-H, Lee KY. Controlled delivery of heat shock protein using an injectable microsphere/hydrogel combination system for the treatment of myocardial infarction. J Control Release. 2009;137(3):196-202.

164. Saranya N, Moorthi A, Saravanan S, Devi MP, Selvamurugan N. Chitosan and its derivatives for gene delivery. Int J Biol Macromol. 2011;48(2):234-8.

165. Alves NM, Mano JF. Chitosan derivatives obtained by chemical modifications for biomedical and environmental applications. Int J Biol Macromol. 2008;43(5):401-14.

166. Mansouri S, Lavigne P, Corsi K, Benderdour M, Beaumont E, Fernandes JC. Chitosan-DNA nanoparticles as non-viral vectors in gene therapy: strategies to improve transfection efficacy. Eur J Pharm Biopharm. 2004;57(1):1-8.

167. Prabaharan M. Chitosan derivatives as promising materials for controlled drug delivery. J Biomater Appl. 2008;23(1):5-36.

168. Calvo P, Remuñan-López C, Vila-Jato JL, Alonso MJ. Chitosan and chitosan/ethylene oxide-propylene oxide block copolymer nanoparticles as novel carriers for proteins and vaccines. Pharm Res. 1997;14(10):1431-6.

169. Boonsongrit Y, Mitrevej A, Mueller BW. Chitosan drug binding by ionic interaction. Eur J Pharm Biopharm. 2006;62(3):267-74.

170. Liu L-S, Liu S-Q, Ng SY, Froix M, Ohno T, Heller J. Controlled release of interleukin-2 for tumour immunotherapy using alginate/chitosan porous microspheres. J Control Release. 1997;43(1):65-74.

171. Remuñán-López C, Bodmeier R. Effect of formulation and process variables on the formation of chitosan-gelatin coacervates. Int J Pharm. 1996;135(1-2):63-72.

172. Fernández-Urrusuno R, Calvo P, Remuñán-López C, Vila-Jato JL, José Alonso M. Enhancement of Nasal Absorption of Insulin Using Chitosan Nanoparticles. Pharm Res. 1999;16(10):1576-81.

173. Calvo P, Remuñán-López C, Vila-Jato JL, Alonso MJ. Novel hydrophilic chitosan-polyethylene oxide nanoparticles as protein carriers. J Appl Polym Sci. 1997;63(1):125-32.

174. Vila A, Sánchez A, Janes K, Behrens I, Kissel T, Vila Jato JL, et al. Low molecular weight chitosan nanoparticles as new carriers for nasal vaccine delivery in mice. Eur J Pharm Biopharm. 2004;57(1):123-31.

175. Kasimova MR, Velázquez-Campoy A, Nielsen HM. On the Temperature Dependence of Complex Formation between Chitosan and Proteins. Biomacromolecules. 2011;12(7):2534-43.

176. Borchard G. Chitosans for gene delivery. Adv Drug Deliv Rev. 2001;52(2):145-50.

177. Lee SH, Kim SH, Park TG. Intracellular siRNA delivery system using polyelectrolyte complex micelles prepared from VEGF siRNA-PEG conjugate and cationic fusogenic peptide. Biochem Biophys Res Commun. 2007;357(2):511-6.

178. Kim SH, Jeong JH, Lee SH, Kim SW, Park TG. Local and systemic delivery of VEGF siRNA using polyelectrolyte complex micelles for effective treatment of cancer. J Control Release. 2008;129(2):107-16.

179. Lin Q-K, Ren K-F, Ji J. Hyaluronic acid and chitosan-DNA complex multilayered thin film as surface-mediated nonviral gene delivery system. Colloids Surf B Biointerfaces. 2009;74(1):298-303.

180. Choi SW, Lee SH, Mok H, Park TG. Multifunctional siRNA delivery system: polyelectrolyte complex micelles of six-arm PEG conjugate of siRNA and cell penetrating peptide with crosslinked fusogenic peptide. Biotechnol Prog. 2010;26(1):57-63.

181. Soliman M, Allen S, Davies MC, Alexander C. Responsive polyelectrolyte complexes for triggered release of nucleic acid therapeutics. Chem Commun (Camb.). 2010;46(30):5421-33.

182. Shah HK, Conkie JA, Tait RC, Johnson JR, Wilson CG. A novel, biodegradable and reversible polyelectrolyte platform for topical-colonic delivery of pentosan polysulphate. Int J Pharm. 2011;404(1-2):124-32.

183. Dhapte V, Pokharkar V. Polyelectrolyte stabilized antimalarial nanosuspension using factorial design approach. J Biomed Nanotechnol. 2011;7(1):139-41.

184. Vergaro V, Scarlino F, Bellomo C, Rinaldi R, Vergara D, Maffia M, et al. Drug-loaded polyelectrolyte microcapsules for sustained targeting of cancer cells. Adv Drug Deliv Rev [Internet]. 2011

185. Izumrudov VA, Galaev IYu, Mattiasson B. Polycomplexes--potential for bioseparation. Bioseparation. 1998 1999;7(4-5):207-20.

186. Shah NJ, Macdonald ML, Beben YM, Padera RF, Samuel RE, Hammond PT. Tunable dual growth factor delivery from polyelectrolyte multilayer films. Biomaterials. 2011;32(26):6183-93.

187. Bechler SL, Lynn DM. Design and Synthesis of a Fluorescently End-Labeled Poly(β-amino ester): Application to the Characterization of Degradable Polyelectrolyte Multilayers. J Polym Sci A Polym Chem. 2011;49(7):1572-81.

188. Yamanlar S, Sant S, Boudou T, Picart C, Khademhosseini A. Surface functionalization of hyaluronic acid hydrogels by polyelectrolyte multilayer films. Biomaterials. 2011;32(24):5590-9.

189. Flessner RM, Jewell CM, Anderson DG, Lynn DM. Degradable Polyelectrolyte Multilayers that Promote the Release of siRNA. Langmuir. 2011;27(12):7868-76.

190. Il'ina AV, Varlamov VP. [Chitosan-based polyelectrolyte complexes: a review]. Prikl Biokhim Mikrobiol. 2005;41(1):9-16.

191. Hamman JH. Chitosan Based Polyelectrolyte Complexes as Potential Carrier Materials in Drug Delivery Systems. Mar Drugs. 2010;8(4):1305-22.

192. Bigucci F, Luppi B, Cerchiara T, Sorrenti M, Bettinetti G, Rodriguez L, et al. Chitosan/pectin polyelectrolyte complexes: Selection of suitable preparative conditions for colon-specific delivery of vancomycin. Eur J Pharm Sci. 2008;35(5):435-41.

193. Mao S, Bakowsky U, Jintapattanakit A, Kissel T. Self-assembled polyelectrolyte nanocomplexes between chitosan derivatives and insulin. J Pharm Sci. 2006;95(5):1035-48.

194. Elsayed A, Al-Remawi M, Qinna N, Farouk A, Al-Sou'od KA, Badwan AA. Chitosan-Sodium Lauryl Sulfate Nanoparticles as a Carrier System for the In Vivo Delivery of Oral Insulin. AAPS PharmSciTech. 2011.

195. Lee H, Jeong C, Ghafoor K, Cho S, Park J. Oral delivery of insulin using chitosan capsules cross-linked with phytic acid. Biomed Mater Eng. 2011;21(1):25-36.

196. Woitiski CB, Sarmento B, Carvalho RA, Neufeld RJ, Veiga F. Facilitated nanoscale delivery of insulin across intestinal membrane models. Int J Pharm. 2011;412(1-2):123-31.

197. Makhlof A, Tozuka Y, Takeuchi H. Design and evaluation of novel pH-sensitive chitosan nanoparticles for oral insulin delivery. Eur J Pharm Sci. 2011;42(5):445-51.

198. Chaudhury A, Das S. Recent advancement of chitosan-based nanoparticles for oral controlled delivery of insulin and other therapeutic agents. AAPS PharmSciTech. 2011;12(1):10-20.

199. Sajeesh S, Sharma CP. Mucoadhesive hydrogel microparticles based on poly (methacrylic acid-vinyl pyrrolidone)-chitosan for oral drug delivery. Drug Deliv. 2011;18(4):227-35.

200. Jintapattanakit A, Peungvicha P, Sailasuta A, Kissel T, Junyaprasert VB. Nasal absorption and local tissue reaction of insulin nanocomplexes of trimethyl chitosan derivatives in rats. J Pharm Pharmacol. 2010;62(5):583-91.

201. du Plessis LH, Kotzé AF, Junginger HE. Nasal and rectal delivery of insulin with chitosan and N-trimethyl chitosan chloride. Drug Deliv. 2010;17(6):399-407.

202. Agrawal AK, Gupta PN, Khanna A, Sharma RK, Chandrawanshi HK, Gupta N, et al. Development and characterization of in situ gel system for nasal insulin delivery. Pharmazie. 2010;65(3):188-93.

203. Wong TW. Chitosan and its use in design of insulin delivery system. Recent Pat Drug Deliv Formul. 2009;3(1):8-25.

204. Cui F, He C, He M, Tang C, Yin L, Qian F, et al. Preparation and evaluation of chitosan-ethylenediaminetetraacetic acid hydrogel films for the mucoadhesive transbuccal delivery of insulin. J Biomed Mater Res A. 2009;89(4):1063-71.

205. Takenaga M, Yamaguchi Y, Kitagawa A, Ogawa Y, Mizushima Y, Igarashi R. A novel sustained-release formulation of insulin with dramatic reduction in initial rapid release. J Control Release. 2002;79(1-3):81-91.

206. Kang F, Singh J. Preparation, in vitro release, in vivo absorption and biocompatibility studies of insulin-loaded microspheres in rabbits. AAPS PharmSciTech. 2005;6(3):E487-494.

207. Ma Z, Yeoh HH, Lim L-Y. Formulation pH modulates the interaction of insulin with chitosan nanoparticles. J Pharm Sci. 2002;91(6):1396-404.

208. Jeong B, Lee DS, Shon J-I, Bae YH, Kim SW. Thermoreversible gelation of poly(ethylene oxide) biodegradable polyester block copolymers. J Polym Sci A Polym Chem. 1999;37(6):751-60.

209. Micro BCA Protein Assay [Internet]. 2011 [cited 2011 Nov 9]. Available from: http://www.piercenet.com/browse.cfm?fldID=02020102

210. Olesen OV, Linnet K. Simplified high-performance liquid chromatographic method for determination of risperidone and 9-hydroxyrisperidone in serum from patients comedicated with other psychotropic drugs. J. Chromatogr. B Biomed. Sci. Appl. 1997 Sep 26;698(1-2):209-16.

211. Hayton WL, Chen T. Correction of perfusate concentration for sample removal. J Pharm Sci. 1982;71(7):820-1.

212. Ibrahim MA, Ismail A, Fetouh MI, Göpferich A. Stability of insulin during the erosion of poly(lactic acid) and poly(lactic-co-glycolic acid) microspheres. J Control Release. 2005;106(3):241-52.

213. Mercodia - Insulin ELISA [Internet]. 2011 [cited 2011 Nov 6]. Available from: http://www.mercodia.se/index.php?page=productview2&prodId=9

214. Gupta S, Chattopadhyay T, Pal Singh M, Surolia A. Supramolecular insulin assembly II for a sustained treatment of type 1 diabetes mellitus. Proc Natl Acad Sci U S A. 2010;107(30):13246-51.

215. Rowland M, Tozer TN. Clinical Pharmacokinetics and Pharmacodynamics: Concepts and Applications. 4th ed. Lippincott Williams & Wilkins; 2010.

216. Langer R. Polymer-controlled drug delivery systems. Acc Chem Res. 1993;26(10):537-42.

217. Jeong B, Bae YH, Kim SW. Drug release from biodegradable injectable thermosensitive hydrogel of PEG-PLGA-PEG triblock copolymers. J Control Release. 2000;63(1-2):155-63.

218. Kinam Park. Superporous Hydrogels for Pharmaceutical & Other Applications. Drug Dev Delivery [Internet]. 2008;2(5).

219. Ganji F, Vasheghani-Farahani S, Vasheghani-Farahani E. Theoretical Description of Hydrogel Swelling: A Review. Iran Polym J. 2010;19(5):375-98.

220. Molina I, Li S, Martinez MB, Vert M. Protein release from physically crosslinked hydrogels of the PLA/PEO/PLA triblock copolymer-type. Biomaterials. 2001;22(4):363-9.

221. Chung S. Chain-end scission in acid catalyzed hydrolysis of poly (d,l-lactide) in solution. J Control Release. 1995;34(1):9-15.

222. Dong WY, KÃ¶rber M, LÃ^{3}pez Esguerra V, Bodmeier R. Stability of poly(d,l-lactide-co-glycolide) and leuprolide acetate in in-situ forming drug delivery systems. J Control Release. 2006;115(2):158-67.

223. Rajeev A J. The manufacturing techniques of various drug loaded biodegradable poly(lactide-co-glycolide) (PLGA) devices. Biomaterials. 2000;21(23):2475-90.

224. Ramchandani M, Pankaskie M, Robinson D. The influence of manufacturing procedure on the degradation of poly(lactide-co-glycolide) 85:15 and 50:50 implants. J Control Release. 1997;43(2-3):161-73.

225. Makadia HK, Siegel SJ. Poly Lactic-co-Glycolic Acid (PLGA) as Biodegradable Controlled Drug Delivery Carrier. Polymers. 2011;3:1377-97.

226. Yu L, Zhang Z, Zhang H, Ding J. Biodegradability and biocompatibility of thermoreversible hydrogels formed from mixing a sol and a precipitate of block copolymers in water. Biomacromolecules. 2010;11(8):2169-78.

227. Zolnik BS, Leary PE, Burgess DJ. Elevated temperature accelerated release testing of PLGA microspheres. J Control Release. 2006;112(3):293-300.

228. BSA: Product Information sheet. Sigma;

229. DrugBank: Risperidone (DB00734) [Internet]. 2011 [cited 2011 Sep 19]. Available from: http://www.drugbank.ca/drugs/DB00734

230. Sandor M, Enscore D, Weston P, Mathiowitz E. Effect of protein molecular weight on release from micron-sized PLGA microspheres. J Control Release. 2001;76(3):297-311.

231. Blanco D, Alonso MJ. Protein encapsulation and release from poly(lactide-co-glycolide) microspheres: effect of the protein and polymer properties and of the co-encapsulation of surfactants. Eur J Pharm Biopharm. 1998;45(3):285-94.

232. Siegel SJ, Kahn JB, Metzger K, Winey KI, Werner K, Dan N. Effect of drug type on the degradation rate of PLGA matrices. Eur J Pharm Biopharm. 2006;64(3):287-93.

233. Shah NH, Railkar AS, Chen FC, Tarantino R, Kumar S, Murjani M, et al. A biodegradable injectable implant for delivering micro and macromolecules using poly (lactic-co-glycolic) acid (PLGA) copolymers. J Control Release. 1993;27(2):139-47.

234. Bittner B, Morlock M, Koll H, Winter G, Kissel T. Recombinant human erythropoietin (rhEPO) loaded poly(lactide-co-glycolide) microspheres: influence of the encapsulation technique and polymer purity on microsphere characteristics. Eur J Pharm Biopharm. 1998;45(3):295-305.

235. Morlock M, Kissel T, Li YX, Koll H, Winter G. Erythropoietin loaded microspheres prepared from biodegradable LPLG-PEO-LPLG triblock copolymers: protein stabilization and in-vitro release properties. J Control Release. 1998;56(1-3):105-15.

236. Park TG, Yong Lee H, Sung Nam Y. A new preparation method for protein loaded poly(D, L-lactic-co-glycolic acid) microspheres and protein release mechanism study. J Control Release. 1998;55(2-3):181-91.

237. Sluzky V, Tamada JA, Klibanov AM, Langer R. Kinetics of insulin aggregation in aqueous solutions upon agitation in the presence of hydrophobic surfaces. Proc Natl Acad Sci U S A. 1991;88(21):9377-81.

238. Banga AK. Preformulation and formulation of therapeutic peptides. Therapeutic peptides and proteins: Formulation, processing, and delivery systems. 2nd ed. Boca Raton FL: CRC Press; 2006. p. 91-128.

239. Dunn MF. Zinc-ligand interactions modulate assembly and stability of the insulin hexamer -- a review. Biometals. 2005;18(4):295-303.

240. Takenaga M, Yamaguchi Y, Kitagawa A, Ogawa Y, Kawai S, Mizushima Y, et al. Optimum formulation for sustained-release insulin. Int J Pharm. 2004;271(1-2):85-94.

241. Brown L, Siemer L, Munoz C, Langer R. Controlled release of insulin from polymer matrices. In vitro kinetics. Diabetes. 1986;35(6):684-91.

242. Strickland EH, Mercola D. Near-ultraviolet tyrosyl circular dichroism of pig insulin monomers, dimers, and hexamers. Dipole-dipole coupling calculations in the monopole approximation. Biochemistry. 1976;15(17):3875-84.

243. Houchin ML, Heppert K, Topp EM. Deamidation, acylation and proteolysis of a model peptide in PLGA films. J Control Release. 2006;112(1):111-9.

244. Chen L, Tianqing L. Interaction behaviors between chitosan and hemoglobin. Int J Biol Macromol. 2008;42(5):441-6.

245. Huus K, Havelund S, Olsen HB, van de Weert M, Frokjaer S. Chemical and thermal stability of insulin: effects of zinc and ligand binding to the insulin zinc-hexamer. Pharm Res. 2006;23(11):2611-20.

246. Shao PG, Bailey LC. Stabilization of pH-induced degradation of porcine insulin in biodegradable polyester microspheres. Pharm Dev Technol. 1999;4(4):633-42.

247. Sajeesh S, Sharma CP. Novel pH responsive polymethacrylic acid-chitosan-polyethylene glycol nanoparticles for oral peptide delivery. J Biomed Mater Res A. 2006;76B(2):298-305.

248. Nyambura BK, Kellaway IW, Taylor KMG. Insulin nanoparticles: stability and aerosolization from pressurized metered dose inhalers. Int J Pharm. 2009;375(1-2):114-22.

249. Jiang G, Woo BH, Kang F, Singh J, DeLuca PP. Assessment of protein release kinetics, stability and protein polymer interaction of lysozyme encapsulated poly(D,L-lactide-co-glycolide) microspheres. J Control Release. 2002;79(1-3):137-45.

250. Miyajima M, Koshika A, Okada J, Ikeda M. Effect of polymer/basic drug interactions on the two-stage diffusion-controlled release from a poly(L-lactic acid) matrix. J Control Release. 1999;61(3):295-304.

251. Mandke R, Singh J. Effect of acyl chain length and unsaturation on physicochemical properties and transfection efficiency of N-acyl-substituted low-molecular-weight chitosan. J Pharm Sci. 2012;101(1):268-82.

252. Wu KK, Huan Y. Streptozotocin-Induced Diabetic Models in Mice and Rats. Curr Protoc Pharmacol. 2008;40:5.47.1-5.47.14.

253. Barichello JM, Morishita M, Takayama K, Nagai T. Absorption of insulin from pluronic F-127 gels following subcutaneous administration in rats. Int J Pharm. 1999;184(2):189-98.

254. Rizza RA, Mandarino LJ, Gerich JE. Dose-response characteristics for effects of insulin on production and utilization of glucose in man. Am J Physiol. 1981;240(6):E630-639.

255. Li J, Johnson JD. Mathematical models of subcutaneous injection of insulin analogues: A mini-review. Discrete Continuous Dyn Syst Ser B. 2009;12(2):401-14.

256. Oak M, Singh J. Controlled delivery of basal level of insulin from chitosan-zinc-insulin-complex-loaded thermosensitive copolymer. J Pharm Sci. 2012;101(3):1079-96.

257. Kwon YM, Kim SW. Biodegradable triblock copolymer microspheres based on thermosensitive sol-gel transition. Pharm Res. 2004;21(2):339-43.

258. International Diabetes Federation. The Global Burden: Diabetes and Impaired Glucose Tolerance (IGT): Prevalence and Projections. IDF Diabetes Atlas [Internet]. 4th ed. Brussels: International Diabetes Federation; 2011. Available from: http://www.idf.org/diabetesatlas

259. Veeramani C, Pushpavalli G, Pugalendi K. Antihyperglycaemic effect of Cardiospermum halicacabum Linn. leaf extract on STZ-induced diabetic rats. J Appl Biomed. 2007;6(1):19-26.

260. Hermeling S, Crommelin DJA, Schellekens H, Jiskoot W. Structure-Immunogenicity Relationships of Therapeutic Proteins. Pharm Res. 2004;21(6):897-903.

261. Schernthaner G. Immunogenicity and allergenic potential of animal and human insulins. Diabetes Care. 1993;16 Suppl 3:155-65.

262. Fineberg SE, Kawabata TT, Finco-Kent D, Fountaine RJ, Finch GL, Krasner AS. Immunological Responses to Exogenous Insulin. Endocr Rev. 2007;28(6):625 -652.

263. Riva R, Ragelle H, des Rieux A, Duhem N, Jerome C, Preat V. Chitosan and chitosan derivatives in drug delivery and tissue engineering. Adv Polym Sci. 2011;244:19-44.

264. Kean T, Thanou M. Biodegradation, biodistribution and toxicity of chitosan. Advanced Drug Delivery Reviews. 2010 Jan 31;62(1):3-11.

265. U.S. Environmental Protection Agency Washington D.C. Toxicological review of zinc and compounds. 2005;CAS No. 7440-66-6.

266. Silva GA, Marques AP, Gomes ME, Coutinho OP, Reis RL. Cytotoxicity Screening of Biodegradable Polymeric Systems. In: Reis RL, Román JS, editors. Biodegradable Systems in Tissue Engineering and Regenerative Medicine 2012.

267. Nwe N, Furuike T, Tamura H. The Mechanical and Biological Properties of Chitosan Scaffolds for Tissue Regeneration Templates Are Significantly Enhanced by Chitosan from Gongronella butleri. Materials. 2009;2(2):374-98.

268. Morais JM, Papadimitrakopoulos F, Burgess DJ. Biomaterials/tissue interactions: possible solutions to overcome foreign body response. AAPS J. 2010;12(2):188-96.

269. Park TG, Lu W, Crotts G. Importance of in vitro experimental conditions on protein release kinetics, stability and polymer degradation in protein encapsulated poly (d,l-lactic acid-co-glycolic acid) microspheres. J Control Release. 1995;33(2):211-22.

270. Daugherty AL, Cleland JL, Duenas EM, Mrsny RJ. Pharmacological modulation of the tissue response to implanted polylactic-co-glycolic acid microspheres. Eur J Pharm Biopharm. 1997;44(1):89-102.

271. Wang F, Li Z, Khan M, Tamama K, Kuppusamy P, Wagner WR, et al. Injectable, rapid gelling and highly flexible hydrogel composites as growth factor and cell carriers. Acta Biomater. 2010;6(6):1978-91.

272. Park M-R, Chun C, Ahn S-W, Ki M-H, Cho C-S, Song S-C. Sustained delivery of human growth hormone using a polyelectrolyte complex-loaded thermosensitive polyphosphazene hydrogel. J Control Release. 2010;147(3):359-67.

273. Toti US, Moon SH, Kim HY, Jun YJ, Kim BM, Park YM, et al. Thermosensitive and biocompatible cyclotriphosphazene micelles. J Control Release. 2007;119(1):34-40.

274. Kim MR, Park TG. Temperature-responsive and degradable hyaluronic acid/Pluronic composite hydrogels for controlled release of human growth hormone. J Control Release. 2002;80(1-3):69-77.